

ADVANCED TOPICS IN SCIENCE AND TECHNOLOGY IN CHINA

Editors Jianping Geng
Weiwei Yan
Wei Xu

Application of the Finite Element Method in Implant Dentistry



Springer



ZHEJIANG UNIVERSITY PRESS
浙江大学出版社

**ADVANCED TOPICS
IN SCIENCE AND TECHNOLOGY IN CHINA**

ADVANCED TOPICS IN SCIENCE AND TECHNOLOGY IN CHINA

Zhejiang University is one of the leading universities in China. In Advanced Topics in Science and Technology in China, Zhejiang University Press and Springer jointly publish monographs by Chinese scholars and professors, as well as invited authors and editors from abroad who are outstanding experts and scholars in their fields. This series will be of interest to researchers, lecturers, and graduate students alike.

Advanced Topics in Science and Technology in China aims to present the latest and most cutting-edge theories, techniques, and methodologies in various research areas in China. It covers all disciplines in the fields of natural science and technology, including but not limited to, computer science, materials science, the life sciences, engineering, environmental sciences, mathematics, and physics.

Jianping Geng
Weiwei Yan
Wei Xu
(Editors)

Application of the Finite Element Method in Implant Dentistry

With 100 figures

EDITORS:

Prof. Jianping Geng
Clinical Research Institute,
Second Affiliated Hospital
Zhejiang University School of Medicine
88 Jiefang Road, Hangzhou 310009
China
E-mail:jp geng2005@163.com

Prof. Weiqi Yan,
Clinical Research Institute,
Second Affiliated Hospital
Zhejiang University School of Medicine
88 Jiefang Road, Hangzhou 310009
China
E-mail: wyan@zju.edu.cn

Dr. Wei Xu,
School of Engineering (H5),
University of Surrey
Surrey, GU2 7XH
UK
E-mail:drweixu@hotmail.com

ISBN 978-7-308-05510-9 Zhejiang University Press, Hangzhou
ISBN 978-3-540-73763-6 Springer Berlin Heidelberg New York
e-ISBN 978-3-540-73764-3 Springer Berlin Heidelberg New York

Series ISSN 1995-6819 Advanced topics in science and technology in China
Series e-ISSN 1995-6827 Advanced topics in science and technology in China

Library of Congress Control Number: 2007937705

This work is subject to copyright. All rights are reserved, whether the whole or part of the material is concerned, specifically the rights of translation, reprinting, reuse of illustrations, recitation, broadcasting, reproduction on microfilm or in any other way, and storage in data banks. Duplication of this publication or parts thereof is permitted only under the provisions of the German Copyright Law of September 9, 1965, in its current version, and permission for use must always be obtained from Springer -Verlag. Violations are liable to prosecution under the German Copyright Law.

© 2008 Zhejiang University Press, Hangzhou and Springer -Verlag GmbH Berlin Heidelberg
Co-published by Zhejiang University Press, Hangzhou and Springer -Verlag GmbH Berlin Heidelberg

Springer is a part of Springer Science + Business Media
springer.com

The use of general descriptive names, registered names, trademarks, etc. in this publication does not imply, even in the absence of a specific statement, that such names are exempt from the relevant protective laws and regulations and therefore free for general use.

Cover design: Joe Piliero, Springer Science + Business Media LLC, New York
Printed on acid-free paper

Foreword

There are situations in clinical reality when it would be beneficial to be able to use a structural and functional prosthesis to compensate for a congenital or acquired defect that can not be replaced by biologic material.

Mechanical stability of the connection between material and biology is a prerequisite for successful rehabilitation with the expectation of life long function without major problems.

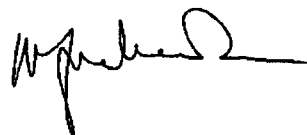
Based on Professor Skalak's theoretical deductions of elastic deformation at/of the interface between a screw shaped element of pure titanium at the sub cellular level the procedure of osseointegration was experimentally and clinically developed and evaluated in the early nineteen-sixties.

More than four decades of clinical testing has ascertained the predictability of this treatment modality, provided the basic requirements on precision in components and procedures were respected and patients continuously followed.

The functional combination of a piece of metal with the human body and its immuno-biologic control mechanism is in itself an apparent impossibility. Within the carefully identified limits of biologic acceptability it can however be applied both in the cranio-maxillofacial skeletal as well as in long bones.

This book provides an important contribution to clinical safety when bone anchored prostheses are used because it explains the mechanism and safety margins of transfer of load at the interface with emphasis on the actual clinical anatomical situation. This makes it particularly useful for the creative clinician and unique in its field. It should also initiate some critical thinking among hard ware producers who might sometimes underestimate the short distance between function and failure when changes in clinical devices or procedures are too abruptly introduced.

An additional value of this book is that it emphasises the necessity of respect for what happens at the functional interaction at the interface between molecular biology and technology based on critical scientific exploration and deduction.



P-I Bränemark

Preface

This book provides the theoretical foundation of Finite Element Analysis(FEA) in implant dentistry and practical modelling skills that enable the new users (implant dentists and designers) to successfully carry out FEA in actual clinical situations.

The text is divided into five parts: introduction of finite element analysis and implant dentistry, applications, theory with modelling and use of commercial software for the finite element analysis. The first part introduces the background of FEA to the dentist in a simple style. The second part introduces the basic knowledge of implant dentistry that will help the engineering designers have some backgrounds in this area. The third part is a collection of dental implant applications and critical issues of using FEA in dental implants, including bone-implant interface, implant-prosthesis connection, and multiple implant prostheses. The fourth part concerns dental implant modelling such as the assumptions of detailed geometry of bone and implant, material properties, boundary conditions, and the interface between bone and implant. Finally, in fifth part, two popular commercial finite element software ANSYS and ABAQUS are introduced for a Bränemark same-day dental implant and a GJP biomechanical optimum dental implant, respectively.

Jianping Geng

Hangzhou

Weiqi Yan

Hangzhou

Wei Xu

Surrey

Contents

1 Finite Element Method	
N. Krishnamurthy	(1)
1.1 Introduction	(1)
1.2 Historical Development	(1)
1.3 Definitions and Terminology	(5)
1.4 Flexibility Approach	(7)
1.5 Stiffness Formulation	(7)
1.5.1 Stiffness Matrix	(7)
1.5.2 Characteristics of Stiffness Matrix	(9)
1.5.3 Equivalent Loads	(10)
1.5.4 System Stiffness Equations	(11)
1.6 Solution Methodology	(11)
1.6.1 Manual Solution	(11)
1.6.2 Computer Solution	(12)
1.6.3 Support Displacements	(13)
1.6.4 Alternate Loadings	(13)
1.7 Advantages and Disadvantages of FEM	(14)
1.8 Mathematical Formulation of Finite Element Method	(15)
1.9 Shape Functions	(16)
1.9.1 General Requirements	(16)
1.9.2 Displacement Function Technique	(17)
1.10 Element Stiffness Matrix	(18)
1.10.1 Shape Function	(18)
1.10.2 Strain Influence Matrix	(18)
1.10.3 Stress Influence Matrix	(19)
1.10.4 External Virtual Work	(19)
1.10.5 Internal Virtual Work	(20)
1.10.6 Virtual Work Equation	(21)
1.11 System Stiffness Matrix	(21)
1.12 Equivalent Actions Due to Element Loads	(24)

1.12.1 Concentrated Action inside Element	(25)
1.12.2 Traction on Edge of Element	(26)
1.12.3 Body Force over the Element	(26)
1.12.4 Initial Strains in the Element	(27)
1.12.5 Total Action Vector	(28)
1.13 Stresses and Strains	(29)
1.14 Stiffness Matrices for Various Element	(29)
1.15 Critical Factors in Finite Element Computer Analysis	(30)
1.16 Modelling Considerations	(30)
1.17 Asce Guidelines	(33)
1.18 Preprocessors and Postprocessors	(35)
1.18.1 Preprocessors	(35)
1.18.2 Postprocessors	(36)
1.19 Support Modelling	(37)
1.20 Improvement of Results	(37)
References	(39)

2 Introduction to Implant Dentistry

Rodrigo F. Neiva, Hon-Lay Wang, Jianping Geng	(42)
2.1 History of Dental Implants	(42)
2.2 Phenomenon of Osseointegration	(43)
2.3 The Soft Tissue Interface	(46)
2.4 Protocols for Implant Placement	(48)
2.5 Types of Implant Systems	(48)
2.6 Prosthetic Rehabilitation	(49)
References	(55)

3 Applications to Implant Dentistry

Jianping Geng, Wei Xu, Keson B.C. Tan, Quan-Sheng Ma, Haw-Ming Huang, Sheng-Yang Lee, Weiqi Yan, Bin Deng, Yong Zhao	(61)
3.1 Introduction	(61)
3.2 Bone-implant Interface	(61)
3.2.1 Introduction	(61)
3.2.2 Stress Transmission and Biomechanical Implant Design Problem	(62)
3.2.3 Summary	(68)
3.3 Implant Prosthesis Connection	(68)
3.3.1 Introduction	(68)
3.3.2 Screw Loosening Problem	(68)
3.3.3 Screw Fracture	(70)
3.3.4 Summary	(70)
3.4 Multiple Implant Prostheses	(71)
3.4.1 Implant-supported Fixed Prostheses	(71)

3.4.2 Implant-supported Overdentures	(73)
3.4.3 Combined Natural Tooth and Implant-supported Prostheses	(74)
3.5 Conclusions	(75)
References	(76)
4 Finite Element Modelling in Implant Dentistry	
Jianping Geng, Weiqi Yan, Wei Xu, Keson B.C. Tan, Haw-Ming Huang, Sheng-Yang Lee, Huazi Xu, Linbang Huang, Jing Chen	(81)
4.1 Introduction	(81)
4.2 Considerations of Dental Implant FEA	(82)
4.3 Fundamentals of Dental Implant Biomechanics	(83)
4.3.1 Assumptions of Detailed Geometry of Bone and Implant	(83)
4.3.2 Material Properties	(84)
4.3.3 Boundary Conditions	(86)
4.4 Interface between Bone and Implant	(86)
4.5 Reliability of Dental Implant FEA	(88)
4.6 Conclusions	(89)
References	(89)
5 Application of Commercial FEA Software	
Wei Xu, Jason Huijun Wang, Jianping Geng, Haw-Ming Huang	(92)
5.1 Introduction	(92)
5.2 ANSYS	(93)
5.2.1 Introduction	(93)
5.2.2 Preprocess	(94)
5.2.3 Solution	(107)
5.2.4 Postprocess	(108)
5.2.5 Summary	(113)
5.3 ABAQUS	(114)
5.3.1 Introduction	(114)
5.3.2 Model an Implant in ABAQUS/CAE	(116)
5.3.3 Job Information Files	(127)
5.3.4 Job Result Files	(130)
5.3.5 Conclusion	(133)
References	(134)
Index	(135)

Contributors

Bin Deng	Department of Mechanical Engineering, National University of Singapore, Singapore
Jianping Geng	Clinical Research Institute, Second Affiliated Hospital, School of Medicine, Zhejiang University, Hangzhou, China
N. Krishnamurthy Sheng -Yang Lee	Consultant, Structures, Safety, and Computer Applications, Singapore School of Dentistry, Taipei Medical University, Taipei, Taiwan, China
Quan -Sheng Ma	Department of Implant Dentistry, Shandong Provincial Hospital, Jinan, China
Haw -Ming Huang	Graduate Institute of Medical Materials & Engineering, Taipei Medical University, Taipei, Taiwan, China
Hom -Lay Wang	School of Dentistry, University of Michigan, Ann Arbor, USA
Huazi Xu	Orthopedic Department, Second Affiliated Hospital, Wenzhou Medical College, Wenzhou, China
Jason Huijun Wang	Worley Advanced Analysis (Singapore), Singapore
Jing Chen	School of Dentistry, Sichuan University, Chengdu, China
Keson B.C. Tan	Faculty of Dentistry, National University of Singapore, Singapore
Linbang Huang	Medical Research Institute, Gannan Medical College, Ganzhou, China
Rodrigo F. Neiva	School of Dentistry, University of Michigan, Ann Arbor, USA
Wei Xu	School of Engineering, University of Surrey, Surrey, UK
Weiwei Yan	Clinical Research Institute, Second Affiliated Hospital, School of Medicine, Zhejiang University, Hangzhou, China
Yong Zhao	School of Dentistry, Sichuan University, Chengdu, China

Finite Element Modelling in Implant Dentistry

Jianping Geng¹, Weiqi Yan², Wei Xu³, Keson B. C. Tan⁴, Haw-Ming Huang⁵, Sheng-Yang Lee⁶, Huazi Xu⁷, Linbang Huang⁸, Jing Chen⁹

^{1,2} Clinical Research Institute, Second Affiliated Hospital, School of Medicine, Zhejiang University, Hangzhou, China

Email: jp geng2005@163.com

³ School of Engineering, University of Surrey, Surrey, UK

⁴ Faculty of Dentistry, National University of Singapore, Singapore

⁵ Graduate Institute of Medical Materials and Engineering, Taipei Medical University, Taipei, Taiwan, China

⁶ School of Dentistry, Taipei Medical University, Taipei, Taiwan, China

⁷ Orthopedic Department, Second Affiliated Hospital, Wenzhou Medical College, Wenzhou, China

⁸ Medical Research Institute, Gannan Medical College, Ganzhou, China

⁹ School of Dentistry, Sichuan University, Chengdu, China

4. 1 Introduction

The use of numerical methods such as FEA has been adopted in solving complicated geometric problems, for which it is very difficult to achieve an analytical solution. FEA is a technique for obtaining a solution to a complex mechanics problem by dividing the problem domain into a collection of much smaller and simpler domains (elements) where field variables can be interpolated using shape functions. An overall approximated solution to the original problem is determined based on variational principles. In other words, FEA is a method whereby, instead of seeking a solution function for the entire domain, it formulates solution functions for each finite element and combines them properly to obtain a solution to the whole body. A mesh is needed in FEA to divide the whole domain into small elements. The process of creating the mesh, elements, their respective nodes, and defining boundary conditions is termed “discretization” of the problem domain. Since the components in a dental implant-bone system is an extremely complex geometry, FEA has been viewed as the most suitable tool to mathematically, model it by numerous scholars.

FEA was initially developed in the early 1960s to solve structural problems in the aerospace industry but has since been extended to solve problems in heat transfer, fluid flow, mass transport, and electromagnetic realm. In 1977, Weinstein¹ was the first to use FEA in implant dentistry. Subsequently, FEA was rapidly applied in many aspects of implant dentistry. Atmaram and Mohammed^{2,4} analysed the stress distribution in a single tooth implant, to understand the effect of elastic parameters and geometry of the implant, implant length variation, and pseudo-periodontal ligament incorporation. Borchers and Reichart⁵ performed a three-dimensional FEA of an implant at different stages of bone interface development. Cook, et al.⁶ applied it in porous rooted dental implants. Meroueh, et al.⁷ used it for an osseointegrated cylindrical implant. Williams, et al.⁸ carried out it on cantilevered prostheses on dental implants. Akpinar, et al.⁹ simulated the combination of a nature tooth with an implant using FEA.

4. 2 Considerations of Dental Implant FEA

In the past three decades, FEA has become an increasingly useful tool for the prediction of stress effect on the implant and its surrounding bone. Vertical and transverse loads from mastication induce axial forces and bending moments and result in stress gradients in the implant as well as in the bone. A key to the success or failure of a dental implant is the manner in which stresses are transferred to the surrounding bone. Load transfer from the implant to its surrounding bone depends on the type of loading, the bone-implant interface, the length and diameter of the implants, the shape and characteristics of the implant surface, the prosthesis type, and the quantity and quality of the surrounding bone. FEA allows researchers to predict stress distribution in the contact area of the implant with cortical bone and around the apex of the implant in trabecular bone.

Although the precise mechanisms are not fully understood, it is clear that there is an adaptive remodelling response of the surrounding bone to this kind of stress. Implant features causing excessive high or low stresses can possibly contribute to pathologic bone resorption or bone atrophy. The principal difficulty in simulating the mechanical behaviour of dental implants is the modelling of human bone tissues and its response to applied mechanical forces. The complexity of the mechanical characterization of bone and its interaction with implant systems have forced researchers to make major simplifications and assumptions to make the modelling and solving process possible. Some assumptions influence the accuracy of the FEA results significantly. They are: (1) detailed geometry of the bone and implant to be modelled¹⁰, (2) material properties¹⁰, (3) boundary conditions¹⁰, and (4) the interface between the bone and implant¹¹.

4.3 Fundamentals of Dental Implant Biomechanics

4.3.1 Assumptions of Detailed Geometry of Bone and Implant

The first step in FEA modelling is to represent the geometry of interest in the computer. In some two- or three-dimensional FEA studies the bone was modeled as a simplified rectangular configuration with the implant¹¹⁻¹³ (Fig. 4.1). Some three-dimensional FEA models treated the mandible as an arch with rectangular section^{14,15}. Recently, with the development of digital imaging techniques, more efficient methods are available for the development of anatomically accurate models. These include the application of specialized softwares for the direct transformation of 2D or 3D information in image data from CT or MRI, into FEA meshes (Fig. 4.2 to Fig. 4.4). The automated inclusion of some material properties from measured bone density values is also possible^{16,17}. This will allow more precise modelling of the geometry of the bone-implant system. In the foreseeable future, the creation of FEA models for individual patients based on advanced digital techniques will become possible and even commonplace.

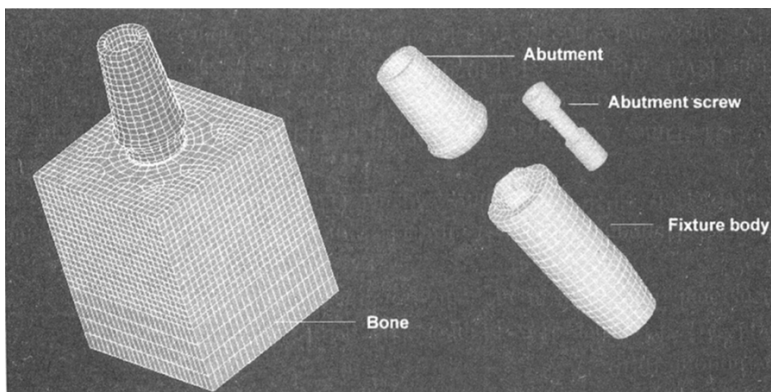


Fig. 4.1 3D Information of a Simplified Rectangular Configuration with the Implant Components (By H.M. Huang and S.Y. Lee)

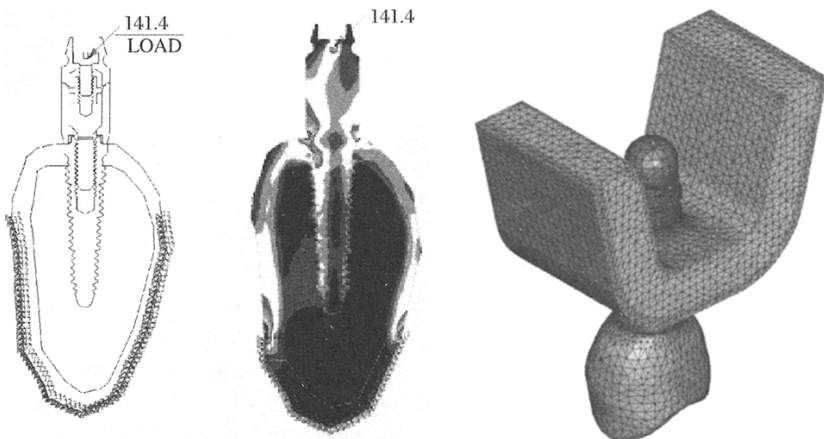


Fig. 4.2 2D Information in Image Data from Mandibular CT and Its FEA Stress Distribution (By J.P. Geng et al.)

Fig. 4.3 3D Information in Image Data from Posterior Maxillary CT and Its FEA Meshes

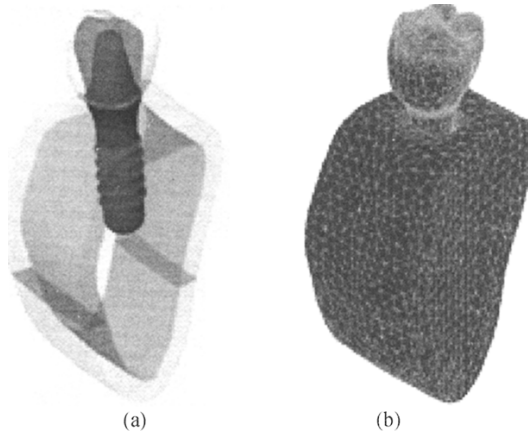


Fig. 4.4 3D Information in Image Data from Mandibular CT and Its FEA Meshes

4.3.2 Material Properties

Material properties greatly influence the stress and strain distribution in a structure. These properties can be modeled in FEA as isotropic, transversely isotropic, orthotropic, and anisotropic. In an isotropic material, the properties are the same in all directions, and therefore there are only two independent material constants. An anisotropic material has its different properties when measured in different directions. There are many material constants depending on the degree of anisotropy (transversely isotropic, orthotropic, etc).

In most reported studies, materials are assumed homogeneous, linear and have elastic material behaviour characterized by two material constants of Young's

modulus and Poisson's Ratio. Early FEA studies ignored the trabecular bone network simply because its pattern was not able to be determined. Therefore, it was assumed that trabecular bone has a solid pattern inside the inner cortical bone shell. Both bone types were simplistically modeled as linear, homogeneous, and isotropic materials. A range of different material parameters have been recommended for use in previous FEA studies (Table 4.1)^{5,18-33}.

Table 4.1 Material Parameters Used in FEA Studies of Dental Implants

	Elastic Modulus (MPa)	Poisson's Ratio	Author, Year	Reference No.
Enamel	4.14×10^4	0.3	Davy, 1981	18
	4.689×10^4	0.30	Wright, 1979	19
	8.25×10^4	0.33	Farah, 1975	20
	8.4×10^4	0.33	Farah, 1989	21
Dentin	1.86×10^4	0.31	Reinhardt, 1984	22
	1.8×10^4	0.31	MacGregor, 1980	23
Parodontal membrane	171	0.45	Atmaram, 1981	24
Cortical bone	69.8	0.45	Reinhardt, 1984	22
	6.9	0.45	Farah, 1989	21
Trabecular bone	2727	0.30	Rice, 1988	25
	1.0×10^4	0.30	Farah, 1989	21
	1.34×10^4	0.30	Cook, 1982	26
	1.5×10^4	0.30	Cowin, 1989	27
Mucosa	150	0.30	Cowin, 1989	27
	250	0.30	MacGregor, 1980	23
	790	0.30	Knoell, 1977	28
	1.37×10^3	0.31	Borchers, 1983	5
Pure Ti	117×10^3	0.30	Ronald, 1995	30
Ti-6Al-4V	110×10^3	0.33	Colling, 1984	31
Type 3 gold alloy	100×10^3	0.30	Ronald, 1995	30
	80×10^3	0.33	Lewinstein, 1995	32
Ag-Pd alloy	95×10^3	0.33	Craig, 1989	33
Co-Cr alloy	218×10^3	0.33	Craig, 1989	33
Porcelain	68.9×10^3	0.28	Lewinstein, 1995	32
Resin	2.7×10^3	0.35	Craig, 1989	33
Resin composite	7×10^3	0.2	Craig, 1989	33

In fact, several studies³⁴⁻³⁷ have pointed out that cortical bone is neither homogeneous nor isotropic (Table 4.2). This non-homogenous, anisotropic, composite structure of bone also possesses different values for ultimate strain and modulus of elasticity when it is tested in compression compared to in tension. Test

conditions will affect the material properties measured too. Rieger, et al.¹² reported that a range of stresses (1.4 MPa to 5.0 MPa) appeared to be necessary for healthy maintenance of bone. Stresses outside this range have been reported to cause bone resorption.

Table 4. 2 Anisotropic Properties of Cortical Bone

Elastic (MPa)	Cortical Shell	
	Diaphyseal	Metaphyseal
Longitudinal	17,500	9,650
Transverse	11,500	5,470

4. 3. 3 Boundary Conditions

Most FEA studies modelling the mandible set boundary conditions as a fixed boundary. Zhou³⁸ developed a more realistic three-dimensional mandibular FEA model from transversely scanned CT image data. The functions of the muscles of mastication and the ligamentous and functional movement of the TMJs were simulated by means of cable elements and compressive gap elements respectively. It was concluded that cable and gap elements could be used to set boundary conditions in their mandibular FEA model, improving the model mimicry and accuracy. Expanding the domain of the model can reduce the influence of inaccurate modelling of the boundary conditions. This however, will be at the expense of computing and modelling time (Fig. 4. 5). Teixeira, et al.³⁹ concluded that in a three-dimensional mandibular model, modelling the mandible at distances greater than 4. 2 mm mesial or distal from the implant did not result in any significant further yield in FEA accuracy. Use of infinite elements can be a good way to model boundary conditions (Fig.4.6).

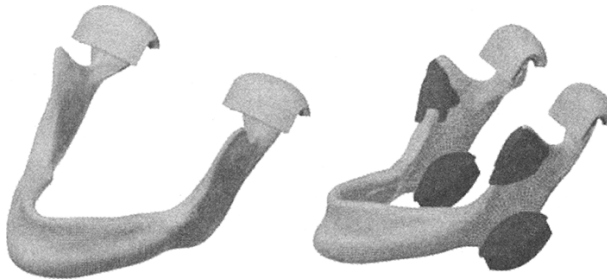


Fig. 4. 5 Three-dimensional FEA Model of the Human Jaw and the Functional Direction of the Muscles of Mastication

4. 4 Interface between Bone and Implant

FEA models usually assume a state of optimal osseointegration, meaning that

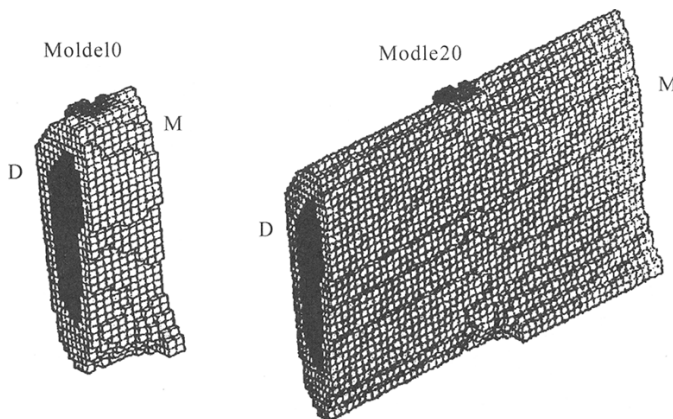


Fig. 4.6 Illustration of the Base Model of the Mandible (left) and the Longest Model (right) (Reproduced from J Oral Rehabil 1998;25:300 with permission)

cortical and trabecular bone is perfectly bonded to the implant. This does not occur exactly in clinical situation. Therefore, the imperfect contact and its effect on load transfer from implant to supporting bone need to be modelled more carefully. Current FEA programs provide several types of contact algorithms to technically conduct simulation of clinical contacts. The friction between contact surfaces can also be modelled with contact algorithms. The friction coefficients, however, have to be determined via experimentation.

Bone is a porous material with complex microstructure. The higher load bearing capacity of dense cortical bone compared to the more porous trabecular bone is generally recognised. Upon implant insertion, cortical and/or trabecular bone, starting at the periosteal and endosteal surfaces, gradually forms a partial to complete encasement around the implant. However, the degree of encasement is dependent on the stresses generated and the location of the implant in the jaw³⁷. The anterior mandible is associated with 100% cortical osseointegration and this decreases toward the posterior mandible. The least cortical osseointegration (< 25%) is seen in the posterior maxilla. The degree of osseointegration appears to be dependant on bone quality and stresses developed during healing and function. To study the influence of osseointegration in greater detail at the bone trabeculae contact to implant level, Sato, et al.⁴⁰ set up four types of stepwise assignment algorithms of elastic modulus according to the bone volume in the cubic cell (Fig 4.7 to Fig 4.8). They showed that a 300 μm element size was valid for modelling the bone-implant interface.

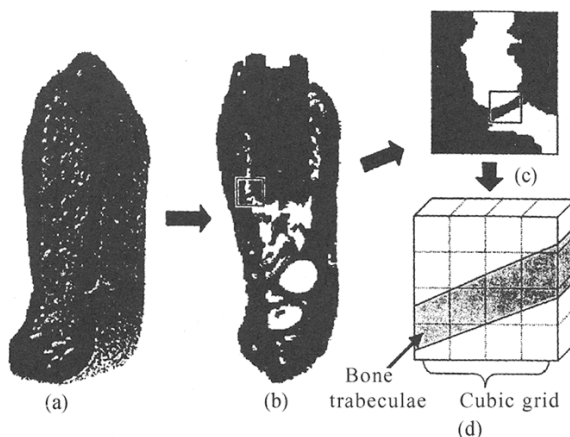


Fig. 4.7 Construction Procedure of Bone Trabecular Model (Reproduced from J Oral Rehabil 1998;26:641 with permission)

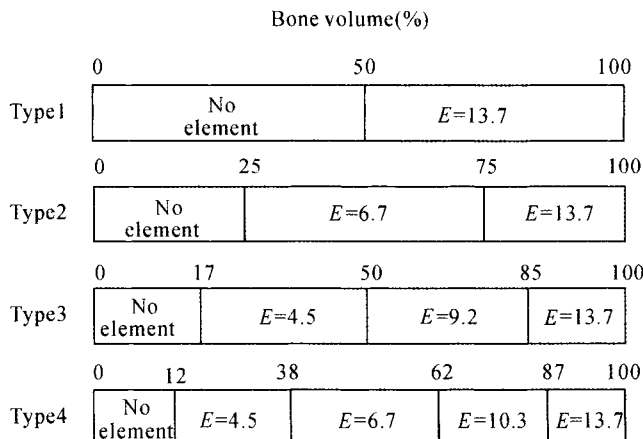


Fig. 4.8 Four Types of Stepwise Assignment Algorithms of Young's Modulus According to the Bone Volume in the Cubic Cell (E: elastic modulus, GPa) (Reproduced from J Oral Rehabil 1999;26:641 with permission)

4.5 Reliability of Dental Implant FEA

Stress distribution depends on assumptions made in modelling geometry, material properties, boundary conditions, and bone-implant interface. To obtain more accurate stress predictions, advanced digital imaging techniques can be applied in modelling more realistical bone geometry; the anisotropic and nonhomogenous nature of materials need to be considered; and boundary conditions have to be carefully

treated using computational modelling techniques. In addition, modelling of the bone-implant interface should incorporate the actual osseointegration contact area in cortical bone as well as the detailed trabecular bone contact pattern, using contact algorithms in FEA.

4.6 Conclusions

FEA has been used extensively in the prediction of biomechanical performance of dental implant systems. Assumptions made in the use of FEA in Implant Dentistry have to be taken into account when interpreting the results.

FEA is an effective computational tool that has been used to analyse dental implant biomechanics. Many optimisations of design feature have been predicted and will be applied to potential new implant systems in the future.

References

1. Weinstein AM, Klawitter JJ, Anand SC, Schuessler R (1977) Stress Analysis of Porous Rooted Dental Implants. *Implantologist* 1:104-109
2. Atmaram GH, Mohammed H (1984) Stress analysis of single-tooth implants. I. Effect of elastic parameters and geometry of implant. *Implantologist* 3:24-29
3. Atmaram GH, Mohammed H (1984) Stress analysis of single-tooth implants. II. Effect of implant root-length variation and pseudo periodontal ligament incorporation. *Implantologist* 3:58-62
4. Mohammed H, Atmaram GH, Schoen FJ (1979) Dental implant design: a critical review. *J Oral Implantol* 8:393-410
5. Borchers L, Reichart P (1983) Three-dimensional stress distribution around a dental implant at different stages of interface development. *J Dent Res* 62:155-159
6. Cook SD, Weinstein AM, Klawitter JJ (1982) A three-dimensional finite element analysis of a porous rooted Co-Cr-Mo alloy dental implant. *J Dent Res* 61:125-129
7. Meroueh KA, Watanabe F, Mentag PJ (1987) Finite element analysis of partially edentulous mandible rehabilitated with an osteointegrated cylindrical implant. *J Oral Implantol* 13:215-238
8. Williams KR, Watson CJ, Murphy WM, Scott J, Gregory M, Sinobad D (1990) Finite element analysis of fixed prostheses attached to osseointegrated implants. *Quintessence Int* 21:563-570
9. Akpinar I, Demirel F, Parnas L, Sahin S (1996) A comparison of stress and strain distribution characteristics of two different rigid implant designs for distal-extension fixed prostheses. *Quintessence Int* 27:11-17
10. Korioth TW, Versluis A (1997) Modelling the mechanical behavior of the jaws and their related structures by finite element (FE) analysis. *Crit Rev Oral Biol Med* 8:90-104

11. Van Oosterwyck H, Duyck J, Vander Sloten, van der Perre G, de Cooman M, Lievens S, Puers R, Naert I (1998) The influence of bone mechanical properties and implant fixation upon bone loading around oral implants. *Clin Oral Impl Res* 9:407-418
12. Rieger MR, Mayberry M, Brose MO (1990) Finite element analysis of six endosseous implants. *J Prosthet Dent* 63:671-676
13. Rieger MR, Adams WK, Kinzel GL (1990) Finite element survey of eleven endosseous implants. *J Prosthet Dent* 63:457-465
14. Meijer GJ, Starmans FJM, de Putter C, van Blitterswijk CA (1995) The influence of a flexible coating on the bone stress around dental implants. *J Oral Rehabil* 22:105-111
15. Sertg ZA (1997) Finite element analysis study of the effect of superstructure material on stress distribution in an implant-supported fixed prosthesis. *Int J Prosthodont* 10:19-27
16. Keyak JH, Meagher JM, Skinner HB, Mote CD (1990) Automated three-dimensional finite element modelling of bone: a new method. *J Biomed Eng* 12: 389-397
17. Cahoon P, Hannam AG (1994) Interactive modelling environment for craniofacial reconstruction. *SPIE Proceedings. Visual Data Exploration and Analysis* 2178: 206-215
18. Davy DT, Dilley GL, Krejci RF (1981) Determination of stress patterns in root-filled teeth incorporating various dowel designs. *J Dent Res* 60:1301-1310
19. Wright KWJ, Yettram AL (1979) Reactive force distributions for teeth when loaded singly and when used as fixed partial denture abutments. *J Prosthet Dent* 42:411-416
20. Farah JW, Hood JAA, Craig RG (1975) Effects of cement bases on the stresses in amalgam restorations. *J Dent Res* 54:10-15
21. Farah JW, Craig RG, Meroueh KA (1989) Finite element analysis of three- and four-unit bridges. *J Oral Rehabil* 16:603-611
22. Reinhardt RA, Pao YC, Krejci RF (1984) Periodontal ligament stresses in the initiation of occlusal traumatism. *J Periodontal Res* 19:238-246
23. MacGregor AR, Miller TP, Farah JW (1980) Stress analysis of mandibular partial dentures with bounded and free-end saddles. *J Dent* 8:27-34
24. Atmaram GH, Mohammed H (1981) Estimation of physiologic stresses with a nature tooth considering fibrous PDL structure. *J Dent Res* 60:873-877
25. Rice JC, Cowin SC, Bowman JA (1988) On the dependence of the elasticity and strength of cancellous bone on apparent density. *J Biomech* 21:155-168
26. Cook SD, Klawitter JJ, Weinstein AM (1982) A model for the implant-bone interface characteristics of porous dental implants. *J Dent Res* 61:1006-1009
27. Cowin SC (1989) Bone Mechanics. Boca Raton, Fla. CRC Press
28. Knoell AC (1977) A mathematical model of an in vivo human mandible. *J Biomech* 10:59-66
29. Maeda Y, Wood WW (1989) Finite element method simulation of bone

- resorption beneath a complete denture. *J Dent Res* 68:1370-1373
- 30. Ronald LS, Svenn EB (1995) Nonlinear contact analysis of preload in dental implant screws. *Int J Oral Maxillofac Implants* 10:295-302
 - 31. Colling EW (1984) *The Physical Metallurgy of Titanium Alloys*. Metals Park, Ohio: American Society for Metals
 - 32. Lewinstein I, Banks-Sills L, Eliasi R (1995) Finite element analysis of a new system (IL) for supporting an implant-retained cantilever prosthesis. *J Prosthet Dent* 10:355-366
 - 33. Craig RG (1989) *Restorative Dental Materials*, ed 8. St Louis: Mosby 84
 - 34. Lewis G (1994) Aparametric finite element analysis study of the stresses in an endosseous implant. *Biomed Mater Eng* 4:495-502
 - 35. Lotz JC, Gerhart YN, Hayes WC (1991) Mechanical properties of metaphyseal bone in the proximal femur. *J Biomech* 24: 317-329
 - 36. Cowin SC (1988) Strain assessment by bone cells. *Tissue Eng* 181-186
 - 37. Patra AK, dePaolo JM, d Souza KS, de Tolla D, Meenaghan MA (1998) Guidelines for analysis and redesign of dental implants. *Implant Dent* 7:355-368
 - 38. Zhou XJ, Zhao ZH, Zhao MY, Fan YB (1999) The boundary design of mandibular model by means of the three-dimensional finite element method. *West China Journal of Stomatology* 17:1-6
 - 39. Teixeira ER, Sato Y, Shindoi N (1998) A comparative evaluation of mandibular finite element models with different lengths and elements for implant biomechanics. *J Oral Rehabil* 25:299-303
 - 40. Sato Y, Teixeira ER, Tsuga K, Shindoi N (1999) The effectiveness of a new algorithm on a three-dimensional finite element model construction of bone trabeculae in implant biomechanics. *J Oral Rehabil* 26:640-643

Applications to Implant Dentistry

Jianping Geng¹, Wei Xu², Keson B. C. Tan³, Quan-Sheng Ma⁴, Haw-Ming Huang⁵, Sheng-Yang Lee⁶, Weiqi Yan⁷, Bin Deng⁸, Yong Zhao⁹

^{1,7} Clinical Research Institute, Second Affiliated Hospital, School of Medicine, Zhejiang University, Hangzhou, China

Email: jp geng2005@163.com

² School of Engineering, University of Surrey, Surrey, UK

³ Faculty of Dentistry, National University of Singapore, Singapore

⁴ Department of Implant Dentistry, Shandong Provincial Hospital, Jinan, China

⁵ Graduate Institute of Medical Materials and Engineering Taipei Medical University, Taipei, Taiwan, China

⁶ School of Dentistry, Taipei Medical University, Taipei, Taiwan, China

⁸ Department of Mechanical Engineering National University of Singapore, Singapore

⁹ School of Dentistry, Sichuan University, Chengdu, China

3. 1 Introduction

Although the precise mechanisms are not fully understood, it is clear that there is an adaptive remodelling response of surrounding bone to stresses. Implant features causing excessive high or low stresses can possibly contribute to pathologic bone resorption or bone atrophy. This chapter reviews the current applications of FEA in Implant Dentistry. Findings from FEA studies will then be discussed in relation to the bone-implant interface; the implant-prosthesis connection; and multiple implant prostheses.

3. 2 Bone-implant Interface

3. 2. 1 Introduction

Analyzing force transfer at the bone-implant interface is an essential step in the overall analysis of loading, which determines the success or failure of an implant. It

has long been recognized that both implant and bone should be stressed within a certain range for physiological homeostasis. Overload can cause bone resorption or fatigue failure of the implant whilst underload may lead to disuse atrophy and to subsequent bone loss as well¹². Using load cells in rabbit calvaria, Hassler, et al.³ showed that the target compressive stress level for maximum bone growth occurs at 1.8 MPa leveling off to a control level at 2.8 MPa. Skalak⁴ states that close apposition of bone to the titanium implant surface means that under loading, the interface moves as a unit without any relative motion and this is essential for the transmission of stress from the implant to the bone at all parts of the interface.

In centric loading, several FEA studies⁵⁻¹⁰ of osseointegrated implants demonstrated that when maximum stress concentration is located in cortical bone, it is in the contact area with the implant; and when maximum stress concentration is in trabecular bone, it occurs around the apex of the implant. In cortical bone, stress dissipation is restricted to the immediate surroundings of the implant, whereas in trabecular bone a fairly broader distant stress distribution occurs¹⁰.

3.2.2 Stress Transmission and Biomechanical Implant Design Problem

FEA can simulate the interaction phenomena between implants and the surrounding tissues. Analysis of the functional adaptation process is facilitated by accessing various loadings and implant and surrounding tissue variables. Load transfer at the bone-implant interface depends on (1) the type of loading, (2) material properties of the implant and prosthesis, (3) implant geometry-length, diameter as well as shape, (4) implant surface structure, (5) the nature of the bone-implant interface, and (6) quality and quantity of the surrounding bone. Most efforts have been directed at optimizing implant geometry to maintain the beneficial stress level in a variety of loading scenarios.

3.2.2.1 Loading

When applying FEA to dental implants, it is important to consider not only axial forces and horizontal forces (moment-causing loads), but also a combined load (oblique bite force), since these are more realistic bite directions and for a given force will cause the highest localized stress in cortical bone¹¹. Barbier, et al.¹² investigated the influence of axial and non-axial occlusal loads on the bone remodelling around IMZ implants in a dog mandible simulated with FEA. Strong correlation between the calculated stress distributions in the surrounding bone tissue and the remodelling phenomena in the comparative animal model was observed. They concluded that the highest bone remodelling events coincide with the regions of highest equivalent stress and that the major remodelling differences between axial and non-axial loading are largely determined by the horizontal stress component of the engendered stresses. The importance of avoiding or minimizing horizontal loads should be emphasized.

Zhang and Chen¹³ compared dynamic with static loading, in three-dimensional FEA models with a range of different elastic moduli for the implant. Their results showed that compared to the static load models, the dynamic load model resulted in

higher maximum stress at the bone-implant interface as well as a greater effect on stress levels when elastic modulus was varied.

In summary, both static and dynamic loading of implants have been modelled with FEA. In static load studies, it is necessary to include oblique bite forces to achieve more realistic modelling. Most studies concluded that excessive horizontal force should be avoided. The effects of dynamic loading requires further investigation.

3.2.2.2 Material Properties

Prosthesis material properties

High rigidity prostheses are recommended because the use of low elastic moduli alloys for the superstructure predicts larger stresses at the bone-implant interface on the loading side than the use of a rigid alloy with the same geometry¹⁴. Stegariou, et al.¹⁵ used three-dimensional FEA to assess stress distribution in bone, implant, and abutment when gold alloy, porcelain, or resin (acrylic or composite) was used for a 3-unit prosthesis. In almost all cases, stress at the bone-implant interface with the resin prostheses was similar to, or higher than that in the models with the other two prosthetic materials. But in his classical mechanical analysis, Skalak¹⁴ stated that the presence of a resilient element in an implant prosthesis superstructure would reduce the high load rates that occur when biting unexpectedly on a hard object. For this reason, he suggested the use of acrylic resin teeth. Nevertheless, several other studies^{16,17} could not demonstrate any significant differences in the force absorption quotient of gold, porcelain or resin prostheses.

Implant material properties

The elastic moduli of different implant materials will influence the implant-bone interface. Implant materials with too low moduli should be avoided and Malaith, et al.¹⁸ suggested implant materials with an elastic modulus of at least 110,000 N/mm². Rieger, et al.¹⁹ indicated that serrated geometry led to high-stress concentrations at the tips of the bony ingrowth and near the neck of the implant. Low moduli of elasticity strengthened these concentrations. The non-tapered screw-type geometry showed high-stress concentrations at the base of the implant when high moduli were modeled and at the neck of the implant when low moduli were modeled. The authors concluded that a tapered endosseous implant with a high elastic modulus would be the most suitable for dental implantology. However, the design must not cause high-stress concentrations at the implant neck that commonly leads to bone resorption. Stoiber²⁰ reported that in the construction of an appropriate screw implant, special attention must be paid to high rigidity of the implant, rather than to thread design.

In summary, although the effect of prosthesis material properties is still under debate, it has been well established that implant material properties can greatly affect the location of stress concentrations at the implant-bone interface.

3.2.2.3 Implant Geometry

Implant diameter and length

Large implant diameters provide for more favourable stress distributions^{18,21}. FEA has been used to show that stresses in cortical bone decrease in inverse proportion

to its increase in implant diameter with both vertical and lateral loads²¹. However, Holmgren, et al.⁵¹ showed that using the widest diameter implant is not necessarily the best choice when considering stress distribution to surrounding bone, but within certain morphological limits, an optimum dental implant size exists for decreasing the stress magnitudes at the bone-implant interface.

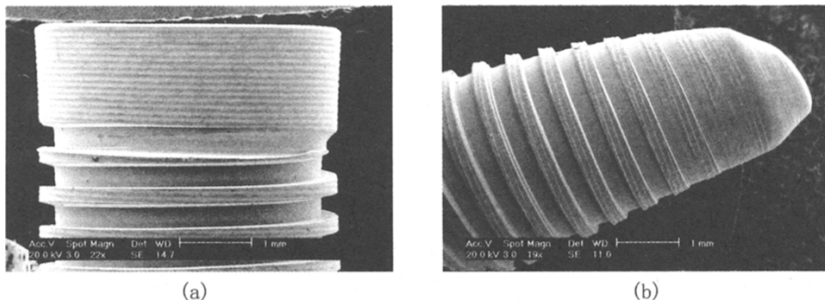


Fig. 3.1 GJP Implant Shape and Its Thread Design(By J.P. Geng)

In general, the use of short implants has not been recommended because it is believed that occlusal forces must be dissipated over a large implant area to preserve the bone. Lum²² has shown that occlusal forces are distributed primarily to the crestal bone rather than evenly throughout the entire surface area of the implant interface. Since masticatory forces are light and fleeting, these forces are normally well-tolerated by the bone. It is the bruxing forces that must be adequately attenuated, and this may be done by increasing the diameter and number of implants. A recent clinical study concluded that short implants are possible when the peri-implant tissues were in good condition²³.

In summary, the optimum length and diameter necessary for long term implantation success depends on the bone support condition. If the bone is in normal condition, length and diameter appear not to be significant factors for implant success. However, if the bone condition is poor, large diameter implants are recommended and short implants should be avoided.

Implant shape

Holmgren, et al.¹¹ report that a stepped cylindrical design for press-fit situations is most desirable from the standpoint of stress distribution to surrounding bone. Using FEA to analyse a parasagittal model digitized from a computed tomography (CT) generated patient data set, these authors simulated various single-tooth, two-dimensional osseointegrated dental implant models. The results suggested that stress is more evenly dissipated throughout the stepped cylindrical implant compared to the straight implant type. Rieger, et al.¹⁹ concluded that a tapered endosseous implant with a high elastic modulus would be the most suitable one after analysing stress concentration patterns using FEA. Also using FEA, Mailath, et al.¹⁸ compared cylindrical to conical implant shapes when exposed to physiologic stresses and examined the occurrence of stress concentrations at the site of implant entry into bone. They reported that cylindrical implants were preferable to conical shapes.

Siegele and Soltesz²⁴ compared cylindrical, conical, stepped, screw and hollow cylindrical implant shapes by means of FEA. Both a fixed bond (simulating complete load transfer with bioactive materials) and a pure contact (only compression transfer with bioinert materials) without friction between implant and bone were considered as interface conditions. The results demonstrate that different implant shapes lead to significant variations in stress distributions in the bone. The authors stated that implant surfaces with very small radii of curvature (conical) or geometric discontinuities (stepped) induced distinctly higher stresses than smoother shapes (cylindrical, screw-shaped). Moreover, a fixed bond between implant and bone in the medullary region (as may be obtained with a bioactive coating) is advantageous to the stress delivered to bone, since it produces a more uniform stress distribution than a pure contact does. Clift, et al.²⁵ reported that the modification of the standard implant design to include a flexible central post resulted in a decrease in the maximum von Mises stresses and equivalent strains in cancellous bone. It was postulated that this would reduce the likelihood of bone fatigue failure and subsequent bone resorption.

Optimum implant shape is related to the bone condition and implant material properties. Implant designs have adopted various shapes and FEA seems to indicate that for commercially pure titanium (CPTi) implants, smoother profiles engender lower stress concentrations. The optimal thread design to achieve the best load transfer characteristics is the subject of current investigations.

3.2.2.4 Implant Surface Structure

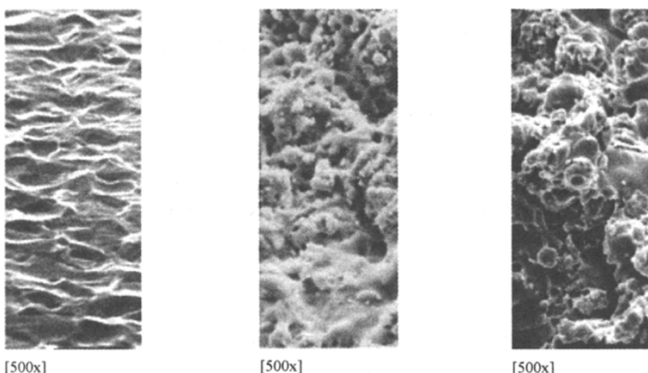


Fig. 3.2 Etched Titanium, Hydroxylapatite-coated (HA-coated) Titanium, and Titanium Plasma Spray (TPS) Surface Treatments (Steri-Oss Implant System)

Bioactive materials are used as coating on titanium implants because they have the potential to encourage bone growth up to the surface of the implant²⁶. It is claimed that these coatings can produce a fully integrated interface with direct bonding between bone and the implant material, leading to a more even transfer of load to the bone along the implant and thus a reduction in stress concentrations²⁴.

Polyactive is a system of poly (ethylene oxide) poly (butylene terephthalate)

segmented co-polymers with bone-bonding capacity. Meijer, et al.²⁷ investigated the influence of a three-layered flexible coating of Polyactive on bone stress distribution using three-dimensional FEA in a mandibular model. In the case of sagittal and transversal loading, the use of a Polyactive coating reduced both the minimum principal stress in the bone and the compressive radial stress at the bone-implant interface. However, it raised the maximum principal and the tensile radial stress. In the case of vertical loading, the application of a flexible coating reduced the compressive radial stress at the bone-implant interface around the neck of the implant by a factor of 6.6 and the tensile radial stress by a factor of 3.6. Variations in composition and thickness of the coating did not significantly affect the results.

3.2.2.5 Nature of Bone-implant Interface

There are two types of contact at the bone-implant interface: bone/implant contact and fibrous tissue/implant contact. The clinical concept of fibrous encapsulation of an implant is considered to be a failure and this condition is no longer modelled in FEA studies.

3.2.2.6 Surrounding Bone Quality and Quantity

The long-term clinical performance of a dental implant is dependent upon the preservation of good quality bone surrounding the implant and a sound interface between the bone and the biomaterial. Good quality bone itself relies on an appropriate level of bone remodelling necessary to maintain the bone density and the avoidance of bone microfracture and failure. Both processes are governed by the stress and strain distribution in the bone.

Crestal bone loss

The crestal bone region is of particular interest due to observation of progressive bone resorption (saucerization). Crestal loss is observed around various designs of dental implants. A possible cause of this loss is related to the low stresses acting on peri-implant bone. An equivalent stress of 1.6 MPa is determined to be sufficient to avoid crestal bone loss from disuse atrophy in the canine mandibular premolar region, based on both histological examination and FEA results^{28,29}.

Wiskott and Belser³⁰ studied the relationship between the stresses applied and bone homeostasis of different implant neck designs. They observed that polished necks of dental implants did not osseointegrate as do textured surfaces. Lack of osseointegration was postulated to be due to increased pressure on the osseous bed during implant placement, establishment of a physiological “biologic width”, stress shielding and lack of adequate biomechanical coupling between the load-bearing implant surface and the surrounding bone. Any viable osseous structure (including the tissue that surrounds the polished implant neck) is subjected to periodic phases of resorption and formation. Hansson³¹ compared implants with smooth necks to implants with retention elements all the way up to the crest. His FEA study found that retention elements at the implant neck resulted in major decrease in peak interfacial shear stresses. He suggests that these retention elements at the implant neck will counteract marginal bone resorption in accordance with Wolff's law.

For the Screw-Vent implant, Clelland, et al.³² showed that under axial loading,

mesial and distal stresses were much lower than those buccal and lingual to the implant. Maximum stress in the bone was lingual to the superior portion of the collar. Previous longitudinal radiographic studies of a similar implant had revealed bone loss mesial and distal to the implant. The authors conclude that the clinical significance of the stress transfer to the bone buccal and lingual to the implant has yet to be determined.

Minimum required load for avoidance of crestal bone loss appears to have been defined^{28, 29}, but the upper limit of the physiological stress range has not yet been investigated.

Cortical bone

The quality and quantity of the surrounding bone influences the load transfer from implant to bone^{8, 33}. In almost all FEA studies of titanium implants, stress concentrations occur around the implant neck. Under oblique loads with high occlusal stress magnitudes, the elastic limit of bone surrounding implants may be surpassed and lead to microfractures in the cortical bone. Clift, et al.⁸ emphasized the importance of having good quality dense bone around the implant neck which can withstand stresses in the range of 9–18 MPa prior to loading. Failure to achieve this after implantation and subsequent healing may result in local fatigue failure and resorption at the neck upon resumption of physiological loading³⁴. Holmes and Loftus³⁵ examined the influence of bone quality on the transmission of occlusal forces for endosseous dental implants using FEA. Placement of implants in bone with greater thickness of the cortical shell and greater density of the core will result in less micro-movement and reduced stress concentration, thereby increasing the likelihood of fixture stabilization and tissue integration.

Papavasiliou, et al.³⁶ showed with a three-dimensional FEA model that the absence of cortical bone increased interfacial stresses at the locations studied. Clift, et al.³⁴ reported that a reduction in the elastic modulus of the bone around the neck of the implant by a factor of 16 only produced a two-fold reduction in the peak stress.

Trabecular (cancellous) bone

Using the degree of direct bone-implant interface as an indicator of endosseous implant success appears to have been over interpreted because 100% bone apposition is almost never obtained at the surface of the endosseous dental implant. Investigating the three-dimensional bone interface to hydroxyapatite-coated titanium alloy implants, Wadamoto, et al.³⁷ generated computer graphics by the integration of data for serial ground surfaces obtained at 75 µm intervals of the tissue block involved with the implant. They found that the bone contact ratio of the whole surface of each of the three implants was 80.8%, 68.1%, and 68.8%, and that for each direction and portion varied with the conditions of implant placement. The bone volume ratios around the implant at the 0 to 300 µm zone were also calculated, and total ratios ranged from 58% to 81%. These results may provide useful quantitative information about the bone structure around implants and contribute to the development of more realistic FEA models based on the biologic bone structure

around implants.

Clelland, et al.³⁸ investigated a Steri-Oss implant in various bone models with different cancellous and cortical bone conditions using two-dimensional FEA. For the all-cancellous bone model, low stresses and high strains surrounded the implant apex. For the models with a layer of cortical bone added, higher crestal stresses and lower apical strains were observed. The thick layer(3mm) of isotropic cortical bone produced stresses at least 50% less than the thin layer(1. 5mm). The assumption of transverse isotropy (orthotropy) for cortical bone layer increased stresses and strains by approximately 25% compared with isotropic bone. They conclude that crestal cortical layer thickness and bone isotropy have a substantial impact on resultant stresses and strains.

3. 2. 3 Summary

Load transmission and resultant stress distribution is significant in determining the success or failure of an implant. Factors that influence the load transfer at the bone-implant interface include the type of loading, material properties of implant and prosthesis, length and diameter of implants, implant shape, structure of implant surface, nature of bone-implant interface, and the quality and quantity of surrounding bone. Of these biomechanical factors, implant length, diameter, and shape are easily changed. The quality and quantity of cortical and cancellous bone needs to be assessed clinically and will influence implant selection.

3. 3 Implant Prosthesis Connection

3. 3. 1 Introduction

Clinical studies have reported a significant incidence of component failure. These include gold screw failures, abutment screw failures, gold cylinder fractures, framework fractures, and implant fractures. The etiology of these failures is complex and involves cyclic fatigue, oral fluids, and varied chewing patterns and loads.

Biomechanically, the following component interfaces can be found in the Bränemark implant: (1) fixture-abutment interface; (2) abutment screw-abutment interface; (3) gold cylinder-abutment interface; (4) gold retaining screw-gold cylinder interface; (5) gold retaining screw-abutment screw interface. Long term screw joint integrity at the fixture-abutment screw joint and abutment-gold cylinder screw joint is essential for prosthetic success. An increasing number of FEA studies are focusing on biomechanical problems involving the screw joint and on screw loosening phenomena³⁹⁻⁴².

3. 3. 2 Screw Loosening Problem

3. 3. 2. 1 Introduction

The screw loosening problem frequently affects dental implants and implant-

supported prostheses. When a screw is fastened to fix a prosthesis, a tensile force (preload) is built up in the shank of the screw. This preload acts on the screw shank from the head of the screw to the threads. It should be as high as possible because it creates a clamping force between the abutment and the implant. The screw elongates when subjected to tensile forces during tightening. The more elongation there is, the better the stability of the screw in place. Thus screw design is of significance and should allow a maximum torque to be introduced on the shank of the screw⁴⁰.

Several authors³⁹⁻⁴² have drawn attention to the fact that repeated loading and unloading cycles result in alternating contact and separation of components. Clinical findings of screw loosening and failure probably result from these separation events and from elevated strains in the screw. Another mechanism of screw loosening is based on the fact that no surface is completely smooth. Because of the microroughness of component surfaces, when the screw interface is subjected to external loads, micromovements occur between the surfaces. Wear of the contact areas might result from these motions, thereby bringing the two surfaces closer to each other and cause a decrease in preload in the set of screws.

With prosthesis superstructure distortion, an external preload can be superimposed on the screw joints of the implant prosthesis. This distortion (or lack of passive fit) can impart additional axial forces and bending moments on the screw joints and increase the likelihood of prosthetic component failure⁴³.

3.3.2 Application of Preload

The load-transfer mechanism between prosthetic components arises from torque application to the abutment screw and gold screw. Sakaguchi, et al.³⁹ developed a two-dimensional FEA model for non-linear contact analysis of Bränemark implant prosthetic components. They found that when the gold retaining screw is fastened to the abutment screw, clamping force on the implant is increased at the expense of decreasing the clamping force at the abutment screw-abutment interface by 50%. Maximum tensile stresses in the screw after preload were less than 55% of the yield stress. Cheong, et al.⁴⁴ used FEA to predict that at a preload tension of 230N in the gold retaining screw shank, the clamping force at the abutment-abutment screw interface was first reduced to zero. With further tightening of the gold retaining screw, the rate of increase of stresses in it was faster than that of the abutment screw and it could be predicted that the gold retaining screw would fail first. Such failure by yielding was expected for a tensile load of around 400N applied to the gold cylinder. At this 400N tensile load, the clamping force at the fixture-abutment interface would be reduced to zero. This would affect the overall stability of the implant-prosthesis connection and eventually lead to component failure.

Because preload application to the gold retaining screw reduces the clamping force at the abutment-fixture interface, it is recommended to find a balance preload between the gold retaining screw and abutment screw to make the whole implant-prosthesis connection more stable⁴⁴. The current manufacturer recommendation for the Bränemark system is to use tightening torques of 20N · cm for titanium

abutment screws and 10N · cm for gold retaining screws.

3.3.2.3 Washer

The addition of a customized washer to dental implant screw joint systems may offer a very simple and inexpensive solution for the persistent problem of screw loosening. Versluis, et al.⁴² studied the effect of a washer in a Bränemark-type implant on the loosening conditions of the retaining screw using FEA. Their simulation indicated that a washer might significantly increase the axial tolerance of a screw against loosening up to 15 times more than a conventional system without washer. The authors state that this is accomplished by increasing the tolerance of the implant against deformation.

3.3.3 Screw Fracture

Factors that contribute to screw failure include the magnitude and direction of loading, the elastic modulus of the prosthesis and the rigidity of the abutment.

Studying the IMZ implant system with FEA, Holmes, et al.⁴⁵ found that with increases in either load magnitude or load angle, stress concentrations in components of the implant system were generally increased. In another study, Holmes, et al.⁴⁶ also showed that in the IMZ implant, stress concentrations in bone and in components were much greater under a 30-degree load than under an equal vertical load. Greater deflection and stress concentrations within the coronal retaining screw were predicted with the use of a resin polyoxymethylene (POM) intramobile element (IME) than with a titanium element in the IMZ implant system. They also found that in FEA model stress transmission to bone was not reduced when the IME was modelled in POM rather than titanium. Maximum stress concentrations occurred in the fastening screw.

Several authors^{45, 47} recommend high elastic modulus prostheses to avoid deflection of the prosthetic superstructure and stress concentrations in the retaining screw. Rigid abutment design is also needed to decrease the peak stresses in the screw and the deflection of the superstructure. Two related studies^{48, 49} described a FEA model of three different IMZ abutment designs: original threaded IME, Abutment Complete (ABC), and Intra-Mobile Connector (IMC). Progressive tightening of the retaining screw (preload) was simulated and the degree of screw tightening necessary to prevent opening of the crown-abutment interface in extreme loading (500 N occlusal load at 45 degrees) was determined individually for each system. A correlation was observed between the peak stresses in the screw and the deflection of the superstructure. Deflections and stress concentrations with the IMC were predicted to be in the same range as with the IME, but much greater than with the ABC.

3.3.4 Summary

The screw loosening problem is of concern especially when considering single tooth implant prostheses. The application of optimal preload has been the main means of preventing loosening. Moreover, a recent FEA study advocates the addition of a

washer as a simple and effective solution for the loosening problem. Stress concentration in fastening screws is influenced by load magnitude and direction. High rigid prostheses and abutments have been found to give more favorable stress distributions in screws.

3. 4 Multiple Implant Prostheses

From a biomechanical viewpoint, there are three main classes of multiple implant prostheses: (1) Implant-supported fixed prostheses (including cantilevered designs), (2) Implant-supported overdentures, and (3) Combined natural tooth and implant-supported prostheses. FEA studies for these prosthetic situations is usually more complex than for the single solitary implant. In most papers, three-dimensional FEA is considered to be necessary and two-dimensional FEA considered inadequate.

Because multiple implants are splinted by the prosthesis framework, stress distribution is more complex compared to a single tooth implant situation. Loading at one point of the prosthesis will cause stress concentrations in all supporting implants to varying degrees. Also, the prosthesis can be loaded not by a single load but by multiple loads and in varying directions. In addition, the flexure of jaw bones, particularly the mandible, under functional loading conditions can cause stress in the bone around the implants and may lead to bone resorption. Stress around the implant can be caused not only by local deformation of the bone due to movement of the implant and interface relative to the surrounding bone, but also by the complex deformation patterns of the mandible.

3. 4. 1 Implant-supported Fixed Prostheses

For implant-supported fixed prostheses, factors affecting bone-implant stress distribution and the ultimate success of prosthesis, include implant inclination, implant number and position, prosthesis splinting scheme, occlusal surface and framework materials properties, and different cross-sectional beam shapes.

Canay, et al.⁵⁰ compared vertically orientated to angled implants and found that inclination of implants greatly influences stress concentrations around the implant-supported fixed prostheses. They found no measurable differences in stress values and contours when a horizontal load was applied to the vertical and angled implants. However, with vertical loading, compressive stress values were five times higher around the cervical region of the angled implant than around the same area in the vertical implant.

Many clinicians are of opinion that the selection of implant positions and the scheme of prosthesis splinting are critical for the longevity and stability of an implant prosthesis. Kregzde⁵¹ reported that induced stresses in bone are sensitive to the scheme of prosthesis splinting and implant positions. He used three-dimensional FEA modelling of jaw bones, teeth and various implant numbers, positions and prosthesis designs to attempt optimisation of stress distribution to the implants.

The induced stresses on implants for different schemes of prosthesis splinting and different implant positions varied as much as 1,000%.

The effect of different cross-sectional beam configuration for implant frameworks has also been investigated using FEA. Korioth and Johann⁵² compared superstructures with different cross-sectional shapes and material properties during a simulated, complex biting task that modeled the deformation patterns of mandible during function. When they submitted their model to loads mimicking simultaneous bending and torsion of the mandibular corpus during a bilateral posterior bite, they found that predicted implant stresses varied significantly between implant sites for different superstructure shapes. The lowest principal stresses were obtained with a vertically orientated rectangular-shaped beam superstructure and contrary to expectations, the ideal “I-beam” superstructure cross section did not yield the lowest stresses. These authors concluded that implant abutment stresses were significantly affected by the cross-sectional shape of the prosthetic superstructure and by diverse mandibular loading conditions.

Implant-supported fixed prostheses with cantilevers add additional factors that can influence stress distribution. These factors include cantilever length, cross-sectional beam shapes and recently, a system for additional support to the distal extension of the cantilever. Young, et al.⁵³ investigated a number of different cross-sectional beam shapes for cantilever fixed prostheses for initiation of permanent deformation at end loading. Straight and curved cantilever beams of 26 mm long were modeled in FEA. They found that a “L” shaped design was more rigid than other designs for a given mass, while an open “I” section framework offered good possibilities particularly when used as curved shapes. “L” shaped cobalt-chromium or stainless steel frameworks of 26 mm cantilever span underwent permanent deformation at end loadings between 130 and 140 N depending on section curvature. They caution that a good framework design is critical to avoid failures since it is known that biting loads can exceed these values.

Different material properties affect stress distribution in different ways. Korioth and Johann⁵² showed that an increase in elastic modulus of prosthetic materials does not necessarily lead to a decrease in stresses on all existing implant abutments. Less rigid superstructures seemed to increase implant abutment stresses overall as well as to decrease tensile stresses on the most anterior implant abutments in the modeled complex biting task.

Using a six implant-supported mandibular complete arch fixed prosthesis three-dimensional FEA model, Sertgöz investigated the effect of different occlusal surface materials (resin, resin composite, and porcelain) and different framework materials (gold, silver-palladium, cobalt-chromium, and titanium alloys) on stress distribution in the fixed prosthesis and surrounding bone. He demonstrated that using a prosthesis superstructure material with lower elastic modulus did not lead to substantial differences in stress patterns or levels in the cortical and cancellous bone surrounding the implants. For a single loading condition investigated, the optimal combination of materials was cobalt-chromium for the framework and porcelain for

the occlusal surface.

Sertgöz and Guvener⁵⁴, with a three-dimensional FEA model of a bilateral distal cantilever fixed prosthesis supported by six implants in the mandible, predicted that maximum stresses occurred at the most distal bone-implant interface on the loaded side and this significantly increased with increase in cantilever length. Nevertheless, they found no significant change in stress levels associated with implant length variation. However, Lindquist, et al.⁵⁵ in a 15-year longitudinal clinical follow-up study, reported that bone at the distal implants of cantilevered mandibular implant-supported prostheses remained very stable and conversely, more bone loss was observed around the anterior implants. However, this may be caused by a multitude of clinical factors. It was concluded that occlusal loading factors such as maximal bite force, tooth clenching and cantilever length were of minor importance to bone loss in their study population. This suggests that extrapolation of FEA studies to clinical situations should be approached with caution.

New systems for additional support to the distal extensions of cantilevered prostheses have been suggested. IL system uses a short implant and a special ball-type attachment to support the distal extension of cantilevered prostheses. Lewinstein, et al.³² compared this new support system to a conventional cantilever prosthesis using two-dimensional FEA. This system dramatically lowered the stresses in bone, cantilever, and implants potentially reducing failures within the implants, prostheses, and surrounding bone. Moreover, employment of a relatively long-span prosthetic extension in the posterior region of the jaw would be possible.

In summary, stress distribution in implant-supported fixed prostheses have been shown by FEA to be influenced by the factors of implant inclination, implant number and positions, prosthetic splinting scheme, superstructure material properties and beam design.

3.4.2 Implant-supported Overdentures

The use of implant-supported overdentures is viewed as a cost-effective treatment modality. Some clinicians are of the opinion that the designed stress-breaking features of overdenture attachments confer more favourable biomechanical characteristics compared to implant-supported fixed prostheses. Implant-supported overdenture attachment systems include bar-clips, balls, O-rings and magnets. For bar-clip attachment systems, some biomechanical factors identified are the number of implants, bar length, stiffener height, and material properties.

Meijer, et al.⁵⁶ set up a three-dimensional model of a human mandible with two endosseous implants in the interforaminal region and compared stress distribution when the two implants were connected by a bar or remained solitary. The most extreme principal stress was found with oblique bite loads whereas vertical bite loads resulted in the lowest stress. The most extreme principal stresses in bone were always located around the necks of the implants. No significant differences in stress distribution were predicted with the highest maximum and lowest minimum principal stresses being 7.4-and-16.2 MPa in the model without the bar and 6.5-and-

16.5 MPa with the bar. It was also found that a bar placed anteriorly of the interconnecting line between the two implants caused extremely large compressive and tensile stress concentrations in the bone around the implants. Therefore, in those cases, it is advised not to connect the implants or, if a bar-clip attachment is preferred, to place additional implants in the frontal region⁵⁷. In a further study, Meijer, et al.⁵⁸ used the same model to study a four implant system with the implants either connected by a bar or remaining solitary. Their results showed that with uniform loading, there were more or less equal extreme principal stresses around the central and lateral implants. With non-uniformly loading on the superstructures, the implant nearest to the load showed the highest stress concentration and with connected implants there was a reduction in the magnitude of the extreme principal stresses compared to solitary implants.

FEA modelling of a two implants round bar⁵⁹ and Hader bar system⁶⁰ as well as a four implant Hader bar system⁶¹ found span length and stiffener height to be more critical factors in the adequacy of the overall design as compared with changing material properties in the range of alloy stiffness tested.

Overdentures supported by two implants ball system have achieved better stress distribution in bone compared to a two implants bar system. Menicucci, et al.⁶² used three-dimensional FEA to evaluate transmission of masticatory load in mandibular implant-retained overdentures. Overdentures retained either by two ball attachments or by two clips on a bar connecting two implants were compared. For the ball attachment system, a 35 N load on the first mandibular molar of the overdenture induced a greater reaction force on the distal edentulous ridge mucosa of the nonworking side compared to the bar-clip attachment. However, when peri-implant bone stress was considered, this was greater with the bar-clip attachment than with the ball attachment.

In summary, FEA has been used to investigate the stress distribution obtained when implants were left solitary, used with ball attachments or connected by bars for clip retention in various configurations and designs. Not all studies modelled the overdenture over the implants and bar superstructure. Bar design factors like stiffener height and span length were found to significantly affect stress distribution whereas the influence of various material moduli was comparatively less significant.

3.4.3 Combined Natural Tooth and Implant-supported Prostheses

Combining natural teeth and implants to support fixed prostheses has been advocated by certain quarters in implant dentistry. Controversy exists as to the advisability of this design philosophy from a biomechanical as well as a clinical perspective. A significant clinical consideration in the restoration of partial edentulism with implant and tooth-supported prostheses is whether implants and natural teeth abutments should be splinted, and if so, in what manner. There is a differential deflection between the viscoelastic intrusion of a natural tooth in its periodontal ligament and the almost negligible elastic deformation of an osseointegrated implant. This difference may induce a fulcrum-like effect and

possibly overstress the implant or surrounding bone. The biomechanical factors that can influence the stress distribution include abutment design, implant material properties, effect of resilient elements, connector design (precision or semi-precision attachments), and degree of splinting implants to natural tooth abutments.

For the implant connected with a natural tooth situation, van Rossem, et al.⁶³ concluded that a more uniform stress was obtained around implants with stress-absorbing elements of low elastic modulus. It was also concluded that the bone surrounding the natural tooth showed a decrease in peak stresses in such a situation.

Charkawi, et al.⁶⁴ studied the use of a resilient layer material under the superstructure of the implant in a connected tooth and implant supported prosthesis model. Their FEA results proposed that this new modification could mimic the structural natural tooth unit by allowing movement of the superstructure without movement of the implant when loaded.

However, Misch and Ismail⁶⁵ conducted a three-dimensional FEA comparing models representing a natural tooth and an integrated implant connected by rigid and non-rigid connectors. Based on similarities in stress contour patterns and the stress values generated in both models, they concluded that advocating a non-rigid connection because of a biomechanical advantage may be erroneous. Melo, et al.⁶⁶ also investigated tooth and implant-supported prostheses in free-end partially edentulous cases. Their two-dimensional FEA predicted that lowest levels of stresses in bone occurred when the prosthesis was not connected to a natural abutment tooth but was supported instead by two free-standing implant abutments. Non-rigid attachments, when incorporated into a prosthesis, did not significantly reduce the level of stresses in bone. A recent comprehensive review of both clinical and laboratory studies concluded that the issue of connecting natural teeth to implants with rigid or non-rigid connectors still remains unresolved⁶⁷.

3.5 Conclusions

FEA has been used extensively in the prediction of biomechanical performance of dental implant systems. This chapter has reviewed the use of FEA in relation to the bone-implant interface, the implant-prosthesis connection, and multiple implant prostheses.

Load transmission and resultant stress distribution at the bone-implant interface has been the subject of FEA studies. Factors that influence load transfer at the bone-implant interface include the type of loading, implant and prosthesis material properties, the length and diameter of implants, implant shape, the structure of implant surface, nature of bone-implant interface, and the quality and quantity of surrounding bone. Of these biomechanical factors, implant length, diameter, and shape are easily modified in the implant design. Cortical and cancellous bone quality and quantity needs to be assessed clinically and can influence implant selection.

Stress distribution in the implant-prosthesis connection has been examined by

FEA studies because of the incidence of clinical problems such as gold screw failures, abutment screw failures, and implant fracture. Design changes to avoid or reduce these prosthetic failures by improving the stress distribution of implant components have been suggested.

When applied to multiple implant prosthesis design, FEA has suggested improved biomechanical situations when factors such as implant inclination, implant positions, prosthetic material properties, superstructure beam design, cantilever lengths, bar system, bar span length and stiffener height, and overdenture attachment type were optimised. For combined natural tooth and implant supported prostheses, FEA studies were inconclusive whether to use a rigid or resilient implant systems.

FEA is an effective computational tool that has been applied from the engineering arena to dental implant biomechanics. Many design feature optimisations have been predicted and will be applied to potential new implant systems in the future.

References

1. Pilliar RM, Deporter DA, Watson PA, Valiquette N (1991) Dental implant design-effect on bone remodelling. *J Biomed Mater Res* 25:467-483
2. Vaillancourt H, Pilliar RM, McCammond D (1996) Factors affecting crestal bone loss with dental implants partially covered with a porous coating: a finite element analysis. *Int J Oral Maxillofac Implants* 11:351-359
3. Hassler CR, Rybicki EF, Cummings KD, Clark LC (1977) Quantitation of compressive stresses and its effects on bone remodelling. *Bull Hosp Bone Joint Res* 38:90-93
4. Skalak R (1983) Biomechanical considerations in osseointegrated prostheses. *J Prosthet Dent* 40:6
5. Ma XX, Li T (1998) Single implant prosthesis. In: Geng Jianping (Ed). Newly-developed Technology of Prosthetic Dentistry in China in 1990s. Chengdu: Sichuan Science and Technology Publishing House 1-20
6. Siegle D, Soltesz U (1986) Implantaten mit intramobilen Emsatzen als Brückenpfeiler-ein Vergleich der im Knochen erzeugten Spanungs Verhältnisse. *Z Zahnartzl Implantol* 11:117-124
7. Richter EJ (1986) Belastung von Implantaten-Theoretische Grundlagen. *Z Zahnartzl Implantol* 11:181-98
8. Clift SE, Fisher J, Watson CJ (1992) Finite element stress and strain analysis of the bone surrounding a dental implant: effect of variations in bone modulus. *Proc Instn Mech Engrs* 206:139-147
9. Geng JP, Liu HC (1999) Exceptional Prosthodontics. Hong Kong, China: Hong Kong Tranfor Publishing Co., Limited 60-76
10. A Natali N, Meroi EA (1996) Biomechanical analysis of dental implant in the

- interaction phenomena with cortical and trabecular bone tissue. Proc 10th Conference of ESB, Leuven 34
11. Holmgren EP, Seckinger RJ, Kilgren LM, Mante F (1998) Evaluating parameters of osseointegrated dental implants using finite element analysis-a two-dimensional comparative study examining the effects of implant diameter, implant shape, and load direction. *J Oral Implantol* 24:80-88
 12. Barbier L, Vander Sloten J, Krzesinski G, Schepers E, van der Perre G (1998) Finite element analysis of non- axial versus axial loading of oral implants in the mandible of the dog. *J Oral Rehabil* 25:847-858
 13. Zhang JK, Chen ZQ (1998) The study of effects of changes of the elastic modulus of the materials substitute to human hard tissues on the mechanical state in the implant-bone interface by three-dimensional anisotropic finite element analysis. *West China Journal of Stomatology* 16:274-278
 14. Benzing UR, Gall H, Weber H (1995) Biomechanical aspects of two different implant-prosthetic concepts for edentulous maxillae. *Int J Oral Maxillofac Implants* 10:188-198
 15. Stegaroiu R, Kusakari H, Nishiyama S, Miyakawa O (1998) Influence of prosthesis material on stress distribution in bone and implant: a 3-dimensional finite element analysis. *Int J Oral Maxillofac Implants* 13:781-790
 16. Hobkirk JA, Psarros KJ (1992) The influence of occlusal surface material on peak masticatory forces using osseointegrated implant-supported prostheses. *Int J Oral Maxillofac Implants* 7:354-362
 17. Cibirka RM (1992) Determining the force absorption on quotient for restorative materials in implant occlusal surfaces. *J Prosthet Dent* 67:361-364
 18. Mailath G, Stoiber B, Watzek G, Matejka M (1989) Bone resorption at the entry of osseointegrated implants-a biomechanical phenomenon. Finite element study. *Z Stomatol* 86:207-216
 19. Rieger MR, Fareed K, Adams WK, Tanquist RA (1989) Bone stress distribution for three endosseous implants. *J Prosthet Dent* 61: 223-238
 20. Stoiber B (1988) Biomechanical principles of endosseous screw implants. *Wien Klin Wochenschr* 100:522-524
 21. Matsushita Y, Kitoh M, Mizuta K, Ikeda H, Suetsugu T (1990) Two-dimensional FEA analysis of hydroxyapatite implants: diameter effects on stress distribution. *J Oral Implantol* 16:6-11
 22. Lum LB (1991) A biomechanical rationale for the use of short implants. *J Oral Implantol* 17:126-131
 23. Stellingsma C, Meijer HJ, Raghoebar GM (2000) Use of short endosseous implants and an overdenture in the extremely resorbed mandible: a five-year retrospective study. *J Oral Maxillofac Surg* 58:382-388
 24. Siegle D, Soltesz U (1989) Numerical investigations of the influence of implant shape on stress distribution in the jaw bone. *Int J Oral Maxillofac Implants* 4: 333-340
 25. Clift SE, Fisher J, Edwards BN (1995) Comparative analysis of bone stresses

- and strains in the Intoss dental implant with and without a flexible internal post. *Proc Inst Mech Eng[H]* 209:139-147
- 26. Oonishi H (1990) Mechanical and chemical bonding of artificial joints. *Clin Mater* 5:217-233
 - 27. Meijer GJ, Starmans FJ, de Putter C, van Blitterswijk CA (1995) The influence of a flexible coating on the bone stress around dental implants. *J Oral Rehabil* 22: 105-111
 - 28. Vaillancourt H, Pilliar RM, McCammond D (1995) Finite element analysis of crestal bone loss around porous-coated dental implants. *J Appl Biomater* 6: 267-282
 - 29. Vaillancourt H, Pilliar RM, McCammond D (1996) Factors affecting crestal bone loss with dental implants partially covered with a porous coating: a finite element analysis. *Int J Oral Maxillofac Implants* 11:351-359
 - 30. Wiskott HW, Belser UC (1999) Lack of integration of smooth titanium surfaces: a working hypothesis based on strains generated in the surrounding bone. *Clin Oral Implants Res* 10:429-444
 - 31. Hansson S (1999) The implant neck: smooth or provided with retention elements. A biomechanical approach. *Clin Oral Impl Res* 10:394-405
 - 32. Clelland NL, Ismail YH, Zaki HS, Pipko D (1991) Three-dimensional finite element stress analysis in and around the Screw-vent implant. *Int J Oral Maxillofac Implants* 6:391-398
 - 33. Lum LB, Osier JF (1992) Load transfer from endosteal implants to supporting bone: an analysis using statics. Part one: Horizontal loading. *J Oral Implantology* 18:343-348
 - 34. Clift SE, Fisher J, Watson CJ (1992) Finite element stress and strain analysis of the bone surrounding a dental implant: effect of variations in bone modulus. *Proc Inst Mech Eng [H]* 206:233-241
 - 35. Holmes DC, Loftus JT (1997) Influence of bone quality on stress distribution for endosseous implants. *J Oral Implantol*, 23:104-111
 - 36. Papavasiliou G, Kamposiora P, Bayne SC, Felton DA (1996) Three-dimensional finite element analysis of stress-distribution around single tooth implants as a function of bony support, prosthesis type, and loading during function. *J Prosthet Dent* 76:633-640
 - 37. Wadamoto M, Akagawa Y, Sato Y, Kubo T (1996) The three-dimensional bone interface of an osseointegrated implant. I: A morphometric evaluation in initial healing. *J Prosthet Dent* 76:170-175
 - 38. Clelland NL, Lee JK, Bimbenet OC, Gilat A (1993) Use of an axisymmetric finite element method to compare maxillary bone variables for a loaded implant. *J Prosthodont* 2:183-189
 - 39. Sakaguchi RL, Borgersen SE (1993) Nonlinear finite element contact analysis of dental implant components. *Int J Oral Maxillofac Implants* 8: 655-661
 - 40. Jorneus L, Jemt T, Carlsson L (1992) Loads and designs of screw joints for single crown supported by osseointegrated implants. *Int J Oral Maxillofac*

Implants 7:353-359

41. Haack JE, Sakaguchi RL, Sun T, Coffey JP (1994) Determination of preload stress in dental implant screws (abstract 808). *J Dent Res* 73(special issue):202
42. Versluis A, Korieth TW, Cardoso AC (1999) Numerical analysis of a dental implant system preloaded with a washer. *Int J Oral Maxillofac Implants* 14:337-341
43. Tan KBC (1995) The Clinical Significance of Distortion in Implant Prosthodontics, "Is there such a thing as Passive Fit?" *Ann Acad Med Singapore* 24:138-157
44. Cheong WM, Tan KBC, Teoh SH, Tan JS (2000) FEA of the Nobel Biocare Standard Abutment during Preload and Applied Axial Loads. *J Dent Res* 77(5): 1329
45. Holmes DC, Haganman CR, Aquilino SA (1994) Deflection of superstructure and stress concentrations in the IMZ implant system. *Int J Prosthodont* 7:239-246
46. Holmes DC, Grigsby WR, Goel VK, Keller JC (1992) Comparison of stress transmission in the IMZ implant system with polyoxymethylene or titanium intramobile element: a finite element stress analysis. *Int J Oral Maxillofac Implants* 7: 450-458
47. Papavasiliou G, Tripodakis AP, Kamposiora P, Strub JR, Bayne SC (1996) Finite element analysis of ceramic abutment restoration combinations for osseointegrated implants. *Int J Prosthodont* 9: 254-260
48. Holmes DC, Haganman CR, Aquilino SA, Diaz-Arnold AM, Stanford CM (1997) Finite element stress analysis of IMZ abutment designs: development of a model. *J Prosthodont* 6:31-36
49. Haganman CR, Holmes DC, Aquilino SA, Diaz-Arnold AM, Stanford CM (1997) Deflection and stress distribution in three different IMZ abutment designs. *J Prosthodont* 6:110-121
50. Canay S, Hersek N, Akpinar I, Asik Z (1996) Comparison of stress distribution around vertical and angled implants with finite-element analysis. *Quintessence Int* 27: 591-598
51. Kregzde M (1994) A method of selecting the best implant prosthesis design option using three-dimensional finite element analysis. *Int J Oral Maxillofac Implants* 8:662-673
52. Korieth TW, Johann AR (1999) Influence of mandibular superstructure shape on implant stresses during simulated posterior biting. *J Prosthet Dent* 82:67-72
53. Young FA, Williams KR, Draughn R, Strohauer (1998) Design of prosthetic cantilever bridgework supported by osseointegrated implants using the finite element method. *Dent Mater* 14:37-43
54. Sertg ZA, Gvener S (1996) Finite element analysis of the effect of cantilever and implant length on stress distribution in an implant-supported fixed prosthesis. *J Prosthet Dent* 76:165-169
55. Lindquist LW, Carlsson GE, Jemt T (1996) A prospective 15-year follow-up study of mandibular fixed prostheses supported by osseointegrated implants: Clinical results and marginal bone loss. *Clin Oral Impl Res* 7:329-336

56. Meijer HJ, Starmans FJ, Steen WH, Bosman F (1993) A three-dimensional, finite-element analysis of bone around dental implants in an edentulous human mandible. *Arch Oral Biol* 38:491-496
57. Meijer HJ, Starmans FJ, Steen WH, Bosman F (1994) Location of implants in the interforaminal region of the mandible and the consequences for the design of the superstructure. *J Oral Rehabil* 21:47-56
58. Meijer HJ, Starmans FJ, Steen WH, Bosman F (1996) Loading conditions of endosseous implants in an edentulous human mandible: a three-dimensional, finite-element study. *J Oral Rehabil* 23:757-763
59. Bidez MW, Chen Y, McLoughlin SW, English CE (1992) Finite element analysis (FEA) studies in 2.5-mm round bar design: the effects of bar length and material composition on bar failure. *J Oral Implantol* 18:122-8
60. Bidez MW, McLoughlin SW, Chen Y, English CE (1993) Finite element analysis of two-abutment Hader bar designs. *Implant Dent* 2:107-114
61. Bidez MW, Chen Y, McLoughlin SW, English CE (1993) Finite element analysis of four-abutment Hader bar designs. *Implant Dent* 2:171-176
62. Menicucci G, Lorenzetti M, Pera P, Preti G (1998) Mandibular implant-retained overdenture: finite element analysis of two anchorage systems. *Int J Oral Maxillofac Implants* 13:369-376
63. Van Rossen IP, Braak LH, de Putter C, de Groot K (1990) Stress-absorbing elements in dental implants. *J Prosthet Dent* 64:198-205
64. El Charkawi HG, el Wakad MT, Naser ME (1990) Modification of osseointegrated implants for distal extension prostheses. *J Prosthet Dent* 64:469-472
65. Misch CM, Ismail YH (1993) Finite element stress analysis of tooth-to-implant fixed partial denture designs. *J Prosthodont* 2:83-92
66. Melo C, Matsushita Y, Koyano K, Hirowatari H, Suetsugu T (1995) Comparative stress analyses of fixed free-end osseointegrated prostheses using the finite element method. *J Oral Implantol* 21:290-294
67. Gross M, Laufer BZ (1997) Splinting osseointegrated implants and natural teeth in rehabilitation of partially edentulous patients. Part I: laboratory and clinical studies. *J Oral Rehabil* 24:863-870

Finite Element Method

N. Krishnamurthy

Consultant, Structures, Safety, and Computer Applications, Singapore
Email: vacnk@yahoo.com

1. 1 Introduction

The finite element method may be applied to all kinds of materials in many kinds of situations: solids, fluids, gases, and combinations thereof; static or dynamic, and, elastic, inelastic, or plastic behaviour. In this book, however, we shall restrict the treatment to the deformation and stress analysis of solids, with particular reference to dental implants.

1. 2 Historical Development

Deformation and stress analysis involves the formulation of force-displacement relationships. These have been used in increasingly sophisticated forms from the 1660s, when Robert Hooke came out with his Law of the Proportionality of Force and Displacement.

The nineteenth and twentieth centuries saw a lot of applications of the force-displacement relationships for the analysis and design of large and complex structures, by manual methods using logarithmic tables, slide rules, and in due course, manually and electrically operated calculators.

Particular mention must be made of the contributions of the following scientists, relevant to modern structural analysis:

1857: Clapeyron Theorem of Three Moments

1864: Maxwell Law of Reciprocal Deflections

1873: Castiglano Theorem of Least Work

1914: Bendixen Slope-deflection Method

References for these works and others to follow are given at the end of the chapter.

These and other early methods and applications to articulated (stick-type)

structures were based on formulas developed from structural mechanics principles, applied to straight, prismatic members such as axial force bars, beams, torsion rods, etc.

All these techniques yielded simultaneous equations relating components of forces and displacements at the joints of the structure. The number of simultaneous equations that could be solved by hand (between 10 and 15) set a practical limit to the size of the structure that could be analysed.

To avoid the direct solution of too many simultaneous equations, successive approximation methods were developed. Among them should be cited the following:

1932: Cross Moment Distribution Method

1940: von Karman and Biot Finite Difference Methods for Field Problems

1942: Newmark Finite Difference Methods for Structural Problems

1946: Southwell Relaxation Methods for Field Problems

These expanded the size limitations outwards by many orders of magnitude, enabling large complex articulated as well as plate-type structures to be analysed and designed.

The appearance of commercial digital computers in the 1940s revolutionised structural analysis. The simultaneous equations were not an obstacle any more. Solutions became even more efficient when the data and processing were organised in matrix form. Thus was matrix analysis of structures born.

It was the aeronautical industry that exploited this new tool to best advantage, but structural designers were quick to follow their lead. By the 1960s, not only could better and bigger aircraft be manufactured, but large bridges and buildings of unconventional design could be built.

This also resulted in the computerised revival of the somewhat abandoned earlier methods of consistent deformation and slope deflection. Not only could much larger problems be handled, but also effects formerly neglected as secondary (out of computational necessity) could be included. Pioneers in matrix computer analysis were:

1958: Argyris-Matrix Force or Flexibility Method

1959: Morice-Matrix Displacement or Stiffness Method

From matrix analysis of articulated structures to finite element analysis of continuous systems, it was a big leap, inspired and spurred on by the digital computer. However, it was not as if the entire idea was new.

Actually, the history of the Finite Element Method is the history of discretisation, the technique of dividing up a continuous region into a number of simple shapes. The progress from conceptualisation and formalisation, to implementation and application, may be summarised as follows:

1774: Concepts of Discretisation of Continua (Euler)

1864: Framework Analysis (Maxwell)

1875: Virtual Work Methods for Force-displacement Relationships (Castigliano)

1906: Lattice Analogy for Stress Analysis (Wieghardt)

1915: Stiffness Formulation of Framework Analysis (Maney)

- 1915: Series Solution for Rods and Plates (Galerkin)
- 1932: Moment Distribution Method for Frames (Hardy Cross)
- 1940: Relaxation (Finite Difference) Methods (Southwell)
- 1941: Framework Method for Elasticity Problems (Hrenikoff)
- 1942: Finite Difference Methods for Beams and Columns (Newmark)
- 1943: Concept of Discretisation of Continua with Triangular Elements (Courant)
- 1943: Lattice Analogy for Plane Stress Problems (McHenry)
- 1953: Computerisation of Matrix Structural Analysis (Levy)
- 1954: Matrix Formulation of Structural Problems (Argyris)
- 1956: Triangular Element for Finite Element Plane Stress Analysis (Turner, et al.)
- 1960: Computerisation of Finite Element Method (Clough)
- 1964: Matrix Methods of Structural Analysis (Livesley)
- 1963: Mathematical Formalisation of the Finite Element Method (Melosh)
- 1965: Plane Stress and Strain, and Axi-symmetric Finite Element Program (Wilson)
- 1967: Finite Element Method in Structural and Continuum Mechanics (Zienkiewicz)
- 1972: Finite Element Applications to Nonlinear Problems (Oden)

Old theories of solid continua were reexamined. Up to the 1950s, only continuous uniform regions of some regular shape such as square and circular plates or prisms could be analysed with closed form solutions. Some extensions were made by conformal mapping techniques. Series and finite difference solutions were developed for certain broader class of problems. But all these remained in the domain of academic pursuit of theoretical advancement, with few general applications and limited practical use.

Again, it was the aircraft industry that pioneered the idea of analysing a region as the assemblage of a number of triangular elements. The force-displacement relationships for each element were formulated on the basis of assumed displacement functions. The governing equations resulted after approximately assembly modelled the behaviour of the entire region. Once the equations were formulated, further solution followed the same steps as the matrix structural analysis.

The idea worked, and very efficiently with computers. It was also confirmed that the finer the division, the better the results. Now the aircraft designers could consider not only the airframe, but the fuselage that covered it and the bulkheads that stiffened it, as a single system of stress bearing components, resisting applied forces as an integrated unit.

This technique came to be called the “Finite Element Method” (“FEM” for short), both because a region could be only broken up into a finite number of elements, and because many of the ideas were extrapolated from an infinitesimal element of the theory to a finite sized element of practical dimensions.

Clough and his associates brought this new technique into the civil engineering profession, and soon engineers used it for better bridges and stronger shells.

Mechanical engineers exploited it for understanding component behaviour and designing new devices.

Computer programs were developed all over the Western world and Japan. The first widely accepted program was "SAP" (for Structural Analysis Package) by E.L. Wilson, which got him a Ph.D. from the University of California, USA. Most programs were in FORTRAN, the only suitable language at the time. Soon there was a veritable explosion in programs, and today, there are scores of packages in recent languages which are menu-driven and automated to the extent that with minimal (self-)training, anybody can do a finite element analysis for better or for worse!

Purists viewed the early applications with considerable reservation, pointing out the lack of mathematical rigour behind the technique. Appropriate responses were not slow in coming. Melosh and others soon connected the assumptions behind the formulation of the element with the already prevalent classical methods of interpolation functions.

Argyris in Europe, Zienkiewicz in UK, and Clough, Wilson, Oden, and numerous others in USA, pushed the frontiers of finite element knowledge and applications fast and wide. Between the 1950s and 1970s, applications of the finite element method grew enormously in variety and size, supported or triggered by fantastic developments in digital computer technology. In the last two decades, new developments have not been so many, but practical applications have become wider, easier, and more sophisticated.

Early users, the author included, considered hundred elements as a boon. A decade later, third generation computers enabled analysts to routinely use thousands of elements. By the 1970s, capacity and speed had increased ten times further. Nothing seemed to be beyond reach of finite element analysis whether it be a nuclear reactor (Fig. 1.1(a),(b),(c)), or a tooth (Fig. 1.1(d))), both of which the author has analysed.

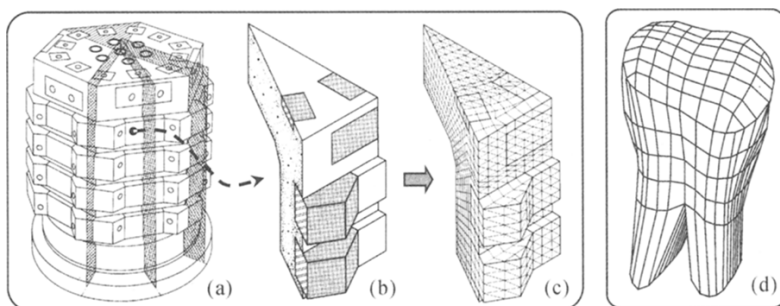


Fig. 1.1 (a) Test Model of Prestressed Concrete Nuclear Reactor; (b) One-twelfth Symmetry Segment for Analysis; (c) 3-D Finite Element Idealisation of the Analysis Segment; (d) 3-D Finite Element Idealisation of a Tooth

Now, computer packages which once demanded a mainframe have come to the desk top, and been loaded with powerful program graphics user interfaces, and interactive, online modelling and solutions.

It was just a small imaginative step to extend the applications beyond linear structural analysis, to non-linear and plastic behaviour, to fluids and gases, to dynamics and stability, to thermal and other field problems, because all of them involved the same kind of differential equations, differing only in parameters and properties, while the overall formulation, assembly, and solution techniques remained the same.

The references of historical importance, given at the end of the chapter, are merely representative, often the earliest in a series of many publications on a topic by the same or other authors. More detailed coverage of the history and further references may be found in the works by Cook, Desai, Gallagher, Huebner, Oden, Przemieniecki, and Zienkiewicz. Readers can refer to these resources for additional information on any of the topics discussed by the author in the following chapters.

Today, there is almost no field of engineering, no subject where any aspect of mechanics is involved, in which the finite element method has not made and is not continuing to make significant contributions to knowledge, leading to unprecedented advances in state of the art and its ultimate usefulness to mankind including contributions to dentistry.

1.3 Definitions and Terminology

The basic procedure for matrix analysis depends on the determination of relationships between the “Actions”, namely forces, moments, torques, etc. acting on the body, and the corresponding “Displacements”, namely deflections, rotations, twists, etc. of the body.

A “structure” is conventionally taken to consist of an assembly of straight “members” (as in trusses, frames, etc.) or curved lines whose shape can be mathematically evaluated, which are connected, supported, and loaded at their ends, called “joints”. Fig 1.2(a) shows a two-storey structure consisting of frames in the vertical plane, grids in the horizontal plane, and trusses for the entrance canopy.

A “system” conventionally consists of a continuous membrane, plate, shell, or solid, single or in combination, each divided for analysis purposes into a finite number of “elements”, connected, supported, and loaded at their vertices and other specified locations on edges or inside, called “nodes”. Systems may include structures as well.

Fig 1.2(b) shows a machine part system consisting of a solid, thin-walled shell, and a projecting plate. The suggested divisions are shown in lines of a lighter shade. Generally, the curved boundaries will be modelled as straight lines. The circular pipe in this case will be simulated as a hexagonal tube.

The principal difference between a structure and a system is this: The articulated structure is automatically, naturally, divided into straight (and certain regularly curved) members such as the truss member AB in Fig. 1.2(a), whose behaviour is well known and can be formulated theoretically. On the other hand, the

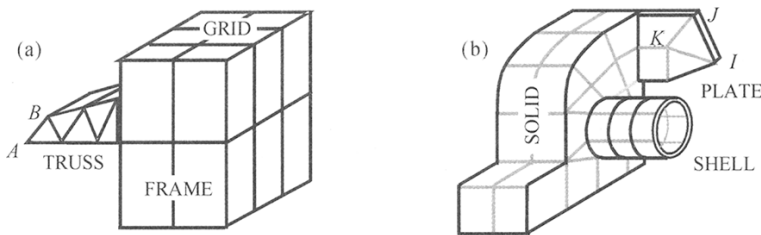


Fig. 1.2 (a) Two-storey Articulated Structure; (b) Machine Part System, Continuum

continuous system has no such theoretical basis and has to be divided into pieces of simple shape, such as the triangle IJK in Fig. 1.2(b), whose behaviour must be formulated by special methods.

Most real-life facilities involve a combination of both types described above. For instance, a building has flat plate-type walls and floors; a machine may sit atop columns and beams. In practice, “member” and “joint” usually apply to a structure, while “element” and “node” apply to a system in particular, and to a structure also in general.

Each node or joint can have a number of independent action (force or moment) or displacement (deflection or rotation) components called “Degrees Of Freedom” (DOF) along a certain direction corresponding to coordinate axes.

A plane truss member such as AB in Fig. 1.2(a) shown enlarged in Fig. 1.3(a) has two DOF at each joint. Hence the member has a total of (2×2) or 4 DOF.

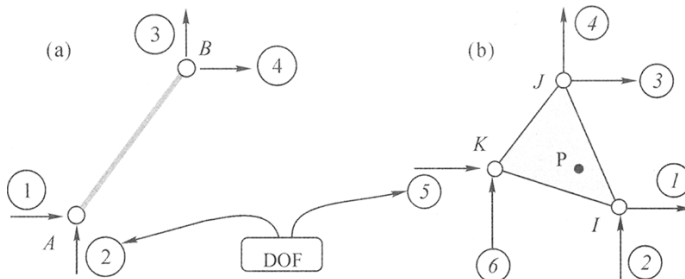


Fig. 1.3 (a) A Truss Member AB; (b) A Triangular Finite Element IJK

A triangular membrane element such as IJK in Fig. 1.2(b) shown enlarged in Fig. 1.3(b) has two DOF at each node. Hence the element has a total of (3×2) or 6 DOF.

Different types of members and elements have different numbers of DOF. For instance, a 3D frame member has two joints and six DOF (3 forces or displacements and 3 moments or rotations) per joint and 12 DOF in total. A solid “brick” element has eight nodes and three DOF (3 forces or displacements) per node and 24 DOF in total.

Additionally, in the case of finite elements, joint the same type of element may

even have different number of nodes in “transition” elements.

1.4 Flexibility Approach

Fig. 1.4 shows a truss member with actions and corresponding displacements along the two DOF at each end. The sets of four actions and displacements can be represented vectorially or in terms of x, y components, as follows:

$\{A\} = \{A_1, A_2, A_3, A_4\} = \{X_i, Y_i, X_j, Y_j\}$, the “Action Vector”

$\{D\} = \{D_1, D_2, D_3, D_4\} = \{u_i, v_i, u_j, v_j\}$, the “Displacement Vector”

The displacement D at every DOF (say I) is a function of the actions A_1, A_2 , at all connected DOF. Within the elastic limit, D_i is a linear combination of the effects of all actions.

Thus, their relationship may be written as:

$$D_i = f_{i1} A_1 + f_{i2} A_2 + f_{i3} A_3 + f_{i4} A_4 \quad (1.1)$$

in which f_{ij} stands for the displacement at DOF I due to a unit action at DOF J , and is known as the “Flexibility Coefficient”.

Three more such equations may be written for D_2 , D_3 , and D_4 . The four equations may be represented in matrix form as:

$$\begin{matrix} \{D\} = [F] \cdot \{A\} \\ 4 \times 1 \quad 4 \times 4 \quad 4 \times 1 \end{matrix} \quad (1.2)$$

in which, the $[F]$ matrix of flexibility coefficients is known as “Flexibility Matrix”.

The flexibility coefficients for prismatic bars can be determined from basic theoretical principles of strength of materials and theory of structures.

The flexibility approach was quite popular as the “Force Method” for manual analysis, the “Method of Consistent Deformation” being a typical application. With the advent of computers, it was found that this approach was not convenient to formulate or solve large and complex problems. Hence, the flexibility approach was not pursued further for practical applications.

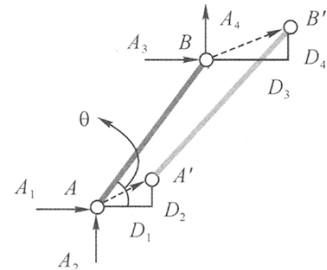


Fig. 1.4 Displaced Truss Member

1.5 Stiffness Formulation

1.5.1 Stiffness Matrix

An alternative formulation, an exact opposite—in fact the inverse—of the flexibility approach, called “stiffness approach” or “displacement approach” was also in use for manual solutions. The “Slope Deflection Method” for continuous beams and the

“Moment Distribution Method” for beams and frames were very popular.

This approach was very convenient for computerisation and became the preferred method for computer solutions, especially for finite element analysis.

In general, the displacement along every DOF needs an action along that DOF and reactions at all the other connected DOFs for equilibrium. For elastic behaviour, the function is a linear combination of all the displacement effects.

Thus, the action-displacement relationships of the truss member in Fig. 1.4 is written as:

$$\begin{aligned} A_1 &= k_{11} D_1 + k_{12} D_2 + k_{13} D_3 + k_{14} D_4 \\ A_2 &= k_{21} D_1 + k_{22} D_2 + k_{23} D_3 + k_{24} D_4 \\ A_3 &= k_{31} D_1 + k_{32} D_2 + k_{33} D_3 + k_{34} D_4 \\ A_4 &= k_{41} D_1 + k_{42} D_2 + k_{43} D_3 + k_{44} D_4 \end{aligned} \quad (1.3)$$

in which k_{ij} stands for the action at DOF I due to a unit displacement at DOF J (with all other displacements set to zero) and is known as the “Stiffness Coefficient”.

The four Eq.(1.3) may be represented in matrix form as:

$$\begin{matrix} \{A\} = [k] \{D\} \\ 4 \times 1 \quad 4 \times 4 \quad 4 \times 1 \end{matrix} \quad (1.4)$$

in which the $[k]$ matrix of stiffness coefficients is known as “Stiffness Matrix”.

The stiffness coefficients for prismatic bars can be determined from basic theoretical principles of strength of materials and theory of structures.

For instance, consider the truss member AB, of length L and cross-sectional area A_t from a material with Young's Modulus of elasticity E, inclined at an angle θ with the horizontal, subjected to a unit displacement along DOF 1, as shown in Fig. 1.5 (a).

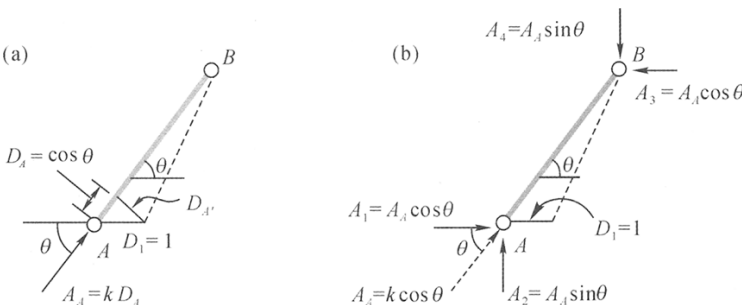


Fig. 1.5 (a) Unit Global Displacement; (b) Action Components

The unit horizontal displacement D_1 resolves into an axial displacement $D_A = 1 \cdot \cos\theta = \cos\theta$ and a transverse displacement $D_A' = 1 \cdot \sin\theta = \sin\theta$.

As the truss member ends are pinned, only the axial displacement D_A needs a force $A_A = kD_A$, or $k\cos\theta$, k being the stiffness of the axial force bar, namely (EA_t/L) .

As shown in Fig. 1.5(b), this axial force A_A may now be resolved into:

$$A_1 = A_A \cos\theta = k \cos^2\theta \quad \text{and} \quad A_2 = A_A \sin\theta = k \cos\theta \sin\theta$$

To keep the bar in equilibrium, equal and opposite reactions must be developed at the end *B*, giving:

$$A_3 = -A_1 = -k \cos^2\theta \quad \text{and} \quad A_4 = -A_2 = -k \cos\theta \sin\theta$$

These four actions corresponding to a unit displacement along DOF 1 are defined by the four stiffness coefficients k_{ij} ($i = 1, 2, 3, 4$) that constitute column 1 of the stiffness matrix $[K]$ in Eq. (1.4), as shown in bold type in Eq. (1.5) below. The other three columns can similarly be determined by the application of unit displacements along DOF 2, 3, and 4 in turn.

The resulting stiffness matrix is as follows:

$$\begin{Bmatrix} A_1 \\ A_2 \\ A_3 \\ A_4 \end{Bmatrix} = \frac{EA_t}{L} \begin{bmatrix} \cos^2\theta & \cos\theta \sin\theta & -\cos^2\theta & -\cos\theta \sin\theta \\ \cos\theta \sin\theta & \sin^2\theta & -\cos\theta \sin\theta & -\sin^2\theta \\ -\cos^2\theta & -\cos\theta \sin\theta & \cos^2\theta & \cos\theta \sin\theta \\ -\cos\theta \sin\theta & -\sin^2\theta & \sin\theta \cos\theta & \sin^2\theta \end{bmatrix} \begin{Bmatrix} D_1 \\ D_2 \\ D_3 \\ D_4 \end{Bmatrix} \quad (1.5)$$

Stiffness matrices can be developed for other straight prismatic members such as beams and torsion bars from similar principles.

However, the situation is quite different when it comes to finite elements.

The triangular plane element *IJK* in Fig. 1.6, under the action of six force components along the 6 DOF, is represented as:

$$\begin{aligned} \{A\} &= \{A_1, A_2, A_3, A_4, A_5, A_6\} \\ &= \{X_i, Y_i, X_j, Y_j, X_k, Y_k\} \text{ also.} \end{aligned}$$

It is displaced to the configuration *I'J'K'*, with the deflection components:

$$\begin{aligned} \{D\} &= \{D_1, D_2, D_3, D_4, D_5, D_6\} \\ &= \{u_i, v_i, u_j, v_j, u_k, v_k\} \text{ also.} \end{aligned}$$

Relationships of actions and displacements at the DOF of this element are of the same kind as Eqs. (1.3) and (1.4) for the truss member, with the difference that for the element, the $\{A\}$ and $\{D\}$ vectors are (6×1) and stiffness matrix $[K]$ is (6×6) .

However, it is unlike Eq. (1.5) that no theoretical method to determine the stiffness coefficients for a general triangle or any other shape exists. Other special techniques must be resorted to, as will be discussed in subsequent chapters.

1.5.2 Characteristics of Stiffness Matrix

The characteristics of the member or element stiffness matrix, most of which may be deduced from Eq. (1.5), are listed below as common to all element stiffness matrices.

(1) The stiffness matrix is square, logically from the fact that there are as many

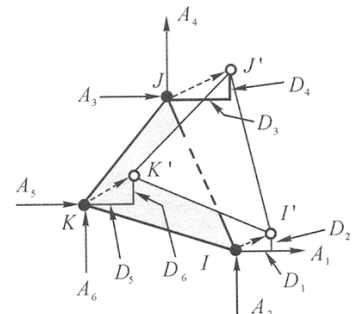


Fig. 1.6 Action and Displacement Components

displacement DOF as action DOF.

- (2) The stiffness matrix is symmetric. This derives from the principle of conservation of energy, commonly developed as Maxwell's Law of Reciprocal Deflections for structural members, which states that the displacement at A due to a unit action at B is equal to the displacement at B due to a unit action at A.
- (3) The matrix is “positive definite”, that is the diagonal terms are positive and (generally) dominant. It simply reflects the fact that a point at which an action is applied, moves along the direction of the action, not opposite to it.
- (4) Each column of the matrix, representing all the actions acting on the element due to the displacement at one DOF, must satisfy statics. If they are all forces, then the alternate terms in a row or column (representing horizontal and vertical components separately) must add up to zero separately. Moments of all the forces about any point must be zero.
- (5) The determinant of the stiffness matrix will be found to be zero. This implies that the matrix is singular, and cannot be inverted. In effect this means that the displacements due to any action on the member will be infinite, that is, not capable of being determined.

The explanation for this apparent anomaly is very simple: The stiffness matrix is just a property of the element. The element can accept and resist a load only when it is supported against rigid-body movement, as along three DOF in 2D. Without such minimal support, even the smallest load along any of its DOF will simply blow the element away to “infinity” as in space!

1.5.3 Equivalent Loads

Loads are often applied between the joints of a member, such as a distributed load on a beam. As matrix analysis deals with loads and displacements at only the joints, the member loads must be replaced by “Equivalent Loads” at the joints. These actions are also called “Consistent Nodal Loads”.

In this case, for straight prismatic members, classical theories provide values for equivalent loads.

For instance, the beam of span L loaded with q per unit length shown in Fig. 1.7(a) can be replaced with the two forces and two moments shown in Fig. 1.7(b), on the basis that both of them produce the same end rotations θ , and satisfy statics.

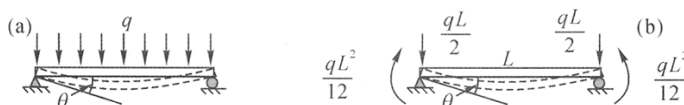


Fig. 1.7 (a) Simply Supported Beam with Uniform Load; (b) Equivalent End Actions

Situations in regard to finite elements are not as simple as this and will need special treatment.

1.5.4 System Stiffness Equations

For a system with n DOF, the governing equation for the i -th DOF of the assemblage of members or elements is obtained by combining the governing equations for the same DOF from the individual pieces, in the form:

$$A_i = k_{i1} D_1 + k_{i2} D_2 + \cdots + k_{in} D_n$$

or, for all the n DOF, in matrix form, similar to the element Eq.(1.4):

$$\{A_s\} = [K_s] \{D_s\} \quad (1.6)$$

where, the action vector $\{A_s\}$ includes the effects of internal loads and is $(n \times 1)$ in size; the displacement vector $\{D_s\}$ is $(n \times 1)$ in size; and the stiffness matrix $[K_s]$ is $(n \times n)$ in size.

Since the system stiffness matrix is the superposition of the element stiffness matrices, all the characteristics of the element stiffness matrix listed in Section 1.4.2 can carry over into the system stiffness matrix.

1.6 Solution Methodology

Typically, the data for a problem in structural and continuum analysis consists of:

- (1) Geometry, namely location of nodes;
- (2) Topology, namely the nodes by which various elements are connected;
- (3) Relevant material properties;
- (4) Locations of supports, and their movements, if any;
- (5) Locations and magnitudes of loads.

To solve a finite element problem, first the region is divided into sufficient numbers of elements of a suitable type, to reflect the geometry and any special features, with nodes located at supports and concentrated loads.

From the data on geometry, topology, and material properties, a stiffness matrix for each element is determined.

The element stiffness matrices are assembled to form the system stiffness matrix, as will be explained in the next chapter.

The supported and loaded DOF in data items (4) and (5) form a complementary set: Those DOF which are constrained can develop reactions and hence must not be loaded. Differently, any action component that happens to be applied on a supported DOF will directly pass on to the support and hence must be excluded from the main analysis. Likewise, those DOF that are loaded (and unconstrained) are free to displace.

1.6.1 Manual Solution

Let a be the number of known actions and unknown displacements and c the number of unknown reactions and known displacement constraints. Note that total DOF n

$$= \mathbf{a} + \mathbf{c}.$$

Thus the action and displacement vectors can be partitioned in a mutually exclusive manner as $\{\mathbf{A}_a | \mathbf{A}_c\}$ and $\{\mathbf{D}_a | \mathbf{D}_c\}$. Note that the action vectors are actually modified action vectors incorporating the effects of any member or element loads.

Subsequently, the stiffness equations can be rearranged to match such partitioning and the stiffness matrix can also be partitioned into four parts.

The partitioned sub-vectors and sub-matrices and their sizes, are as follows:

$$\left\{ \begin{array}{l} \mathbf{A}_a \\ (\mathbf{a} \times 1) \\ \mathbf{A}_c \\ (\mathbf{c} \times 1) \end{array} \right\} = \left[\begin{array}{c|c} \mathbf{K}_{aa} & \mathbf{K}_{ac} \\ (\mathbf{a} \times \mathbf{a}) & (\mathbf{a} \times \mathbf{c}) \\ \hline \mathbf{K}_{ca} & \mathbf{K}_{cc} \\ (\mathbf{c} \times \mathbf{a}) & (\mathbf{c} \times \mathbf{c}) \end{array} \right] \cdot \left\{ \begin{array}{l} \mathbf{D}_a \\ (\mathbf{a} \times 1) \\ \mathbf{D}_c \\ (\mathbf{c} \times 1) \end{array} \right\} \quad (1.7)$$

This can be separated into two matrix equations as follows:

$$\{\mathbf{A}_a\} = [\mathbf{K}_{aa}]\{\mathbf{D}_a\} + [\mathbf{K}_{ac}]\{\mathbf{D}_c\} \quad (1.8a)$$

$$\text{and } \{\mathbf{A}_c\} = [\mathbf{K}_{ca}]\{\mathbf{D}_a\} + [\mathbf{K}_{cc}]\{\mathbf{D}_c\} \quad (1.8b)$$

In Eq. (1.8a), all the terms except $\{\mathbf{D}_a\}$ are known, and $\{\mathbf{D}_a\}$ can be computed from:

$$\begin{aligned} \{\mathbf{A}_a\} - ([\mathbf{K}_{ac}]\{\mathbf{D}_c\}) &= [\mathbf{K}_{aa}]\{\mathbf{D}_a\} \\ \text{i.e. } \{\mathbf{D}_a\} &= [\mathbf{K}_{aa}]^{-1}(\{\mathbf{A}_a\} - [\mathbf{K}_{ac}]\{\mathbf{D}_c\}) \end{aligned} \quad (1.9a)$$

Designating the term $(-[\mathbf{K}_{ac}]\{\mathbf{D}_c\})$ as $\{\mathbf{A}_d\}$, Eq. (1.9a) may be written as:

$$\{\mathbf{D}_a\} = [\mathbf{K}_{aa}]^{-1}(\{\mathbf{A}_a\} + \{\mathbf{A}_d\}) \quad (1.9b)$$

If all known (support) displacements $\{\mathbf{D}_c\}$ are zero, $\{\mathbf{A}_d\}$ is zero. Eqs. (1.9) simplify to:

$$\{\mathbf{D}_a\} = [\mathbf{K}_{aa}]^{-1}\{\mathbf{A}_a\} \quad (1.10a)$$

Now, with all the displacements known, the unknown reactions $\{\mathbf{A}_c\}$ may be found from Eq. (1.8b).

Further, if all the known (support) displacements $\{\mathbf{D}_c\}$ are zero, then $\{\mathbf{A}_d\}$ is zero, and Eq. (1.8b) simplifies to:

$$\{\mathbf{A}_c\} = [\mathbf{K}_{ca}]\{\mathbf{D}_a\} \quad (1.10b)$$

1.6.2 Computer Solution

While the partitioning procedure described may be suitable for manual solution of small problems, obviously the reordering of the terms in, and partitioning of, large vectors and matrices in computer solutions will be inefficient and time consuming.

Instead, the equation set is retained as assembled. The action vector $\{\mathbf{A}_a\}$ is still modified to $\{\mathbf{A}_a^*\}$ for the c known displacements according to Eq. (1.9a), but without rearranging the equations. The stiffness coefficients k_i in the columns corresponding to the known displacements are set to zero as their effect has already been incorporated into the action vector.

As those a equations are the only ones needed for solution of the unknown displacements, the other c equations corresponding to Eq. (1.8b) involving the known displacements and unknown reactions are replaced by dummy equations in the form of $\{A_c^*\} = [K_\infty]\{D_c\}$, in which each A_i^* is set equal to the known value of $k^i D_i$, so that when D_i is solved for, it will return the known value of D_i .

The equations thus modified, still in their original order, can be written as:

$$\{A^*\} = [K^*]\{D^*\} \quad (1.11)$$

Because of the incorporation of the support conditions, the modified $[K^*]$ matrix is not singular any more. Hence the displacements may be found as:

$$\{D^*\} = [K^*]^{-1}\{A^*\} \quad (1.12)$$

Then all the displacements can be computed, including the known displacements at their original input values. Once the displacements are known, the unknown reactions can be computed from the full set of original equations, Eq. (1.6).

Needless to say, the computer is also heavily involved in the automation of the input preparation and output evaluation of such large scale analyses.

1.6.3 Support Displacements

It may be noted that Eqs. (1.9) are in general form wherein some or all the known displacements may be non-zero, implying support settlement or yielding.

The minimum supports that a system must be provided before analysis can proceed is strong enough to prevent rigid body displacement. For instance, in a 2D plane region, three non-collinear DOF must be supported to prevent rigid body deflection and rotation.

In such a minimally supported system, any support displacement will only cause a change in the position of the body and will not introduce deformations. Hence no internal actions will be developed due to support displacement. The reactions at the supports can be found from statics, and the only internal actions will be due to external applied loading, if any.

However, as is more common, if the system is supported at more than the minimum required number of DOF, then it becomes “statically indeterminate”. Any support displacement will introduce internal deformations and actions, even without external applied loading. Eqs.(1.7), (1.8), and (1.9) will take care of all these effects.

The notation $\{A_d\} = [K_\infty]\{D_c\}$ introduced in Eqs. (1.9), may now be interpreted as the “Equivalent Load” vector to account for support displacements.

1.6.4 Alternate Loadings

Note that Eqs. (1.9) involve the applied loading conditions $\{A_a\}$ on the right hand side only. Hence if we need the results for different applied loadings, we can simply save the $[K_\infty]^{-1}$ matrix and the $\{A_d\}$ vector, and carry out the matrix multiplication in Eqs. (1.9) for the new applied load vector $\{A_a\}$.

From the displacements $\{D_a\}$ due to the new loading, the corresponding

reactions, $\{A_c\}$ may be found from Eq. (1.8b) or Eq. (1.10b).

This facility is of great use when different loadings have to be applied to the same object in the same support conditions, as is very often the case.

Thus, if the results can be computed for a few basic independent loadings, then for various combinations of these loadings, the stiffness equations do not have to be solved afresh. Only the already computed results of the basic loadings need to be combined in the same proportions as the loads in the combinations.

As should be evident, the solution methodology described is standard practice and quite routine with today's computers. The art and science of finite elements thus revolves entirely around the determination of the stiffness matrix and the equivalent load vector.

1. 7 Advantages and Disadvantages of FEM

The advantages of FEM, some already touched upon, may be summarised as follows:

- (1) Any domain with curved boundaries, heterogeneous material properties, irregular support constraints, and varying loading conditions, may be sub-divided into a suitable number of finite elements, appropriate material and behaviour properties may be ascribed to them, and the resulting governing equations may be solved quickly and accurately by computers.
 - (2) It is equally applicable to statics and dynamics; solids, fluids, and gases and combinations; linear and nonlinear; elastic, inelastic, or plastic; special effects such as crack propagation; events and processes such as bolt pretensioning, etc.
 - (3) The massive amounts of data itself can be efficiently generated by computer " preprocessors ", and the even more voluminous output can be effectively analysed and presented by " postprocessors ". Hence a larger problem does not involve undue additional effort for users.
 - (4) Problems of size and complexity hitherto unimaginable and infeasible can be handled by FEM, enabling analysts to extend their investigations into fresh areas, and inspiring designers to create new forms and new solutions.
 - (5) Where formerly only a few alternatives could be examined, with FEM quite a large number of possible solutions could be tested, resulting in optimal solutions.
- However, certain disadvantages and limitations of FEM should also be recognised:
- (1) Every finite element is based on an assumed shape function expressing internal displacements as functions of nodal displacements. A certain element may give accurate answers for a particular type and location of support and loading, but inaccurate answers for another type and location.
 - (2) Even with " well-behaved " elements, the solution is heavily dependent on the mesh, not only on the number of elements into which the region is divided, but also on their shape and arrangement.

- (3) Modelling of the geometry, material properties, support conditions, and loading conditions, is very subjective and depends on analyst's judgement a lot. The same problem, when solved with the same computer program by different analysts, will often result in answers differing to a smaller or larger degree.
- (4) Precision of the output to a large number of significant digits is no guarantee of the accuracy of the solution. Even convergence with refinement of mesh is not absolute proof of the correctness of solution.
- (5) As finite elements become necessary only when other methods are not available or economically viable, in many cases there will be not many ways to confirm whether the solution is right or exact.

Hence FEM needs considerable experience in the problem modelling and result interpretation aspects. In the wrong hands it can lead to wrong and even dangerous results. One must simply investigate the system with various mesh sizes and types, different modelling treatments, and under all possible material, support and loading conditions, and look for consistent and convergent behaviour.

Before results from any analysis are used in real-life situations, they must be backed by justification of the model, evaluation of convergence, and an estimate of the accuracy, at least in relative terms.

At the same time, there is no cause for undue alarm. Fortunately, in the last few decades, innumerable types of problems have been analysed by many researchers and application engineers around the world, and a massive amount of practical experience has been accumulated in applications of FEM.

Most of the packages have built-in checks for catching obvious errors. Hence the chances of a user making a large error in applying FEM are very little.

As long as users are aware of the factors that could influence the result and techniques for eliminating or at least minimising the errors, results from FEA should be reliable.

1.8 Mathematical Formulation of Finite Element Method

As already mentioned, there is no theory that can yield the force-displacement relationships for a general triangle or quadrilateral. We have to make some reasonable assumption on the behaviour of the element and then use the fact that as we increase the number of elements the answer converges, to lead us to a usable solution.

In the stiffness approach, the assumption is usually made at the displacement level. This will ensure compatibility of displacements between elements but not continuity of stresses. Rarely and in special cases, stress distributions may be assumed and a flexibility analysis made. More often however, a hybrid approach is used, enforcing partial continuity of both stress and deformation distributions across element boundaries.

In this book, the pure displacement approach will be described, with comments

on hybrid elements where necessary.

In the displacement or stiffness method, the internal displacements are assumed as functions of nodal displacements, and these functions are known as “Shape Functions”. It is on the basis of those shape functions that stiffness matrices and equivalent actions for element loads are developed.

1. 9 Shape Functions

1. 9. 1 General Requirements

Let a point inside or on the boundary of a finite element displace by the amount $\{U\}$ under some loading. The components of the internal displacement vector $\{U\}$ will depend on the particular problem being analysed.

For instance, in the case of plate bending it will be $\{\theta_x, \theta_y, w\}$, the rotations about the x and y axes and the vertical (z) deflection. To illustrate, we shall use 2D plane analysis with deflection components i.e. x and y movements $\{u, v\}$, because it is the simplest and the most common case, and is easily extendable to the solid elements which are of the greatest importance to our topic.

The general internal displacements $\{U\}$ are related to nodal displacements $\{D\}$. Thus, for an element with nodes I, J, ..., with nodal displacements $(u_i, v_i), (u_j, v_j), \dots$, the x and y displacements u and v at any point will be:

$$u = N_i u_i + N_j u_j + \dots, \\ \text{and} \quad v = N_i v_i + N_j v_j + \dots.$$

This relationship is called “Shape Function” and the relating matrix is designated [N].

$$\{U\} = [N] \{D\} \quad (1.13)$$

Internal displacements of a point will depend on the location of the point, and hence shape functions will depend on the coordinates $\{x, y\}$ of the point.

The shape functions must be true for the entire element, in particular on its boundaries and at the nodes. Hence at the node I, where, $x = x_i$ and $y = y_i$, u must equal u_i , and v must equal v_i . This means that at I, N_i must equal 1, and N_j and N_k must equal zero.

Similarly, at J, $N_j = 1$, and N_i and $N_k = 0$; and at K, $N_k = 1$, and N_i and $N_j = 0$.

Thus the shape function may be visualised as a surface which has ordinate of 1 at the node to which it applies, and zero at the other nodes. Fig. 1.8 shows the shape function N_i for the node I, for a rectangular element with (a) four nodes I, J, K, L, and, (b) eight nodes I, J, K, L, P, Q, R, S, illustrating the analogy.

Obviously, the more nodes an element has, the more terms can be incorporated into the shape function, and the better the solution surface can approximate the real behaviour.

For straight prismatic members and certain regular shapes, shape functions can

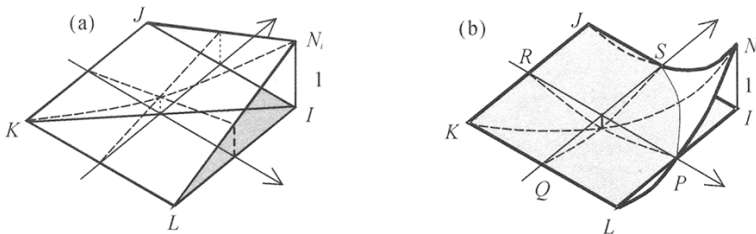


Fig. 1.8 Shape Functions for (a) 4-node Rectangle, (b) 8-node Rectangle

be obtained from theoretical principles. But, for general shapes, some assumptions will have to be made, to be validated and refined subsequently.

1.9.2 Displacement Function Technique

For certain simple cases such as a plane triangle, it is easier to express the displacements of a point in the element as functions of its position, rather than to assume a shape function directly.

Then the shape functions may be developed through such “Displacement Functions” as follows:

Step 1 :

Write the displacements at any point as functions of its coordinates and undetermined coefficients, through an assumed “Displacement Function” [P], in the form:

$$\begin{aligned} u &= C_1 x + C_2 \\ \text{and } v &= C_1 y + C_2 \quad \text{or in general} \\ \{U\} &= [P]\{C\} \end{aligned} \tag{1.14}$$

with $\{C\}$ being the vector of undetermined coefficients C_1, C_2, \dots , the number of the coefficients being equal to the number of DOF for the element, say m .

Step 2 :

The displacement function Eq. (1.14) is true for the whole domain, and in particular at the nodes such as I, J . When we substitute the nodal coordinates and their displacements into Eq. (1.14), we get:

$$\begin{aligned} u_i &= C_1 x_i + C_2 \\ \text{and } v_i &= C_1 y_i + C_2 \quad \text{or in general} \\ \{D\} &= [M]\{C\} \end{aligned} \tag{1.15}$$

The $[M]$ matrix is square, $(n \times n)$ in size.

Step 3 :

The coefficient vector $\{C\}$ in Eq. (1.15) may be determined by inverting $[M]$:

$$\{C\} = [M]^{-1}\{D\} \tag{1.16}$$

Step 4:

Upon substitution of Eq. (1.16) into Eq. (1.14), we get the internal displacements as functions of nodal displacements in the form:

$$\{U\} = [P][M]^{-1}\{D\} = [N]\{D\} \quad (1.17)$$

defining the Shape Function as: $[N] = [P][M]^{-1}$

This is feasible where the $[M]$ matrix can be inverted, and is of reasonable size for closed form inversion or economical computation.

For all but the simplest of cases such as a plane triangle or rectangle, this approach is not practical and more general and direct methods have been discovered and developed.

1.10 Element Stiffness Matrix

Although we would use the triangular finite element IJK of Fig. 1.9 to develop the general procedure for developing the finite element stiffness matrix, the technique will apply to other shapes with different DOF as well.

As the entire element deforms, a typical interior point such as $P = (x, y)$ moves to the position P' , by an amount $\{U\}$, with components $\{u, v\}$, as shown in Fig. 1.9. The rectangle around the point denotes an infinitesimal element $dx dy$ of the triangle.

The general procedure for the determination of a stiffness matrix may be outlined as follows:

1.10.1 Shape Function

Except for very simple cases, internal displacements $\{U\}$ are written as an assumed function of node displacements $\{D\}$:

$$\{U\} = [N]\{D\} \quad (1.18)$$

where, $[N]$ is the shape function matrix.

The individual shape function expressions will be functions of coordinates (x_i, y_i, x_m, y_m) of the m nodes of the element and variable general point coordinates (x, y) . That is,

$$N_i = f_i(x, y), N_j = f_j(x, y), \dots \quad (1.19)$$

1.10.2 Strain Influence Matrix

Strains are derivative functions of displacements. For example, in the plane stress situation shown in Fig. 1.10, we have:

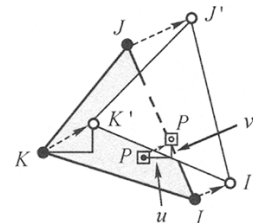


Fig. 1.9 Displaced Triangular Finite Element

situation shown in Fig. 1.10, we have:

$$\epsilon_x = \frac{\partial u}{\partial x}, \quad \epsilon_y = \frac{\partial v}{\partial y}, \quad \text{and} \quad \gamma_{xy} = \frac{\partial v}{\partial x} + \frac{\partial u}{\partial y}$$

Symbolically, the strain vector may be written as:

$$\{\epsilon\} = [L]\{U\} \quad (1.20)$$

where $[L]$ consists only of the partial derivative operators such as $\{\frac{\partial}{\partial x}\}$ and is called the “Operator Matrix”, implying that its terms operate on (rather than multiply) the terms of the displacement vector.

From Eqs. (1.18) and (1.20), we get:

$$\{\epsilon\} = [L]\{N\}\{D\} = [B]\{D\} \quad (1.21)$$

where $[B] = [L][N]$, representing the result of $[L]$ operating on the shape function matrix $[N]$. The author will refer to the $[B]$ matrix as the “Strain Influence Matrix” as it gives the strains when multiplied by the nodal displacements.

1.10.3 Stress Influence Matrix

Stresses are functions of strains by the generalised Hooke’s Law. In the plane stress situation of Fig. 1.10, we have:

$$\sigma_x = \frac{E(\epsilon_x + v\epsilon_y)}{1-v^2}, \quad \sigma_y = \frac{E(v\epsilon_x + \epsilon_y)}{1-v^2}, \quad \text{and} \quad \gamma_{xy} = \frac{E\tau_{xy}}{2(1+v)}$$

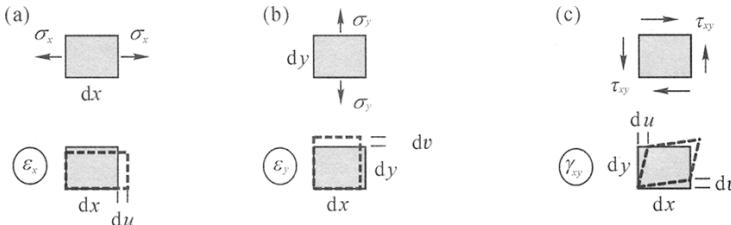


Fig. 1.10. (a) Normal x-strain; (b) Normal y-strain; (c) Shear xy-strain

Thus, the stress vector may be written, using Eq. (1.21):

$$[\sigma] = [E]\{\epsilon\} = [E][B]\{D\} = [S]\{D\} \quad (1.22)$$

where $[E]$ is the elasticity matrix, involving the material properties E the Young’s Modulus, v the Poisson’s Ratio, and the product matrix $[S]$ ($= [E][B]$) may be referred to as the “Stress Influence Matrix” because it gives the stresses when multiplied by the displacement vector.

1.10.4 External Virtual Work

Now consider the element subjected to additional virtual (imaginary) displacements $\{D^*\}$ at the nodes, with the asterisk (*) superscript indicating virtual quantities.

to be an elastically deformed region under actual loads $\{A\}$, and then an additional virtual displacement may be imposed on it, shifting it to the position indicated by the thin-line triangle $I'J'K'$.

The external virtual work done by the actual actions $\{A\}$ moving through the virtual displacements $\{D^*\}$ is given by:

$$W_e^* = D_1^* A_1 + D_2^* A_2 + \dots = \{D^*\}^T \{A\} \quad (1.23)$$

the vector transpose $\{D^*\}^T$ being necessary to convert the $\{D^*\}$ vector to a row matrix, thus enabling the actions and displacements to be multiplied and added, and hence to yield a scalar work quantity.

1.10.5 Internal Virtual Work

The nodal displacements will result in additional general internal virtual displacements $\{U^*\}$ and hence virtual strains $\{\varepsilon^*\}$. The actual stresses $\{\sigma\}$ in the element moving through the virtual strains $\{\varepsilon^*\}$ will cause internal virtual work, that is to say, will store internal virtual strain energy.

The same relationships that we developed for the real displacements and strains will also hold true for the virtual displacements also, and hence we may write:

$$\{U^*\} = [N] \{D^*\} \quad (1.13a)$$

$$\{\varepsilon^*\} = [L][N] \{D^*\} = [B] \{D^*\} \quad (1.21a)$$

Fig. 1.11 shows an element of unit sides and unit thickness, so that stresses are equal in magnitude to the forces, and strains are equal in magnitude to the displacements.

For this unit cube, the virtual internal work done (or strain energy stored) by the actual stresses $\{\sigma_x, \sigma_y\}$ moving through virtual strains $\{\varepsilon_x^*, \varepsilon_y^*\}$ is given by:

$$dW_{(1)}^* = \varepsilon_x^* \sigma_x + \varepsilon_y^* \sigma_y + \dots = \{\varepsilon^*\}^T \{\sigma\}$$

the transpose $\{\varepsilon^*\}^T$ of the strain vector being necessary to convert it to a row matrix and yield the scalar work (or energy) quantity on multiplication.

For an elemental volume of the body $dV (= dx dy dz)$, the virtual internal work is:

$$dW_i^* = \{\varepsilon^*\}^T \{\sigma\} dV \quad (1.24)$$

From Eq. (1.21a), we can write: $\{\varepsilon^*\}^T = \{D^*\}^T [B]^T$

Substituting this into Eq. (1.24) and applying Eq. (1.22), for the entire finite element, the internal virtual work done, we get:

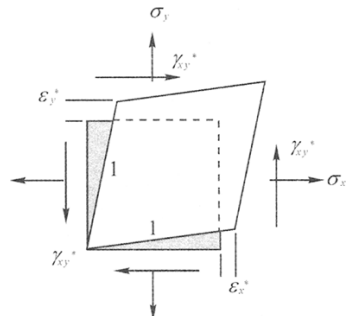


Fig. 1.11 Real Stresses and Virtual Strains

$$\begin{aligned}
 W_i^* &= \int_{\text{VOL}} \{D^*\}^T [B]^T [E] [B] \{D\} dV \\
 &= \{D^*\}^T \left(\int_{\text{VOL}} [B]^T [E] [B] dV \right) \{D\}
 \end{aligned} \tag{1.25}$$

1.10.6 Virtual Work Equation

Total virtual work ($W_e - W_i^*$) must be zero. Hence from Eqs. (1.23) and (1.25) we get:

$$\begin{aligned}
 \{D^*\}^T \{A\} &= \{D^*\}^T \left(\int_{\text{VOL}} [B]^T [E] [B] dV \right) \{D\} \\
 \text{or } \{A\} &= \left(\int_{\text{VOL}} [B]^T [E] [B] dV \right) \{D\}
 \end{aligned} \tag{1.26}$$

Eq. (1.26) may be symbolically written in the same form as Eq.(1.4):

$$\{A\} = [K]\{D\}$$

in which, $[K]$, relating action and displacement vectors $\{A\}$ and $\{D\}$, may be termed as the “Stiffness Matrix”, and may be determined for any element as:

$$[K] = \int [B]^T [E] [B] dV \tag{1.27}$$

Note that in the above, $\{A\}$ and $\{D\}$ are $(m \times 1)$, and $[K]$ is $(m \times m)$, where, m is the number of DOF for the element, 6 in the case of the triangle considered.

1.11 System Stiffness Matrix

For an assemblage of elements, similar action-displacement relationships exist as for individual elements. Each action on the system is a linear function of the displacements at all the DOF connected to the DOF of the particular action.

The basic approach to develop these relationships is the same, namely, to determine the actions at all the DOF in the system due to unit displacement at each DOF in turn. But this can become very tedious for large systems. Instead, a simpler method, based on equilibrium and compatibility at the nodes, is used.

For illustration, consider the two elements $P (\equiv IJK)$ and $Q (\equiv IKL)$ of the machine part in Fig. 1.12(a). The DOF for all the elements of the system are sequentially numbered, and the eight DOF corresponding to the four nodes of the two elements P and Q are marked in Fig. 1.12(b). The curved surface of the pipe is now shown modelled as flat plate elements.

$IJKL$ is deformed to the shape $I'J'K'L'$ by actions(not shown) on this part as shown in Fig. 1.12(c), with displacement components $\{D_1, D_2, \dots, D_8\}$.

Fig. 1.13 shows elements P and Q with their separate nodal displacements and

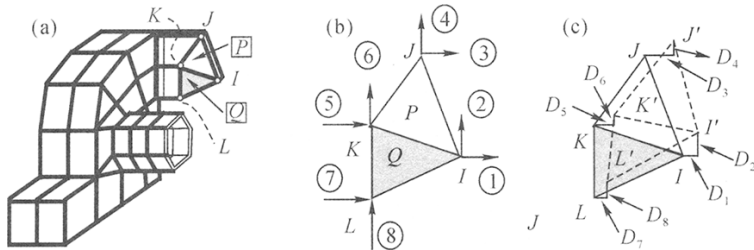


Fig. 1.12 (a) Machine Part; (b) Two Plane Elements IJK, IKL; (c) Displacements

actions. The displacements at the common nodes I and K, namely D_1 , D_2 , D_5 , and D_6 , will be the same for both elements for compatibility, that is, to maintain continuity of the material.

As already described, the stiffness matrices of the two elements can be determined and the nodal actions may be written in terms of the nodal displacements for each element.

Thus, for instance, with superscripts within brackets identifying the elements:

$$A_1^{(P)} = k_{11}^{(P)} D_1 + k_{12}^{(P)} D_2 + k_{13}^{(P)} D_3 + k_{14}^{(P)} D_4 + k_{15}^{(P)} D_5 + k_{16}^{(P)} D_6$$

and, $A_1^{(Q)} = k_{11}^{(Q)} D_1 + k_{12}^{(Q)} D_2 + k_{15}^{(Q)} D_5 + k_{16}^{(Q)} D_6 + k_{17}^{(Q)} D_7 + k_{18}^{(Q)} D_8$

Then, $A_1 = A_1^{(P)} + A_1^{(Q)}$

$$= (k_{11}^{(P)} + k_{11}^{(Q)}) D_1 + (k_{12}^{(P)} + k_{12}^{(Q)}) D_2 + k_{13}^{(P)} D_3 + k_{14}^{(P)} D_4$$

$$+ (k_{15}^{(P)} + k_{15}^{(Q)}) D_5 + (k_{16}^{(P)} + k_{16}^{(Q)}) D_6 + k_{17}^{(Q)} D_7 + k_{18}^{(Q)} D_8$$

Write: $A_1 = k_{11} D_1 + k_{12} D_2 + k_{13} D_3 + k_{14} D_4 + k_{15} D_5 + k_{16} D_6 + k_{17} D_7 + k_{18} D_8$

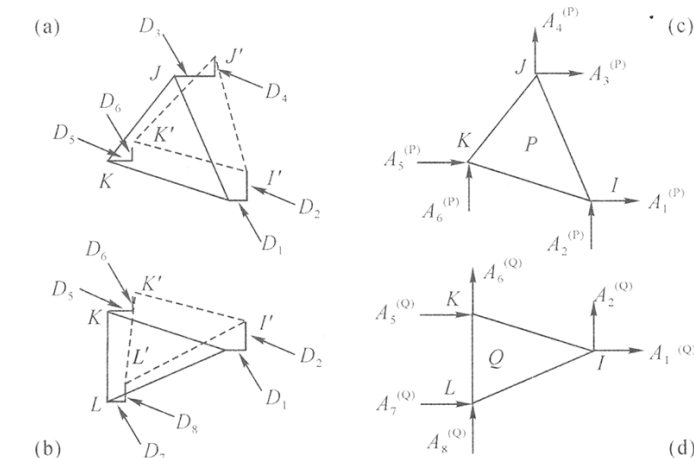


Fig. 1.13 (a) Displacements of IJK; (b) Displacements of IKL; (c) Actions for IJK; (d) Actions for IKL

It is seen that the system stiffness coefficients at the common DOF 1, 2, 5, and 6 are the (algebraic) sums of stiffness coefficients of the elements connected at these

DOFs. Thus,

$$k_{11} = k_{11}^{(P)} + k_{11}^{(Q)}, \quad k_{12} = k_{12}^{(P)} + k_{12}^{(Q)}, \quad k_{15} = k_{15}^{(P)} + k_{15}^{(Q)}, \quad k_{16} = k_{16}^{(P)} + k_{16}^{(Q)}$$

Similarly writing the equilibrium equations for the forces along the other three common DOF 2, 5, and 6, we will get:

$$\begin{aligned} k_{21} &= k_{21}^{(P)} + k_{21}^{(Q)}, \quad k_{22} = k_{22}^{(P)} + k_{22}^{(Q)}, \quad k_{25} = k_{25}^{(P)} + k_{25}^{(Q)}, \quad k_{26} = k_{26}^{(P)} + k_{26}^{(Q)} \\ k_{51} &= k_{51}^{(P)} + k_{51}^{(Q)}, \quad k_{52} = k_{52}^{(P)} + k_{52}^{(Q)}, \quad k_{55} = k_{55}^{(P)} + k_{55}^{(Q)}, \quad k_{56} = k_{56}^{(P)} + k_{56}^{(Q)} \\ k_{61} &= k_{61}^{(P)} + k_{61}^{(Q)}, \quad k_{62} = k_{62}^{(P)} + k_{62}^{(Q)}, \quad k_{65} = k_{65}^{(P)} + k_{65}^{(Q)}, \quad k_{66} = k_{66}^{(P)} + k_{66}^{(Q)} \end{aligned}$$

In fact, considering all the four elements connected at the node K in Fig. 1.12(a), as shown in Fig. 1.14, the stiffness coefficient k_{51} will not be just $(k_{51}^{(P)} + k_{51}^{(Q)})$ as given earlier, but will be as follows:

$$k_{51} = k_{51}^{(P)} + k_{51}^{(Q)} + k_{51}^{(R)} + k_{51}^{(S)}$$

R and S being the elements to the left of elements P and Q.

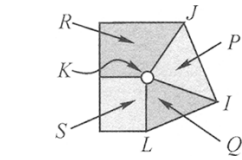


Fig. 1.14 Four Elements around K

In general, a typical system stiffness coefficient in the system stiffness matrix $[K_s]$ may be written, summed up all the M elements connected along the DOFs I and J,

$$k_{ij} = \sum_{m=1}^M k_{ij}^{(m)} \quad (1.28)$$

More than the mathematical justification, it can be intuitively appreciated that for a node to displace along any of its DOF, it has to exert actions to overcome the stiffnesses of all the elements attached at that node. In other words, the stiffness at a node is the sum of the contributions from all the elements meeting at the node.

The technique used in the computer assembly of the stiffness matrix for a system with n DOF from m individual member stiffness matrices may be now summarised as follows, with reference to Table 1.1 for the two elements P and Q:

- (1) Set up an (empty) system stiffness matrix $[K_s]$, $(n \times n)$ in size;
- (2) Determine the stiffness matrices $[K_m]$ of all the m elements, identified with their appropriate system DOF;
- (3) Add each term of the stiffness matrix of every element into the row and column of the system stiffness matrix, according to the system row and column DOF.

It schematically tabulates the two (6×6) stiffness matrices of the two elements P and Q in Table 1.1(Top), as well as the (8×8) system stiffness matrix assembled from them in Table 1.1(Bottom). For ease of presentation, $k_{ij}^{(P)}$ and $k_{ij}^{(Q)}$ have been shown as p_{ij} and q_{ij} , respectively.

Blank cells such as at the intersection of rows and columns for DOF (3,4) and (7, 8) imply that the nodes corresponding to them, J and L in this case, are not directly connected.

Thus, the system stiffness equation can be developed as:

$$\{A_s\} = [K_s]\{D_s\} \quad (1.29)$$

Table 1.1 Element Stiffness Matrices, (Bottom) System Stiffness Matrix

node	→	<i>I</i>		<i>J</i>		<i>K</i>		node	→	<i>I</i>		<i>J</i>		<i>K</i>	
↓	DOF	1 ^(P)	2 ^(P)	3 ^(P)	4 ^(P)	5 ^(P)	6 ^(P)	↓	DOF	1 ^(Q)	2 ^(Q)	3 ^(Q)	4 ^(Q)	5 ^(Q)	6 ^(Q)
<i>I</i>	1 ^(P)	P_{11}	P_{12}	P_{13}	P_{14}	$\boxed{P_{15}}$	P_{16}	<i>I</i>	1 ^(Q)	q_{11}	q_{12}	$\boxed{q_{15}}$	q_{15}	q_{17}	q_{18}
	2 ^(P)	P_{21}	P_{22}	P_{23}	P_{24}	P_{25}	P_{26}		2 ^(Q)	q_{21}	q_{22}	$\boxed{q_{23}}$	q_{26}	q_{27}	q_{28}
<i>J</i>	3 ^(P)	P_{31}	P_{32}	P_{33}	P_{34}	P_{35}	P_{36}	<i>J</i>	5 ^(Q)	q_{51}	q_{52}	$\boxed{q_{53}}$	q_{56}	q_{57}	q_{58}
	4 ^(P)	P_{41}	P_{42}	P_{43}	P_{44}	P_{45}	P_{46}		6 ^(Q)	q_{61}	q_{62}	$\boxed{q_{63}}$	q_{64}	q_{65}	q_{66}
<i>K</i>	5 ^(P)	P_{51}	P_{52}	P_{53}	P_{54}	P_{55}	P_{56}	<i>K</i>	7 ^(Q)	q_{71}	q_{72}	$\boxed{q_{73}}$	q_{74}	q_{75}	q_{76}
	6 ^(P)	P_{61}	P_{62}	P_{63}	P_{64}	P_{65}	P_{66}		8 ^(Q)	q_{81}	q_{82}	$\boxed{q_{83}}$	q_{84}	q_{85}	q_{86}

node	→	<i>I</i>		<i>J</i>		<i>K</i>		node	→	<i>I</i>		<i>J</i>		<i>K</i>	
↓	DOF	1	2	3	4	5	6	↓	DOF	1	2	3	4	5	6
<i>I</i>	1	$p_{11}+q_{11}$	$p_{12}+q_{12}$	p_{13}	p_{14}	$p_{15}+q_{15}$	$p_{16}+q_{16}$	<i>I</i>	1	$p_{11}+q_{11}$	$p_{12}+q_{12}$	p_{13}	p_{14}	$p_{15}+q_{15}$	$p_{16}+q_{16}$
	2	$p_{21}+q_{21}$	$p_{22}+q_{22}$	p_{23}	p_{24}	$p_{25}+q_{25}$	$p_{26}+q_{26}$		2	$p_{21}+q_{21}$	$p_{22}+q_{22}$	p_{23}	p_{24}	$p_{25}+q_{25}$	$p_{26}+q_{26}$
<i>J</i>	3	p_{31}	p_{32}	p_{33}	p_{34}	p_{35}	p_{36}	<i>J</i>	3	p_{31}	p_{32}	p_{33}	p_{34}	p_{35}	p_{36}
	4	p_{41}	p_{42}	p_{43}	p_{44}	p_{45}	p_{46}		4	p_{41}	p_{42}	p_{43}	p_{44}	p_{45}	p_{46}
<i>K</i>	5	$p_{51}+q_{51}$	$p_{52}+q_{52}$	p_{53}	p_{54}	$p_{55}+q_{55}$	$p_{56}+q_{56}$	<i>K</i>	5	$p_{51}+q_{51}$	$p_{52}+q_{52}$	p_{53}	p_{54}	$p_{55}+q_{55}$	$p_{56}+q_{56}$
	6	$p_{61}+q_{61}$	$p_{62}+q_{62}$	p_{63}	p_{64}	$p_{65}+q_{65}$	$p_{66}+q_{66}$		6	$p_{61}+q_{61}$	$p_{62}+q_{62}$	p_{63}	p_{64}	$p_{65}+q_{65}$	$p_{66}+q_{66}$
<i>L</i>	7	p_{71}	p_{72}			p_{75}	p_{76}	<i>L</i>	7	p_{71}	p_{72}			p_{75}	p_{76}
	8	p_{81}	p_{82}			p_{85}	p_{86}		8	p_{81}	p_{82}			p_{85}	p_{86}

As the system stiffness matrix $[K_s]$ is simply the superposition of the component member stiffness matrices, all the characteristics of member or element stiffness matrices, listed in Section 1.5.2 in Chapter 1, carry over into the system stiffness matrix. In particular, the system stiffness matrix at this point is singular, and cannot be inverted.

1.12 Equivalent Actions Due to Element Loads

The matrix formulation and solution can be only applied to express the effects of actions at the nodes. But in practical problems, the loads which cause deformations and consequent strains and stresses, may be on or inside the boundary of the elements. Such non-nodal loads are referred to as "Element Loads". Examples are:

- (1) Concentrated action A_c , applied on the boundary or within an element;
- (2) Distributed "Tensions" q , along the edge or surface of an element;
- (3) Distributed "Body Force" g , acting on all the particles of the element, as gravity, magnetic effect, or centrifugal action; and
- (4) Distributed "Initial Strain" ϵ_0 , due to temperature change, force fit of slightly larger or smaller component parts, etc.

The set of nodal actions that will cause the same deformations as each of these element loads, and hence may be substituted in their place, are referred to as

“Equivalent Loads”.

We have already used the term in Chapter 1, during the discussion of the effects of uniformly distributed on fixed-ended beams in Section 1.5.3.

We shall invoke the principle of zero virtual work to derive expressions for the equivalent loads. In Fig. 1.15, the IJK is defined as an elastically deformed shape of the finite element. Consider an additional virtual displacement $\{D^*\}$ imposed on each node. The corresponding equivalent nodal actions are $\{A_e\}$.

These will become are the equivalent nodal actions when the virtual work done by these actions equals that by the applied element loads. Note that each of the actions and displacements which have been identified with the node subscripts i , j , and k , will have the usual components along the coordinate directions.

1.12.1 Concentrated Action inside Element

Consider the element IJK loaded with a concentrated force $\{C\}$, at the point $P(x, y)$, as in Fig. 1.16. Note that P may also be on the boundary.

An additional virtual displacement described before is given to the element and the point P correspondingly moves to the position P' by the amount $\{U^*\} = \{u^*, v^*\}$.

External virtual work done by the applied action $\{C\}$, noting that $\{U^*\} = [N_p]\{D_e^*\}$,

$$W_a = \{U^*\}^T \{C\} = \{D_e^*\}^T [N_p]^T \{C\} \quad (1.30)$$

Then replace the applied force $\{C\}$ by equivalent actions $\{A_c\} = \{A_{c1}, A_{c2}, \dots\}$ at the nodes (similar to $\{A_e\}$ of Fig. 1.15 so as to cause the same displacements at the nodes as $\{C\}$ would).

The virtual work done by the equivalent nodal loads through the virtual nodal displacements,

$$W_c = \{D_e^*\}^T \{A_c\} \quad (1.31)$$

Equating the two values of virtual work from Eq. (1.30) and Eq. (1.31), we get:

$$\{A_c\} = [N_p]^T \{C\} \quad (1.32)$$

Thus, the equivalent load vector $\{A_c\}$ may be computed with the shape function $[N]$ evaluated at the location of $\{C\}$, and for the known value of $\{C\}$.

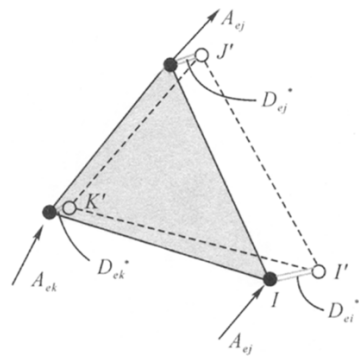


Fig. 1.15 Virtual Nodal Displacements

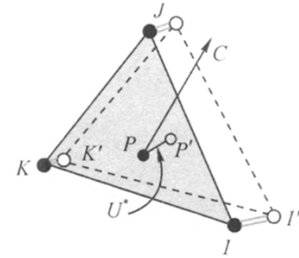


Fig. 1.16 Concentrated Force inside Element

1.12.2 Traction on Edge of Element

Let the element IJK be loaded with a traction $\{q\} = \{q_x, q_y\}$ per unit length, along the edge IJ, as shown in Fig. 1.17. Consider an element dS of the edge as marked with a thicker line.

The element is given an additional virtual displacement $\{D^*\}$ at the nodes I, J, K, and then move to the position shown by the broken lines. The edge element dS correspondingly moves by the amount $\{U^*\} = \{u^*, v^*\}$.

The applied traction $\{q\}$ is replaced by equivalent actions $\{A_q\} = \{A_{q1}, A_{q2}, \dots\}$ at the nodes (similar to $\{A_c\}$ of Fig. 1.15) so as to cause the same displacements at the nodes as $\{q\}$ would.

External virtual work done by the applied traction $\{q\}$ on the edge element dS , noting that $\{U^*\} = [N]\{D^*\}$,

$$dW_a = \{U^*\}^T \{q\} dS = \{D^*\}^T [N]^T \{q\} dS$$

For the entire edge, external virtual work done by the traction is:

$$W_a = \{D^*\}^T \int_{I \rightarrow J} [N]^T \{q\} dS \quad (1.33)$$

The integration to extend over the entire edge IJ subjected to the traction.

As in the case of the concentrated action, external virtual work done by the equivalent actions $\{A_q\}$,

$$W_q = \{D^*\}^T \{A_q\} \quad (1.34)$$

Equating W_a and W_q , the two values of virtual work from Eqs. (1.33) and (1.34), we get:

$$A_q = \int_{\text{EDGE}} [N]^T \{q\} dS \quad (1.35)$$

1.12.3 Body Force over the Element

The element IJK is loaded with a body force $\{g\}$ per unit volume, $\{g_x, g_y\}$ in this plane case, over the entire element, as shown in Fig. 1.18.

Consider an infinitesimal element $dx dy$ of the finite element as marked. Elemental volume $dV = t dx dy$, t being the element thickness in this plane case.

The element is given an additional virtual displacement $\{D^*\}$ at the nodes I, J, K, and then move to the position shown by the broken lines. The area element correspondingly moves by the amount $\{U^*\} = \{u^*, v^*\}$.

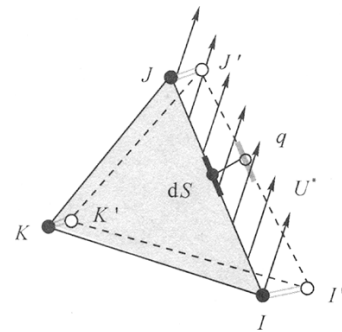


Fig. 1.17 Uniform Traction along One Edge

The applied body force $\{g\}$ is replaced by equivalent actions $\{A_g\} = \{A_{g1}, A_{g2}\}$ at the nodes (similar to $\{A_e\}$ of Fig. 1.15) so as to cause the same displacements at the nodes as $\{g\}$ would.

External virtual work done by the applied traction $\{g\}$ on the volume element dV , noting that $\{U^*\} = [N]\{D^*\}$,

$$\begin{aligned} dW_a &= \{U^*\}^T \{g\} dV \\ &= \{D^*\}^T [N]^T \{g\} dV \end{aligned}$$

For the entire element, external virtual work done by the body force is:

$$W_a = \{D^*\}^T \int_{VOL} [N]^T \{g\} dV \quad (1.36)$$

the integration to extend over the entire area (and hence volume) of the element.

As before, external virtual work done by the equivalent actions $\{A_g\}$,

$$W_g = \{D^*\}^T \{A_g\} \quad (1.37)$$

Equating W_a and W_g , the two values of virtual work from Eqs. (1.36) and (1.37), we get:

$$A_g = \int_{VOL} [N]^T \{g\} dV \quad (1.38)$$

1.12.4 Initial Strains in the Element

Initial strains may be introduced to a body due to temperature change, the necessity to force fit a component into place, and so on.

For example, when the temperature of a body changes by T , it experiences normal strains of $\alpha \cdot T$, where α is the thermal expansion coefficient of the material. No shear strains are developed.

Then the element IJK is loaded with initial strain $\{\epsilon_0\} = \{\epsilon_{x0}, \epsilon_{y0}, \gamma_{xy0}\}$, over the entire element, as shown in Fig. 1.19.

Consider an infinitesimal element $dx dy$ of the finite element as marked. As before, elemental volume for the plane case, $dV = t dx dy$.

The element is now given an additional virtual displacement $\{D^*\}$ at the nodes I , J , K , to the position shown by the broken lines.

The applied initial strain $\{\epsilon_0\}$ is replaced by equivalent actions $\{A_e\} = \{A_{e1}, A_{e2}\}$ at the nodes (similar to $\{A_e\}$ of Fig. 1.15) so as to cause the same displacements at

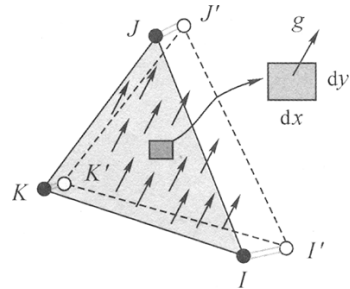


Fig. 1.18 Body Force on Element

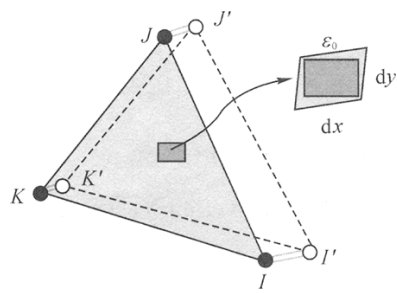


Fig. 1.19 Initial Strains in Element

the nodes as $\{\epsilon_0\}$ would.

In the case of initial strain, it must be remembered that only the elastic component of the strain (total strain minus the initial strain) would cause stresses in the material.

Hence Eq.(1.22) must be modified as:

$$[\sigma] = [E]\{\epsilon - \epsilon_0\} = [E][B]\{D\} - [E]\{\epsilon_0\} \quad (1.39)$$

Then, the expression for the internal work done, Eq. (1.25) gets modified as:

$$\begin{aligned} W_i^* &= \{D^*\}^T \left[\left(\int_{VOL} [B]^T [E] [B] dV \right) \{D\} \right. \\ &\quad \left. - \int_{VOL} [B]^T [E]\{\epsilon_0\} dV \right] \end{aligned} \quad (1.40)$$

The virtual work equation leading to the stiffness relation Eq. (1.26) is modified to:

$$\begin{aligned} \{A\} &= \left(\int_{VOL} [B]^T [E] [B] dV \right) \{D\} - \int_{VOL} [B]^T [E]\{\epsilon_0\} dV \\ &= [K]\{D\} - \int_{VOL} [B]^T [E]\{\epsilon_0\} dV \end{aligned} \quad (1.41)$$

The second term on the right-hand side represents the effect of initial strain and has the dimensions of force, or action in general. It may be designated as the equivalent load $\{A_\epsilon\}$ corresponding to initial strain, and shifted to the left-hand side, to give:

$$\{A_n\} + \{A_\epsilon\} = [K]\{D\} \quad (1.42)$$

where $\{A_n\}$ represents the actions directly applied at the nodes, and

$$\{A_\epsilon\} = \int_{VOL} [B]^T [E]\{\epsilon_0\} dV \quad (1.43)$$

Incidentally, $[E]\{\epsilon_0\}$ may be a directly applied “Initial Stress Vector” $\{\sigma_0\}$ also.

1.12.5 Total Action Vector

Thus for an element subjected to all the four element loads described in the preceding sections, the total action vector will be:

$$\{A\} = \{A_n\} + \{A_c\} + \{A_q\} + \{A_g\} + \{A_\epsilon\} \quad (1.44)$$

where $\{A_n\}$ equals concentrated actions applied at nodes, and $\{A_c\}$, $\{A_q\}$, $\{A_g\}$, and $\{A_\epsilon\}$ are known from Eqs. (1.32), (1.35), (1.38) and (1.44).

Eq. (1.44) is evaluated for all the elements, and then summed up to give the system action vector $\{A_s\}$. The stiffness equation will continue to be:

$$\{A_s\} = [K_s]\{D_s\}$$

with stiffness matrix $[K_s]$ being the superposition of individual element stiffness matrices given by Eq. (1.27).

Further solution will proceed according to the methodology described in Section 1.6 of Chapter 1, to yield displacements and support reactions.

1.13 Stresses and Strains

Apart from the deformations of the body analysed, the critical information always needed is the ability of the body to resist the applied loads without yielding or breaking.

In matrix analysis of structures, the end results of matrix analysis are the internal axial and shear forces and bending moments in the members. In finite element analysis of continua, the end results are strains and stresses.

Strains are simply obtained from Eq. (1.21), with the $[B]$ matrices recalled from storage, if stored earlier. If we are only interested in a few critical locations, it may be cheaper to re-compute the $[B]$ matrices for the specific elements.

Stresses can likewise be obtained from the strains using Eq.(1.22). Storage or re-computation of the stress influence matrix $[S]$ is not necessary.

The numerical output from finite element analysis will be overwhelming, too much to understand and digest. These days, with so many automated graphical facilities available on the computer, most packages have modules to present the results in graphical form. Deformed shapes, with displacements increased hundred-to thousand-fold to make them visibly meaningful, and strain and stress distributions displayed as contours with lines and colour bands depicting various value ranges, are excellent tools for understanding.

1.14 Stiffness Matrices for Various Elements

In many standard texts on the finite element method, at this point, actual stiffness matrices are usually developed and/or presented for various shapes and types of elements by application of the principles described in the preceding sections.

This would include: Plane stress, plane strain, axi-symmetric, solid, plate bending and shell elements, with various DOFs; and refinements such as isoparametric formulation, varying orders of integration, etc.

However, in this book, such development or even presentation of stiffness matrices will not serve such purposes. If readers wish to learn more about these specific topics, they may consult standard references such as Przemieniecki, J.S. and Zienkiewicz, O.C.

In each of these, in spite of the mathematical rigour of the actual development of

the stiffness matrix, the starting point is the shape function, which is an assumption and this is why the finite element method requires caution in its practical applications.

1. 15 Critical Factors in Finite Element Computer Analysis

Computers are used for solving problems with a large amount of calculation; finite element method is used to solve complex problems. Their combination leads to some special factors that must be considered and resolved, such as the following:

Computer modelling

The process of transforming and transferring details of an actual system into a form that the computer can recognise and work upon is called “computer modelling” or “idealisation”. It must be remembered that the computer will never know or handle the object itself. It can only manipulate numbers representing the various parts of the object and the actions which it is subjected to.

As such, the way users translate the object into input information will be the most critical aspect of the analysis. In certain cases, the modelling may be obvious and suggested by the configuration of the object itself. But in objects of continuous solids of a general irregular shape, much care and planning become important. Validation of the model may be critical to the acceptability of the results.

Input preparation

Large problems require large amounts of data, in terms of the coordinates of large numbers of nodes and the incidences (i.e. node connectivities) of large numbers of elements, as well as other items relating to material properties, boundary conditions, loading conditions, etc. Special means must be taken to produce and transfer them to the computer quickly and without error. Programs used for this purpose are called “Preprocessors”.

Output evaluation

Similarly, the results from the analysis will also be massive, which must be evaluated carefully to identify the magnitude, nature and location of worst effects, again quickly and correctly. In finite element analysis of unusual problems, ways must be provided for users to view summaries of critical results. Where the object is complex and assumptions (as in support conditions) have been made, some means of bounding the magnitude of possible error must be provided. Programs used for this purpose are called “Postprocessors”.

As a case study on all three aspects cited above, the author cites his paper on the finite element analysis for the stress concentration in a steel pressure vessel.

1. 16 Modelling Considerations

Most finite element problems are unique and deserve special attention in modelling.

Even experienced analysts who investigate a finite element problem using the same software, may come up with varying results sometimes differing by orders of magnitude!

Except for the simplest and most conventional cases, modelling of a structure or system for computer analysis is a skill involving subjective decisions and interpretations. The main fact to be remembered is that the computer deals only with and in numbers, without the implication of any physical quantity or real entity.

Hence two important steps must be included in the modelling/analysis cycle, namely:

- (1) Model validation, and
- (2) Result verification.

With computers, engineers and scientists can analyse larger and more complicated systems, and include more of the surrounding domain, more of the supporting media, and so on, than before the advent of computers.

Under these circumstances, idealisation becomes even more important than when the structures were simpler. Furthermore, intelligent assumptions and decisions will still have to be made on the following questions:

- (1) Should a 2D analysis or 3D analysis be done?
- (2) Should every little detail be included, and if not, what can be omitted?
- (3) How much of the supporting medium should be included?

The question of 2D vs. 3D is a subjective one. With today's powerful computers, users tend to go to 3D as a rule. However, while it may seem more realistic, there are two counter-arguments:

- (1) Is 3D really necessary all the time?
- (2) Does it involve extra information, further assumptions, etc. in the input?

The answer is often "No" to the first, and "Yes" to the second one. There is considerable published material on this topic to convince one to use discretion and experience before launching a full-blown 3D effort.

The author has occasionally run various cases of a particular problem by both 2D and 3D, and extracted a "Correlation Factor" between 2D and 3D (for specific results), and later run only 2D cases of the same problem, applying the correlation factor to predict the more realistic 3D result.

One difficulty which is unique to finite element analysis is that the magnitude of the "discretisation error" arising from the division of the domain into elements is often unpredictable, and needs independent validation. Errors may also occur due to wrong choice of type of element, wrong modelling of the boundary or loading conditions, etc.

The best protection against making a wrong choice of mesh or input parameters is experience developed by long use, or knowledge borrowed from experts, through publications or otherwise.

Lacking these, users may need to adopt one or more of the following methods to evaluate the validity of the computed findings and extract dependable results from

finite element analysis:

(1) Physical testing some typical continua of the type and general dimensions analysed and comparing the experimental and computed results. But test specimens and tests are often too costly, involve delays, and may or may not conform to the object and conditions of the actual problem.

Furthermore, most of the time, finite element analyses are resorted to only when the other classical or matrix methods cannot be applied, and as such, it may not be feasible to apply experimental methods to them.

(2) Making the finite element model self-validating as follows:

1) Sensitivity studies must be made on computer models including various parameters and their combinations likely to influence the object's behaviour, and their results evaluated to ascertain which of the parameters will be more critical and which less.

If this is not done, important parameters may be left out by oversight or assumed insignificance. Alternatively, any and every parameters may be included, over-burdening the computer input, processing and evaluation.

2) Convergence studies must be conducted on at least two meshes to obtain an estimate of the discrepancy in the critical stresses.

If the difference in results from two different meshes is beyond tolerable percentage, a third (perhaps even a fourth) finer mesh analysis will be needed to check the convergence of the results to some asymptotic value. In the author's experience, most problems give rise to wide variations for the same problem from different meshes.

In this case, the results for critical stresses or displacements from three or more meshes must be utilised to extrapolate an improved (predicted) result for the continuum, as described later, and as demonstrated in the author's paper (Ref.3.1), and summarised in a later section.

(3) In many cases, solution to a similar (simpler) configuration of the subject case may be available by other methods, or from other sources. Such problems may be analysed by finite elements, and the type and density of mesh that best predicts the known values may be adopted for the complex case on hand.

(4) Occasionally, the configuration of the object may be close to a problem which is amenable to classical or approximate solutions. In such cases, an analysis may provide a rough check on the validity of the finite element solution. However, with complex structural forms and combinations commonly analysed by finite element method, approximate solutions may be far away from the exact solution, and comparison with computer solutions in such cases may be misleading.

Then, "self-validation" by running a few more cases of the same problem with slight modifications of supports, connectivities, element idealisations, etc. may be quite informative.

Once a model has been validated, parameter studies wherein significant parameters governing the problem are varied between their maximum and minimum practical values (and preferably even a middle value), and the results for significant

variables evaluated by regression analysis, to obtain good prediction equations for the continua.

1.17 Asce Guidelines

A publication of the American Society of Civil Engineers gives some guidelines for finite element idealisation. Some relevant ones are listed hereunder:

- (1) Finite element gridworks should be uniform where this is practical. However, nonuniformity is often necessary to achieve refinement of the gridwork in regions of rapid changes in loading and/or behaviour.
- (2) Quadrilateral finite elements should be used except where triangular shapes are necessary to effect grid refinement or accommodate irregularity in geometry and/or loading.
- (3) Analyses to obtain displacement (or force) behaviour do not require as refined a gridwork as is required to obtain strain (or stress) behaviour.
- (4) Analyses including nonlinearity in geometry or material usually require a more refined idealization than linear analyses.
- (5) Where possible, gridpoints should be numbered from regions of large displacement toward regions of small displacement (e.g. from tip toward root for a cantilever beam).
- (6) Monotonic convergence characteristics are seldom guaranteed with respect to behaviour at a point; an exception may be the displacement under a single concentrated load.
- (7) When flat elements are used in the polygonal approximation of curved shell surfaces, rotation about the normal to the curved surface should usually be retained as a degree of freedom. However, the retention of such degrees of freedom may yield an ill-conditioned stiffness matrix. If these degrees of freedom are suppressed, it is important to check that the resulting reactions are acceptably small.
- (8) The use of constraint equations as a means of imposing special connections and boundary conditions may increase the bandwidth substantially.
- (9) The use of constant strain triangle finite elements should be avoided wherever possible.
- (10) The recommended first checks on predicted behaviour are equilibrium checks using loads, reactions and forces.
- (11) Aspect Ratio (length/height) limits vary from element to element; however, a general guideline is to keep element aspect Ratios below 10 for deformation analysis and below 5 for stress analysis.
- (12) Curvature of sides of iso-parametric elements should be employed only to represent curved boundary geometry or curvature of stress iso-clinics (where this can be reasonably inferred from the geometry and loading).
- (13) Non-uniform distribution of intermediate nodes on the sides of higher order

- elements should be avoided wherever possible.
- (14) With higher order elements, special care must be exercised in defining boundary conditions because the solutions for some elements are sensitive to this choice.
 - (15) Elements of extreme shape (high aspect Ratio rectangles, large angled triangles, re-entrant corner pentagons) are unfavorable with respect to manipulation error and should be avoided.
 - (16) If the structure and loading possess symmetry, advantage should be taken into account of this fact.
 - (17) For anisotropic materials, the subscript on Poisson's Ratio must be clearly defined. In addition, the theoretical limits on ν , E and C should be checked.
 - (18) For isotropic materials in "compressible solids" programs, the value of Poisson's Ratio must not be too close to 0.5.
 - (19) Rapid changes in element size should be minimized.
 - (20) Do not try to fake internal openings by using a very soft (i.e. very low E) material unless all the "free" nodes in the opening are restrained. (This is used in conjunction with some mesh generators which do not permit internal openings.)
 - (21) When modelling reduced portion of the structure for evaluation of local effects, make the boundary of this local area far enough away from the area of interest to avoid boundary effects on the information at the area of interest.
 - (22) Connecting high order elements to low order elements can cause stress irregularities which should either be smoothed or ignored.
 - (23) For complex structures consider a "staged" analysis. Analyze the entire structure with a coarse mesh and then study the areas of interest with a fine mesh, using as boundary loads the results of the coarse analysis.
 - (24) If flat shell elements are used to model a curved shell, the pressure load should be applied as concentrated loads at the nodal points.
 - (25) In modelling long cylindrical shells, the model should include at least three wavelengths on either side of any perturbation in geometry and/or loading.
 - (26) Two elements through the wall thickness of a thick-walled pressure vessel will usually give reasonable results with incompatible displacement elements.
 - (27) Solutions for structures with uniform stiffness distribution are more accurate than those for structures with stiff and flexible regions.
 - (28) A boundary layer of width equal to plate thickness usually exists along the edges of shells. There are high stress gradients in the boundary layers. To properly reproduce these stress gradients, there should be a double row of elements along the edge, the overall width of the row being equal to the boundary layer width.
 - (29) A boundary layer of width t may exist along the edge of a plate which undergoes shear deformation, in addition to bending deformation. Remarks similar to Guideline 28 apply.
 - (30) If the solution routine is band-width dependent, the band width should be minimized. Likewise, if a solution routine is dependent on the element

numbering scheme, an optimum sequence should be used.

- (31) For convergence studies, one must refine (i.e. sub-divide) the original mesh, otherwise a new approximating sequence is begun.

Most of the guidelines must be taken only as suggestions or recommendations, but not as rules, because with finite elements, decisions must be made based on merits of each case, unless it happens to be almost identical with others already successfully analysed earlier.

1.18 Preprocessors and Postprocessors

1.18.1 Preprocessors

Fig. 1.20 depicts a machine part, a continuous solid that has been divided into a mesh of 188 solid elements, connected at 396 nodes. This is given only for illustrative purposes. Actual finite element models would be much more complex and have thousands of nodes and elements.

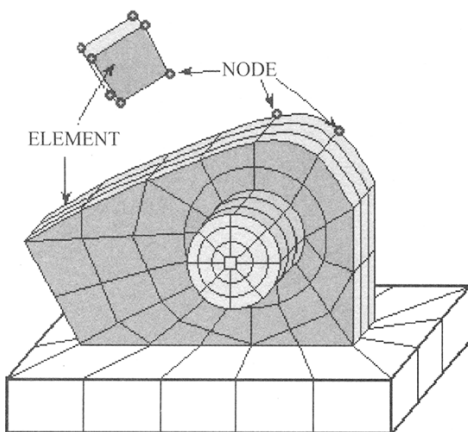


Fig. 1.20 Machine Part Discretised into Finite Elements

As listed in Section 1.5, the input normally includes: 1) Geometry, 2) topology, 3) material properties, 4) element types and cross-sectional properties, 5) boundary conditions, and 6) loading conditions.

Each item would typically involve an average of five to ten items of data for each node and element. The total could run to millions of numbers, every one of which had to be right for the analysis program to work, and then for the answers to be correct.

Even if a large number of people were employed to generate these numbers, it would be a monumental if not impossible task to detect and eliminate all the errors that would inevitably creep in.

So computer programs for special purpose are used to generate and display the data for matrix structural and finite element programs for the analysis of different objects. These programs are called “Preprocessors”.

In due course, computer graphics offered powerful display and manipulative capabilities. Soon after computer analysis package developers added preprocessor modules to display and edit the input and generated data on the monitor.

Now the analyst could literally see his model and confirm the correctness of his data, or locate and correct the errors, and then proceed with the analysis without delay of time or waste of computation.

The automatic generation of data in regions of regular geometry and topology, selective data display, zooming and rotation facilities, text annotation and colour coding, and on-screen editing capabilities, have now freed the analyst from struggling with the data preparation, checking, and correction.

One might almost say that without these preprocessors, practical application of the matrix and finite element analysis would not have developed and been applied to the extent it has been applied and it is being applied today.

Current preprocessors may be categorised into the following broad groups:

- (1) Numerical routines to interpolate omitted node coordinates and element incidences at equal or specified (proportionate) intervals.
- (2) Graphic input modules by which users can “create” and sub-divide his structure.
- (3) Menu-driven text help (input instructions) mode to guide users into developing the input commands.
- (4) “Wizards”, namely user-friendly, icon-based, menu-driven guidelines for automatic generation of data required for the analysis, based on a few input parameters from the user, mostly by mouse-click selection. Many assumptions are built in to minimise input data.

1. 18. 2 Postprocessors

If the situation of the large input was bad, the problem with the voluminous output became worse. For each node and each element, large number of displacements, forces and reactions, moments and torques, stresses and strains, etc. were computed.

Printed output for a single analysis could fill boxes, and it was impossible for analysts to go over all the numbers and keep track of the changes, to find the critical values necessary for design. It was too easy to get lost in the maze of numbers and miss the big picture.

So analysts sought selective output in critical regions. Large number of draftsmen toiled to plot critical quantities across specified sections and lines. Again, computer programs were written to digest the massive output into manageable and understandable summaries. These came to be called “Postprocessors”.

Here too, computer graphics came to the rescue, to even greater effect than with the input. Results could be superposed over the image of the object, also selectively, zoomed up in specific regions, and displayed in desired orientations. Images of the distorted object, force and moment diagrams for articulated structures, and stress

and strain distributions for continuous solids could all be viewed on the click of a button.

This feature enabled immediate validation of the computer model and interactive analysis for changed configurations and for different boundary and loading conditions, eventually leading to optimum design.

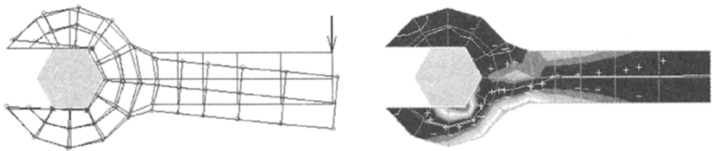


Fig. 1.21 Spanner (a) Deformed Shape, and (b) Stress Contours

Fig. 1.21 depicts the computer “Scope” display from GTSTRUDL (Georgia Tech STRUctural Design Language) an integrated structural and finite element analysis package, for the analysis of a spanner tightening a hexagonal nut.

The left sketch shows the original and deformed shapes. The right sketch displays the stress distribution contours.

This is just an illustrative example, as real-life situations would be much bigger in data size and complexity.

1.19 Support Modelling

In earlier times, any component being analysed was assumed to rest on a firm foundation, often fixed to the base. In reality, however, there is a large interaction between the components and their support, the magnitude of which may be quite significant. Modern computerised methods enable the designer to take account of these effects.

It is very important to decide whether a node is constrained in all its DOFs (namely “fixed”), or constrained on certain DOF (“pinned”, “sliding”, etc.), or not constrained at all (“free”). In axi-symmetric solids or shells and in symmetric halves of components, the support conditions may not be obvious, and wrong choices will lead to very erroneous results.

The support medium may also be modelled by finite elements with actual properties being input. The extent of the support medium should be at least 2 to 3 times the size of the component being analysed, and would involve quite a bit of discretisation. Alternatively and with sufficient accuracy, they are usually modelled as springs under the component.

1.20 Improvement of Results

The result from analysis with a single mesh, unless substantiated by other evidence,

is really good only for general qualitative interpretation, and may not be sufficiently accurate for dependable quantitative conclusions.

It is well known as one of the strengths of the finite element method, that for well defined problems, the results converge asymptotically as the mesh is refined, that is as n , the number of DOF (or the number of nodes or elements) is increased.

Many studies have tried to develop a means to extrapolate the results from two or more meshes to the asymptotic result, assumed to be “exact”, corresponding to an infinite number of elements corresponding to the actual continuum.

One conclusion is that when a mesh is progressively divided so that a mesh is developed from another mesh by sub-dividing the coarser equally in all coordinate directions, then the error (for a certain class of elements and for square shapes) is the order of h^2 , where h is the element size parameter. Note that the element size is (roughly) proportional to $(1/n)$.

Thus, if a rectangle 6 cm by 4 cm is first analysed with square elements of 2 cm side, and then analysed with square elements of 1 cm side (obtained by sub-dividing the original mesh equally in both directions), then the error is reduced to $(1 \text{ cm}/2 \text{ cm})^2$ or one-fourth of the starting value.

This observation has been utilised to extrapolate known results for two or more meshes to the continuum by what is known as “Richardson’s Extrapolation”, which has been widely used in finite difference applications.

However, in the general case, square (or cube shaped) elements are not the norm, where mesh is often not uniform but graded, and it is very difficult to get mesh sequences increasing 4 times for 2D or 8 times for 3D for every successive refinement.

Hence in general situations not conforming to the theoretical requirements of mesh variations, a strategy successfully adopted by the author is a modification of Richardson’s Extrapolation as follows:

- (1) Solve the problem by three or more meshes with DOF numbering n_1, n_2, n_3, \dots , not necessarily in any sequence of sub-division. (Note that the technique must not be applied to results from two meshes!)
- (2) Confirm that corresponding values of any critical result, say s_1, s_2, s_3, \dots tend to converge. Fig. 1.22(a) shows the plot of raw data. Note that at this stage, attempting to estimate the asymptotic value may be very subjective, as indicated by the two possible curves shown by full and broken lines in the figure, both passing through the three points.
- (3) Plot s_1, s_2, s_3, \dots against $(1/n_1)^2, (1/n_2)^2, (1/n_3)^2, \dots$
- (4) If the three points happen to be in a straight line (or at least nearly so) as shown by the full line in Fig. 1.22(b), then extend the line through them backwards to the vertical axis, to obtain the best estimate for continuum from the three meshes.
- (5) In general, the three points will not lie on a straight line, but in a curve as shown by the broken line in Fig. 1.22(b). By trial and error, find the value of the exponent m in $(1/n)^m$ for which the three points lie in a (nearly) straight line.

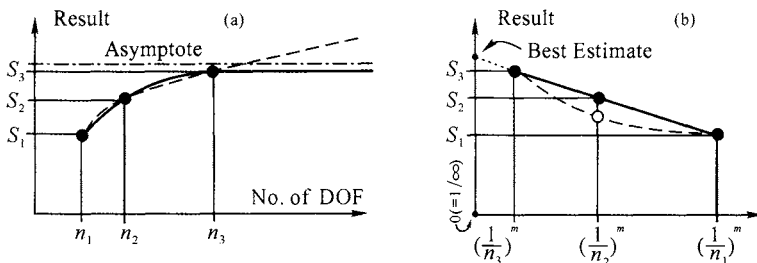


Fig. 1.22 Results from Three Meshes for (a) Linear Plot, and (b) Exponential Plot

Then extend the line backwards to obtain the best estimate.

This procedure is simply a practical way to get a best estimate from three (or more) sets of results on hand, and not a theoretically valid method to obtain the asymptotic value. Furthermore, such extrapolation and the estimated value are valid only locally and for the specific critical value plotted. The more the number of meshes, the better the estimate of the asymptotic value.

References

1. Argyris JH (1995) Energy Theorems and Structural Analysis. Aircraft Engineering 27
2. Bendixen A (1914) Die Methode der Alpha Gleichungen zur Bererchnung von Rahmenkonstruktionen, Berlin
3. Castigliano A (1875) Nuova Teoria Intorno dell Equilibrio dei Sistemi Elastici. Atti Acc Sci Torino
4. Clapeyron (1857) Theorem of Three Moments. Comptes Rendus 45:1076
5. Clough RW (1960) The Finite Element Method in Plane Stress Analysis. J Struc Div, ASCE, Proc. 2nd Conf. on Electronic Computation 345-378
6. Cook RD, Malcus DS, Plesha ME (1989) Concepts and Applications of Finite Element Analysis, Third Ed. New York, USA:John Wiley & Sons
7. Corum JM, N Krishnamurthy (1969) A Three-dimensional Finite Element Analysis of a Prestressed Concrete Reactor Vessel Model, Proc. of Symposium on Application of Finite Element Methods in Civil Engineering. Vanderbilt University, Nashville, Tennessee, USA 63-94
8. Courant R (1943) Variational Methods for the Solution of Problems of Equilibrium and Vibration. Bull Am Math Soc 49:1-23
9. Cross H (1932) Analysis of Continuous Frames by Distributing Fixed-End Moments. Trans ASCE 96:1-10
10. Desai CS, JF Abel (1972) Introduction to the Finite Element Method. New York, USA:van Nostrand Reinhold Co.
11. Euler L (1774) Methods Inveniendi Lineas Curvas Maximi Minimine Proprietate Gaudentes. Lausanne and Geneva: M. Bousquet

12. Galerkin BG (1915) Series Solution of Some Problems of Elastic Equilibrium of Rods and Plates (Russian). *Vestn Inzh Tech* 19:897-908
13. Gallagher RH (1975) *Finite Element Analysis Fundamentals*. New Jersey, USA: Prentice Hall, Inc.
14. Hrenikoff A (1941) Solution of Problems in Elasticity by the Framework Method. *J Appl Mech* 8:A169-A175
15. Huebner KH (1975) *The Finite Element Method for Engineers*. New York, USA: John Wiley & Sons 9-13
16. Krishnamurthy N (1983) *Finite Elements for the Practicing Engineer*. Singapore: Inst Engrs 23(1)
17. Levy S (1953) Structural Analysis and influence Coefficients for Delta Wings. *J Aero Sci* 20 (7): 449-454
18. Livesley RK (1964) *Matrix Methods in Structural Analysis*. Pergamon Press
19. Maney GB (1915) *Studies in Engineering (No. 1)*. Minneapolis, Minnesota: University of Minnesota
20. Maxwell JC (1864) On the Calculations of the Equilibrium and Stiffness of Frames. *Phil Mag* 4(27): 294
21. McHenry D (1944) A Lattice Analogy for The Solution of Plane Stress Problems. *Proc Inst Civ Engrs* 21(2):59-82
22. Melosh RJ (1963) Basis for Derivation of Matrices for the Direct Stiffness Method. *AIAA J* 1(7):1631-1637
23. Morice PB (1959) *Linear Structural Analysis*. New York, USA: The Ronald press Co.
24. Newmark NM (1943) Numerical Procedure for Computing Deflections, Moments, and Buckling Loads. *Trans ASCE* 68-69
25. Oden JT (1972) *Finite Elements of Nonlinear Continua*. New York, USA: McGraw-Hill Book Co.
26. Przemieniecki JS (1968) *Theory of Matrix Structural Analysis*, New York, USA: McGraw-Hill Book Co.
27. Rubin Carol, N Krishnamurthy, E Capilouto, H Yi (1983) Stress Analysis of the Human Tooth Using a Three-dimensional Finite Element Model. *J Dent Res* 62 (2):82-86
28. Southwell RV (1940) *Relaxation Methods in Engineering Science*. Oxford, UK: Clarendon Press
29. Turner MJ, Clough RW, Martin HC, Topp LJ (1956) Stiffness and Deflection Analysis of Complex Structures. *J Aero Sci* 23(9):805-823
30. Von Karman, T MA Biot (1940) *Mathematical Methods in Engineering*. New York, USA: McGraw-Hill Book Co.
31. Wieghardt K (1906) Ber einen Grenz Bergang der Elastizit Tslehre und Seine Anwendung auf die Statik Hochgradig Statisch Unbestimmter Fachwerke. *Verhandlungen des Vereins z. Bef rderung des Gewerbefleisses. Abhandlungen* 85:139-176
32. Wilson EL (1963) Finite Element Analysis of Two-dimensional Structures,

- Report No. 63. Dept of Civil Eng Univ of California, Berkeley
- 33. Zienkiewicz OC, Cheung YK (1967) The Finite Element Method in Structural and Continuum Mechanics, London, UK: McGraw-Hill Publishing Co.
 - 34. Krishnamurthy, N (1971) Three dimensional Finite Element Analysis of Thick Walled Pipe Nozzle Junctions with Curved Transitions, Preprints of the First International Conference on Structural Mechanics In Reactor Technology, Berlin, Germany, 3. Reactor pressure vessels, Part G Steel Pressure Vessels. Organised by: Bundesanstalt fur Materialprufung (BAM), Berlin, Commission of the European Communities, Brussel
 - 35. Task Committee on Automated Analysis and Design, Committee on Electronic Computation, Guidelines for Finite Element Idealization, Meeting Preprint 2504 (1975) ASCE National Structural Engineering Convention, New Orleans, Louisiana, USA

Introduction to Implant Dentistry

Rodrigo F. Neiva¹, Hom-Lay Wang², Jianping Geng³

^{1,2}School of Dentistry, University of Michigan, Ann Arbor, USA

Email: homlay@umich.edu

³Clinical Research Institute, Second Affiliated Hospital, School of Medicine, Zhejiang University, Hangzhou, China

2. 1 History of Dental Implants

Dentistry aims at replacing missing teeth since it was first recognized as a profession. For centuries, dental practitioners have relied on their own skills and various artifacts to develop esthetic and functional alternatives to minimize sequelae that occur as a result of edentulism. Partial, complete, fixed, or removable dentures are by far the most commonly used forms of tooth replacement applied. In other words, these devices have been incorporated into the oral cavity anchored on either remaining teeth and/or other anatomical structures. Only scarce archeological reports have demonstrated attempts of incorporating prosthetic devices into the jaws as more natural and functional replacements. However, predictability of these methods was not achieved until recently. (Table 2.1)

Table 2. 1 Advantages & Disadvantages of Implant Therapy

Advantages	Disadvantages
Highly predictable	Surgical intervention
Preservation of osseous structures	Higher costs
Natural masticatory function	Esthetics

In 1952, in a modestly appointed laboratory in the university town of Lund, Sweden, Professor Per-Ingvar Bränemark had an extremely fortunate accident, what most scientists call serendipity. Much to his irritation, Dr. Bränemark observed that it was virtually impossible to recover any of the bone-anchored titanium microscopes he used in his orthopedic research. The titanium had apparently bonded irreversibly to living bone tissue, an observation which contradicted contemporary scientific theory. Metal implants in contact with living bone were thought to be embedded in

soft tissue, a term known as fibro-osseous integration. This form of metal-to-bone integration was never capable of achieving strong anchorage to bone. Dr. Bränemark subsequently duplicated his findings and demonstrated that under carefully controlled conditions, titanium could be structurally integrated into living bone.¹ This titanium-to-bone integration was found to be extremely rigid, in contrast to the previously known concept of fibro-osseous integration. Dr. Bränemark named this phenomenon. Osseointegration has been described as a direct structural and functional connection between living bone and the surface of a load-bearing implant. This concept was later modified with more advanced imaging techniques. Scanning electron microscopy revealed that a thin proteoglycan layer exists between titanium and bone.

Soon after presenting osseointegration, Dr. Bränemark realized that his discovery would have uncountable applications beyond the field of orthopedics. The most significant application would probably be anchorage to intra-oral prosthesis. Leonard Linkow was the first to utilize titanium in intra-oral rehabilitation. He reported utilization of titanium blade-form intra-osseous implants to provide stability and enhanced function to partial and complete dentures.² These findings triggered developments of a series of studies to better illustrate the potential of osseointegration in treating edentulism.³⁻⁵ Later, Dr. Bränemark revisited this concept by introducing hollow titanium screws for the same purpose.⁶ An increased success rate, clinical applicability, and reduced rate of complications were obtained with this type of fixtures when compared to previously used blade-form implants.⁷ This screw has a very similar morphology and configuration with currently used endosseous implants. The hallmark paper of modern implant dentistry was published by Dr. Bränemark in 1977 in which the first long-term longitudinal study in this field was reported. This 10-year report provided scientific data for the development of the currently used implantation protocols and implant systems.⁸ The replacement of missing teeth with implant-supported prostheses has been a widely accepted treatment modality. Implants as a treatment option will be extensively used due to their high success rate and wide array of restorative options.⁹⁻¹¹

2. 2 Phenomenon of Osseointegration

The interactions between synthetic materials and host tissues require achievement of an optimal biological interface between the implant and the surrounding tissue. Adhesion molecule/cytokine interactions, specially osteopontin, an adhesion molecule as well as a cytokine, seem to play an important role during the wound healing process of dental implants¹². An acute inflammatory response occurs after implant osteotomy preparation that includes the releasing and activation of a variety of cytokines and growth factors, which mediate initial events. Most of these factors come from platelets, and the others are released by PMNs and macrophages. As a result, mesenchymal cells migrate onto clots and synthesize a collagen network that becomes a scaffold for wound repairing. Local factor production determines the

quality of bone formation or the formation of fibrosis^{13,14}. (Fig. 2.1)

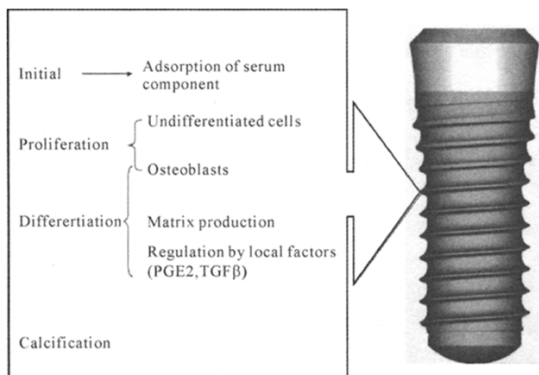


Fig. 2.1 Sequence of Events During Osseointegration of Dental Implants

The earliest events following implant placement are adsorption of water, ions and small biomolecules and are followed by adsorption and exchange of larger biomolecules such as proteins. The properties of the implant surface and those of individual proteins dictate the organization of the adsorbed protein layer, which in turn determines the cellular response to implant surface.

Following adsorption of water, ions and small biomolecules, cell proliferation begins. Cell proliferation is modulated and influenced by TGF- β 1, PGE₂, BMP-2, and 1,25-(OH)₂D₃ (vitamin D). The proliferation of undifferentiated mesenchymal cells is followed by differentiation of osteoblast-like cells. Appropriate mineral deposition is critical to ensure that the subsequent remodeling cycle on the implant surface will be optimal. Matrix production is necessary for the correct interrelationship between the apatite crystals and collagen¹⁵. Integrins are transmembrane proteins that mediate attachment to extracellular matrix proteins. Integrins as ECM receptors are believed to play a role in signal transduction and gene regulation, potentially influencing cellular migration, differentiation, and maturation. Cells are not actually attached to titanium itself, but to the organic material that adheres to the surface of that material. In this way, they form focal attachments through their integrin receptors, with arginine-glycine-aspartic acid (RGD) sequences in proteins such as fibronectin and vitronectin¹⁶.

The formation of a TiO₂ layer is considered to be the key to ideal interaction between titanium and bone¹⁷. The result of dissociative adsorption of water on TiO₂ is a hydroxylated surface with two different types of hydroxyl groups. TiO₂ is an amphoteric surface and has the ability to bind with both acids and bases¹⁸. For cell attachment to be possible, the active sites of proteins have to be accessible to the corresponding sites on cell membrane, which means that globular proteins such as fibronectin have to be adsorbed in a non-denatured state similar to their conformation in solution. The high biocompatibility of titanium can be explained

since the amorphous TiO₂ layer is a favorable surface for protein adsorption¹⁹. Four interrelated properties of biomaterials (chemical composition, surface energy, surface roughness, and surface topography) affect mesenchymal cells in vitro. Attachment, proliferation, metabolism, matrix synthesis, and differentiation of osteoblast-like cell lines and primary chondrocytes are sensitive to one or more of these properties²⁰. Osteogenesis around implants is affected by the physical and chemical characteristics of the biomaterials used. The osteoprogenitor cells must migrate to the implant site and synthesize and secrete a mineralizable extracellular matrix. Because this is new bone formation, the mechanism by which the cells calcify their matrix involves extracellular organelles called matrix vesicles in a process termed "primary mineralization"²¹. However, this process has shown to be delayed when compared to normal primary bone formation during bone healing. The delay in mineralization is compensated by an enhancement of primary mineralization by titanium²².

The healing response of bone to the injury of implant insertion is similar to its response to fracture. If there is absolute stability between the bone and the implant, the injury to the bone will result in bone formation conforming to the surface configuration of the implant. There is first appositional bone growth and subsequently bone ingrowth into the interstices of the surface. The newly formed bone is not an uninterrupted layer of bone. If the implant is relatively stable after insertion, the healing response results in the implant becoming enveloped by densely organized fibrous tissue with occasional area of fibrocartilage, without any area of resorption in the surrounding bone. If the implant is unstable after insertion the healing response causes the implant to become surrounded by loosely organized fibrous tissue with active bone resorption occurring in the surrounding bone²³.

The process of ossification around implants is composed of three stages. At first incorporation by woven bone formation occurs, followed by bone remodeling and maturation. Woven bone is the primitive type of bone characterized by random orientation of collagen fibrils, numerous osteocytes, and low mineral density. Woven bone formation dominates the first 4-6 weeks after surgery²⁴. Lamellar bone is the most elaborate bone tissue. Packing collagen fibrils into parallel layers with alternating course gives it the highest ultimate strength. Lamellar bone replaces woven bone by apposition²⁵. Intense remodeling in lamellar bone adjacent to endosseous implants characterizes the last stage of the healing process. Intense remodeling begins at around 3 months and decreases after several weeks, but continues for the rest of life.²⁶ Remodeling starts with osteoclastic resorption, followed by lamellar bone deposition.²⁴

Little information is available on the bone-resorptive activity that occurs around implants during osseointegration. However, the role of osteoclasts, macrophages, and stromal cells in those catabolic processes associated with bone remodeling has been demonstrated.²⁷ The integrity of connective tissues surrounding dental implants may be influenced by a balance between matrix metalloproteinases (MMPs) and tissue inhibitors of metalloproteinases (TIMPs). A significant increase in the TIMP-1 level at 1 week after implantation compared with that in gingival crevicular fluid (GCF)

from healthy periodontium has been reported. Four weeks after implantation it had reached the same level as that in the GCF of healthy subjects. The data has also disclosed a higher post-implantation collagenase activity level at 1 week than those at weeks 2, 4, and 12. This may be due to the increase in MMP-1 and -8. The overproduction of TIMP-1 in the wound area after implantation could, to some extent, inhibit excessive tissue destruction and degradation of the neo-matrix in wound repair due to MMPs²⁸.

Four biomechanical parameters (peak force, vertical displacement, interface stiffness, and strain energy) were measured at implant placement and after 3 months of healing during push-in tests on implants placed in the mandibles of dogs. Results showed increasing values of peak force, interface stiffness, and strain energy after 3 months of healing, but decreasing value of vertical displacement. These findings suggest that the interface stiffness, which is considered as a major factor for implant success, increases during 3 months of healing in dogs (correspondent to a 4 to 6 month healing period in human mandibles), which indicates that a 4 to 6 month healing period for dental implants is justifiable.²⁹

Tissue damage due to inadequate surgical techniques, resulting in excessive bone necrosis; bacterial contamination of the implant and/or the wound in course of surgery or insufficient maintenance care procedures in the healing phase of 1-stage implants; and the instability of the implant and/or premature loading, are considered to be the key factors that can influence bone healing around titanium implants³⁰. Studies on the effect of bacterial infection on the peri-implant tissues revealed a decrease in woven bone formation due to infection³¹.

2.3 The Soft Tissue Interface

Epithelial cells have the capacity to proliferate and to move on surfaces. Following implant/abutment placement, epithelial migration from adjacent soft tissues begins. The epithelium moves in apico-coronal direction as soon as it reaches the implant surface, giving rise to a junctional epithelium about 2mm long³²⁻³⁴. The formation of a junctional epithelium in the implant/mucosal interface can be considered the first barrier of defense against oral microflora. Research has shown that once epithelial cells have reached the implant surface, their attachment occurs directly via a basal lamina (< 200nm) and hemidesmosomes.³⁵⁻³⁷ Another form of attachment, where a glycoprotein layer of approximately 200nm forms exists between the cell wall without direct epithelium/implant contact was also proposed.^{38,39} Nonetheless, it is agreed that this seal is probably viable and adequate in function since there were minimal histologic inflammatory reactions in the underlying connective tissues.^{40,41}

The surface topography has also played a role in the soft tissue attachment to titanium surfaces, since polished surfaces have shown higher compatibility to fibroblasts when compared to rough surfaces.⁴²⁻⁴⁷ A prerequisite to a successful dental implant should obtain a peri-implant mucosal seal on the implant surface.^{48,49}

Failure to achieve or maintain this seal results in apical migration of epithelium into the bone/implant interface and possibly caused partially or completely encapsulation of endosseous implant.^{50,51} In a natural dentition, the junctional epithelium provides a seal at the base of the sulcus against the penetration of chemical and bacterial substances. If the seal is disrupted and/or the fibers apical to the epithelium are destroyed, epithelia cells migrate apically, forming a periodontal pocket after cleavage of the soft tissue from the radicular surface. The importance of the biologic seal should be emphasized due to the absence of cementum and fiber insertion into the implant surface which may cause formation of a “peri-implant pocket” extending into the osseous structures.

For the connective tissue attachment to the implant, collagen fibers form a tight cuff around the implant abutment. The length of the connective tissue attachment ranges from 1.3 to 1.8mm^{32,52}, and is also dependent on the design of the implant (one- or two-part implant). There are reports in the literature that the use of a plasma sprayed surface promotes connective tissue adherence with fibers inserted functionally at 90° into the plasma sprayed surface of the implant.^{44,53} However, most reports have shown that connective tissue fibers are not inserted into the implant surface. Dense bundles of thick collagen fibers are oriented only longitudinally due to a lack of fiber insertion.^{54,55} The connective tissue of the peri-implant mucosa can be subdivided into two distinct zones. The outer zone located under the junctional epithelium, composed of collagen Types I and III, is responsible for the transformation of collagen. The inner supracrestal connective tissue zone, composed mainly of Type I collagen, is responsible for mechanical resistance and stability of the peri-implant mucosa.^{54,56} The connective tissue surrounding dental implants possess fewer capillaries as compared to that surrounding natural teeth.⁵⁷ The blood supply of the peri-implant mucosa is composed of terminal branches of larger vessels originating from the periosteum of alveolar bone, while the vasculature of the gingiva and the supracrestal connective tissue at teeth is derived from the supraperiosteal vessels lateral of the alveolar process and the vessels of the periodontal ligament.⁵⁷ The peri-implant mucosa has also shown to exhibit an inflammatory response, similar to gingival tissues, characterized by increased proportions of T- and B-cells in the inner connective tissue. However, the host response is less pronounced than in gingival tissues.⁵⁸⁻⁶⁰

Animal and human studies have shown that an adequate biological width/seal can only be achieved if there is a supracrestal smooth titanium surface of at least 3 mm long in the apico-coronal direction.^{32,50,61-64} The junctional epithelium(JE) occupies approximately 2 mm of this surface, while the rest of it is occupied by the connective tissue (CT). The values for two-part implants were 2.0 mm for JE, and 1.3 to 1.8 mm for CT.⁵² The values for a biological width/seal around one-part implants at 3-month unloaded implants were reported to be 0.49 mm for sulcus depth (SD), 1.16 mm for JE attachment, and 1.36 mm for CT attachment. These dimensions slightly varied in the loaded implants, 0.50 mm for SD, 1.44 mm for JE, and 1.01 mm for CT. After a 12-month loading period, these values were 0.16 mm

for SD, 1.88mm for JE, and 1.05mm for CT.³² It can be speculated that the biological width/seal increases approximately 1mm after implant loading possibly due to crestal bone resorption. Table 2.2 summarizes the comparison between dental implants and natural teeth.

Table 2.2 Dental Implants vs. Natural Teeth

	Dental Implants	Natural Teeth
Hard Tissue Interface	Only bone (functional ankylosis)	Bone, PDL, cementum
Soft Tissue Interface	Hemidesmosomes and basal lamina	Hemidesmosomes, and basal lamina
CT Fiber Apparatus	Parallel	Perpendicular
Collagen Fibers	More	Less

2.4 Protocols for Implant Placement

A dental implant is said to be biomechanically osseointegrated if no progressive relative motion of living bone and implant occur under functional levels and types of loading for the entire life of the patient.

The surgical phase of most dental implant systems involves two distinctive stages, the placement of the implant and its subsequent uncovering. Research reported no significant differences in wound healing of implants exist in one-stage and two-stage procedures.^{65,66} However, when two-stage implants were inserted using a one-stage technique, failure rate of 16.7% was observed, suggesting that two-stage implants can be used in a one-stage approach but with increased risks of failure.^{67,68} Primary stability of dental implant is considered to be a key factor to promote close bone-to-implant contact. Less bone to titanium contact and lower bone level in the threads have been determined in initially mobile implants compared to initially stable ones.⁶⁹

2.5 Types of Implant Systems

Advances in oral implantology research have led to the development of several different types of implants, and it is anticipated that continued research will lead to even improved systems. The different implant systems are classified according to their morphology and method of osseous incorporation that are subperiosteal, transosteal, and endosseous implants. The most frequently used implants are endosseous implants while other forms have been slowly replaced by consumers.

Endosseous implant systems include a range of sizes, shapes, coatings, and prosthetic components (Table 2.3). A variety of lengths and widths should be available to better incorporate the implant fixture within osseous structures. Prosthetic components can also be selected in a variety of sizes and angles to perfectly accommodate the final restoration. Implant surface morphology has been

shown to influence osseointegration. Porous coatings (i.e. acid-etched, sand-blasted) can achieve more bone-to-implant contact than smooth subcrestal surfaces.⁷⁰ Chemical coating of implant surfaces (i.e. hydroxyapatite) has also been shown to promote enhanced bone-to-implant contact and faster osseointegration.

Table 2.3 Classification of Implant Fixtures According to Surgical Protocol, Interface Connection, and Body Geometry

Surgical Protocol	Interface Connection	Body Geometry
— One-stage	— Internal connection	— Threaded screws
	— External connection	— Straight
— Two-stage	— Octagonal	— Tapered
	— Hexagonal	— Stepped
	— Cone Screw	— Expansive
	— Cone Hex	
	— Spline	

With an immense variety of available implant systems, the clinician should follow appropriate criteria for selection of an implant system (Table 2.4). However, these systems appeared to be similar and very few have been subjected to a variety of clinical trials to determine their success. The majority of implant systems currently available were modifications of those few systems that have been properly evaluated. However, the data of one system should not be applied to another. It is important to know the long-term stability of the fixtures and the degree of tolerance of the peri-implant tissues for extended periods of time. An ideal implant system should also be easy-to-use and flexible to a variety of clinical scenarios. Only systems that provide numerous restorative options can predictably result in pleasing esthetic outcomes.

Table 2.4 Dental Implant Selection Criteria

Selection Criteria
— High success rate
— Predictable Osseointegration demonstrated in scientific data
— Prosthetic flexibility in a variety of clinical applications
— Tissue friendly
— Interface stability
— User friendly
— Optimal esthetics
— Reasonable cost

2.6 Prosthetic Rehabilitation

The exact position and angulation of the implants in jaw bone is planned before surgery. Utilization of surgical guides are often needed to precisely locate ideal implant position during placement. Varying degrees of edentulism can be treated by prosthetic rehabilitation with implants. These range from a fully edentulous jaw to

partially edentulous segments to single tooth replacements.(Fig.2.2a-2.2j).



Fig. 2. 2a Pre-operative View Demonstrates Edentulous Area (# 5)



Fig. 2. 2b Radiograph Demonstrates Adequate Bone Height for Implant Placement



Fig. 2. 2c Implant Osteotomy Is Prepared under Guidance of a Surgical Stent

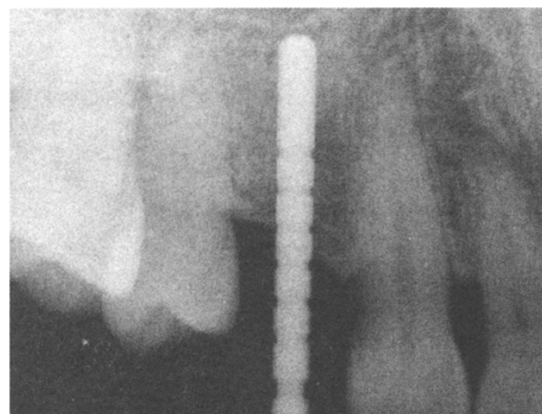


Fig. 2.2d Intra-surgical Radiograph Shows Ideal Angulation for Implantation

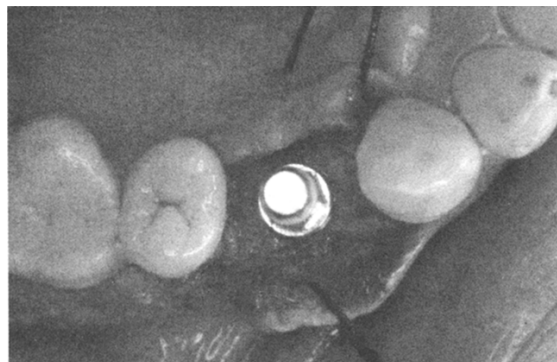


Fig. 2.2e Implant Is Placed in a One-stage Approach with Satisfactory Position



Fig. 2.2f Interrupted Sutures Reposition the Flaps

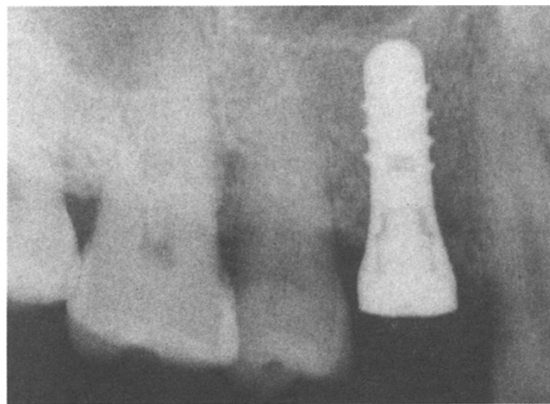


Fig. 2. 2g Post-surgical Radiograph Confirms Adequate Relation between Implant and Adjacent Teeth

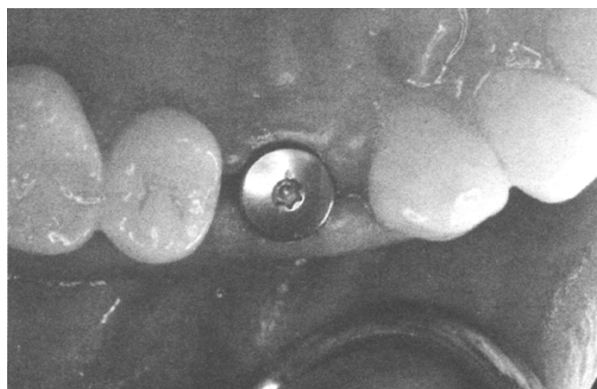


Fig. 2. 2h Adequate Healing Is Observed 2 Weeks Later



Fig. 2. 2i Four Months Later, the Final Crown Is Cemented



Fig. 2. 2j Radiograph Demonstrates the Final Restoration

Complete dentures are always confronted with the problems of retention and stability, especially in patients with advanced alveolar ridge resorption. Implant supported dentures allow for much improved masticatory function and comfort. Commonly, the lower complete denture is the more problematic and thus it frequently indicates for implant supported rehabilitation. (Fig. 2.3a – 2.3e)

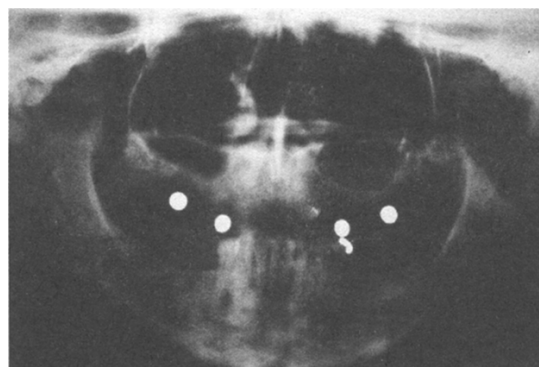


Fig. 2. 3a Radiograph Demonstrates Edentulous Maxilla with Insufficient Alveolar Bone Height for Implant Placement

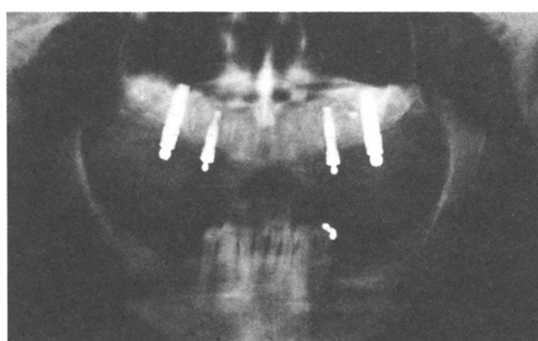


Fig. 2. 3b Following Augmentation of the Maxillary Sinuses, Four Implants Are Placed

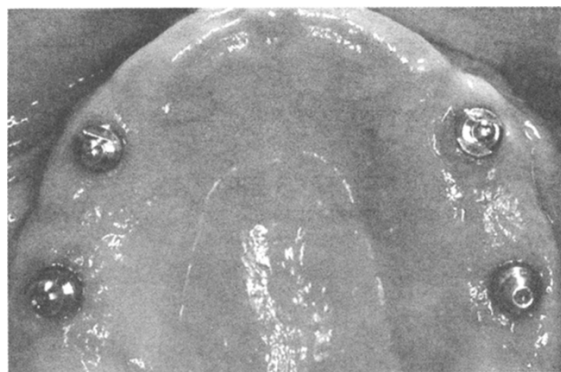


Fig. 2.3c Abutments Are Connected Six Months Later



Fig. 2.3d An Open-palate Overdenture Is Fabricated



Fig. 2.3e Satisfactory Esthetics and Occlusal Function Are Achieved

Even when the patient retains some teeth, some edentulous spans are too long for predictable treatment with conventional bridges. When the edentulous span has no terminal abutment tooth at the end of the arch to support a bridge, a so-called free-end saddle situation is said to exist. Such patients had no choice but to wear removable partial dentures in the past. Implant supported bridges are now possible in these situations. Increasing numbers of patients are opting for the restoration of a single or multiple adjacent missing teeth with implant-supported crowns. In conventional dental treatment, the teeth adjacent to the edentulous space have to be altered to serve as abutments for fixed partial prostheses. If these abutment teeth are untouched by previous episodes of caries then such a treatment modality would be destructive to healthy tooth structure. Before the advent of implants, this was the best restorative option for partial edentulism. Replacement of these teeth with implant-supported crown has become the standard of treatment in the last decade (Table 2.5).

Table 2.5 Dental Implants vs. Natural Teeth

	Dental Implants	Natural Teeth
Hard Tissue Interface	Only bone (functional ankylosis)	Bone, PDL, cementum
Soft Tissue Interface	Hemidesmosomes, and Basal Lamina	Hemidesmosomes, and Basal Lamina
CT Fiber Apparatus	Parallel	Perpendicular
Collagen Fibers	More	Less
Soft Tissue Vascularity	Less	More
Fibroblasts	Less	More
Probing Depth in Health	Deeper (3-4 mm)	Shallower (< 3mm)
Inflammation Progression	Faster	Slower

References

1. Brånenmark PI, Adell R, Breine U, Hansson BO, Lindstrom J, Ohlsson A (1969) Intra osseous anchorage of dental prostheses. I. Experimental studies. Scand J Plast Reconstr Surg 3:81-100
2. Linkow LI (1966) Clinical evaluation of the various designed endosseous implants. J Oral Implant Transplant Surg 12:35-46
3. Linkow L (1966) The age of endosseous implants. Dent Concepts 8:4-10
4. Linkow LI (1967) The era of endosseous implants. J Dist Columbia Dent Soc 42: 46-47
5. Linkow LI (1967) Prefabricated endosseous implant prostheses. Dent Concepts 10:2-10
6. Brånenmark PI, Adell R, Hansson BO (1971) Reconstruction of jaws and intraosseous anchorage of dental prosthesis. Tandläkartidningen 63:486-497

7. Bränemark PI (1971) Jaw reconstruction and intraosseous anchorage of dental prosthesis. *Lakartidningen* 68:3105-3116
8. Bränemark PI, Hansson BO, Adell R, Breine U, Lindstrom J, Hallen O, et al. (1977) Osseointegrated implants in the treatment of the edentulous jaw. Experience from a 10-year period. *Scand J Plast Reconstr Surg Suppl* 16:1-132
9. Brocard D, Barthet P, Baysse E, Duffort JF, Eller P, Justumus P, et al. (2000) A multicenter report on 1, 022 consecutively placed ITI implants: a 7-year longitudinal study. *Int J Oral Maxillofac Implants* 15:691-700
10. Jones JD, Lupori J, van Sickels JE, Gardner W (1999) A 5-year comparison of hydroxyapatite-coated titanium plasma-sprayed and titanium plasma-sprayed cylinder dental implants. *Oral Surg Oral Med Oral Pathol Oral Radiol Endod* 87: 649-652
11. Karoussis IK, Salvi GE, Heitz-Mayfield LJ, Bragger U, Hammerle CH, Lang NP (2003) Long term implant prognosis in patients with and without a history of chronic periodontitis: a 10-year prospective cohort study of the ITI Dental Implant System. *Clin Oral Implants Res* 14:329-339
12. O Neal RB, Sauk JJ, Somerman MJ (1992) Biological requirements for material integration. *J Oral Implantol* 18:243-255
13. Schwartz Z, Lohmann CH, Cochran DL, Sylvia VL, Dean DD, Boyan BD (1999) Bone regulating mechanisms on implant surfaces. *Proceedings of the Third European Workshop on Periodontology-Implant Dentistry* 1:41-54
14. Kasemo B, Lausmaa J (1994) Material-tissue interfaces: the role of surface properties and processes. *Environ Health Perspect*, 102 Suppl 5:41-45
15. Cassiede P, Dennis JE, Ma F, Caplan AI (1996) Osteochondrogenic potential of marrow mesenchymal progenitor cells exposed to TGF-beta 1 or PDGF-BB as assayed in vivo and in vitro. *J Bone Miner Res* 11:1264-1273
16. Sinha RK, Tuan RS (1996) Regulation of human osteoblast integrin expression by orthopedic implant materials. *Bone* 18:451-457
17. Steinemann SG (1996) Metal implants and surface reactions. *Injury*, 27 Suppl 3: SC16-22
18. Henrich V (1996) The Surface Science of Metal Oxides. Cambridge, UK: Press Syndicate of the University of Cambridge, 1st ed:464
19. Descouts P (1999) Influence of surface configuration on adsorption of molecules. *Proceedings of the Third European Workshop on Periodontology-Implant Dentistry* 1:30-40
20. Schwartz Z, Boyan BD (1994) Underlying mechanisms at the bone biomaterial interface. *J Cell Biochem* 56:340-347
21. Sela J, Gross UM, Kohavi D, Shani J, Dean DD, Boyan BD, et al.(2000) Primary mineralization at the surfaces of implants. *Crit Rev Oral Biol Med* 11:423-436
22. Kohavi D, Schwartz Z, Amir D, Mai CM, Gross U, Sela J (1992) Effect of titanium implants on primary mineralization following 6 and 14 days of rat tibial healing. *Biomaterials* 13:255-260
23. Schatzker J (1995) Osseointegration of metal. *Can J Surg* 38 Suppl 1:S49-54

24. Schenk RK, Buser D (2000) Osseointegration: a reality. *Periodontol* 17:22-35
25. Cochran DL, Schenk RK, Lussi A, Higginbottom FL, Buser D (1998) Bone response to unloaded and loaded titanium implants with a sandblasted and acid-etched surface:a histometric study in the canine mandible. *J Biomed Mater Res* 40:1-11
26. Huja SS, Katona TR, Burr DB, Garetto LP, Roberts WE (1999) Microdamage adjacent to endosseous implants. *Bone* 25:217-222
27. Minkin C, Marinho VC (1999) Role of the osteoclast at the bone implant interface. *Adv Dent Res* 13:49-56
28. Nomura T, Ishii A, Shimizu H, Taguchi N, Yoshie H, Kusakari H, et al. (2000) Tissue inhibitor of metalloproteinases 1, matrix metalloproteinases-1 and -8, and collagenase activity levels in periimplant crevicular fluid after implantation. *Clin Oral Implants Res* 11:430-440
29. Brosh T, Persovski Z, Binderman I (1995) Mechanical properties of bone implant interface: an in vitro comparison of the parameters at placement and at 3 months. *Int J Oral Maxillofac Implants*, 10:729-735
30. Tonetti MS, Schmid J (2000) Pathogenesis of implant failures. *Periodontol*, 4: 127-138
31. Sela J, Gross UM, Kohavi D, Shani J, Boyan BD, Schwartz Z, et al. (1999) Woven bone formation around implants and the effect of bacterial infection. *J Long Term Eff Med Implants* 9:47-65
32. Cochran DL, Hermann JS, Schenk RK, Higginbottom FL, Buser D (1997) Biologic width around titanium implants. A histometric analysis of the implantogingival junction around unloaded and loaded nonsubmerged implants in the canine mandible. *J Periodontol* 68:186-198
33. Listgarten MA (1996) Soft and hard tissue response to endosseous dental implants. *Anat Rec* 245:410-425
34. Lindhe J, Berglundh T (2000) The interface between the mucosa and the implant. *Periodontol* 17:47-54
35. Gould TR, Brunette DM, Westbury L (1981) The attachment mechanism of epithelial cells to titanium in vitro. *J Periodontal Res* 16:611-616
36. Hansson HA, Albrektsson T, Bränemark PI (1983) Structural aspects of the interface between tissue and titanium implants. *J Prosthet Dent* 50:108-113
37. McKinney RV, Steflik DE, Koth DL (1985) Evidence for a junctional epithelial attachment to ceramic dental implants. A transmission electron microscopic study. *J Periodontol* 56:579-591
38. Kawahara H, Kawahara D, Mimura Y, Takashima Y, Ong JL (1998) Morphologic studies on the biologic seal of titanium dental implants. Report II. In vivo study on the defending mechanism of epithelial adhesions/attachment against invasive factors. *Int J Oral Maxillofac Implants* 13:465-473
39. Kawahara H, Kawahara D, Hashimoto K, Takashima Y, Ong JL (1998) Morphologic studies on the biologic seal of titanium dental implants. Report I. In vitro study on the epithelialization mechanism around the dental implant. *Int*

- J Oral Maxillofac Implants 13:457-464
- 40. Adell R, Lekholm U, Rockler B, Bränemark PI, Lindhe J, Eriksson B, et al. (1986) Marginal tissue reactions at osseointegrated titanium fixtures (I). A 3-year longitudinal prospective study. *Int J Oral Maxillofac Surg* 15:39-52
 - 41. Lekholm U, Adell R, Lindhe J, Bränemark PI, Eriksson B, Rockler B, et al. (1986) Marginal tissue reactions at osseointegrated titanium fixtures. (II) A cross-sectional retrospective study. *Int J Oral Maxillofac Surg* 15:53-61
 - 42. Fitton JH, Dalton BA, Beumer G, Johnson G, Griesser HJ, Steele JG (1998) Surface topography can interfere with epithelial tissue migration. *J Biomed Mater Res* 42:245-257
 - 43. Cochran D, Buser D (1994) Attachment and growth of periodontal cells on smooth and rough titanium. *Int J Oral Maxillofac Implants* 9:289-297
 - 44. Schroeder A, van der Zypen E, Stich H, Sutter F (1981) The reactions of bone, connective tissue, and epithelium to endosteal implants with titanium-sprayed surfaces. *J Maxillofac Surg* 9:15-25
 - 45. Wennstrom J, Lindhe J (1983) Plaque-induced gingival inflammation in the absence of attached gingiva in dogs. *J Clin Periodontol* 10:266-276
 - 46. Jansen JA, de Wijn JR, Wolters-Lutgerhorst JM, van Mullem PJ (1985) Ultrastructural study of epithelial cell attachment to implant materials. *J Dent Res* 64:891-896
 - 47. Lauer G, Wiedmann-Al-Ahmad M, Otten JE, Hubner U, Schmelzeisen R, Schilli W (2001) The titanium surface texture effects adherence and growth of human gingival keratinocytes and human maxillary osteoblast-like cells in vitro. *Biomaterials* 22:2799-2809
 - 48. Liljenberg B, Gualini F, Berglundh T, Tonetti M, Lindhe J (1996) Some characteristics of the ridge mucosa before and after implant installation. A prospective study in humans. *J Clin Periodontol* 23:1008-1013
 - 49. Liljenberg B, Gualini F, Berglundh T, Tonetti M, Lindhe J (1997) Composition of plaque-associated lesions in the gingiva and the periimplant mucosa in partially edentulous subjects. *J Clin Periodontol* 24:119-123
 - 50. Ericsson I, Lindhe J (1993) Probing depth at implants and teeth. An experimental study in the dog. *J Clin Periodontol* 20:623-627
 - 51. Ericsson I, Persson LG, Berglundh T, Marinello CP, Lindhe J, Klinge B (1995) Different types of inflammatory reactions in periimplant soft tissues. *J Clin Periodontol* 22:255-261
 - 52. Berglundh T, Lindhe J (1996) Dimension of the periimplant mucosa. Biological width revisited. *J Clin Periodontol* 23:971-973
 - 53. Buser D, Warrer K, Karring T, Stich H (1990) Titanium implants with a true periodontal ligament: an alternative to osseointegrated implants? *Int J Oral Maxillofac Implants* 5:113-116
 - 54. Chavrier CA, Couble ML (1999) Ultrastructural immunohistochemical study of interstitial collagenous components of the healthy human keratinized mucosa surrounding implants. *Int J Oral Maxillofac Implants* 14:108-112

55. Comut AA, Weber HP, Shortkroff S, Cui FZ, Spector M (2001) Connective tissue orientation around dental implants in a canine model. *Clin Oral Implants Res* 12:433-440
56. Chavrier C, Couble ML, Hartmann DJ (1994) Qualitative study of collagenous and noncollagenous glycoproteins of the human healthy keratinized mucosa surrounding implants. *Clin Oral Implants Res* 5:117-124
57. Berglundh T, Lindhe J, Jonsson K, Ericsson I (1994) The topography of the vascular systems in the periodontal and periimplant tissues in the dog. *J Clin Periodontol* 21:189-193
58. Zitzmann NU, Berglundh T, Marinello CP, Lindhe J (2001) Experimental periimplant mucositis in man. *J Clin Periodontol* 28:517-523
59. Tonetti MS, Imboden M, Gerber L, Lang NP (1995) Compartmentalization of inflammatory cell phenotypes in normal gingiva and periimplant keratinized mucosa. *J Clin Periodontol* 22:735-742
60. Marchetti C, Farina A, Cornaglia AI (2002) Microscopic, immunocytochemical, and ultrastructural properties of periimplant mucosa in humans. *J Periodontol* 73:555-563
61. Abrahamsson I, Berglundh T, Wennstrom J, Lindhe J (1996) The periimplant hard and soft tissues at different implant systems. A comparative study in the dog. *Clin Oral Implants Res* 7:212-219
62. Abrahamsson I, Berglundh T, Lindhe J (1997) The mucosal barrier following abutment dis/reconnection. An experimental study in dogs. *J Clin Periodontol* 24: 568-572
63. Ericsson I, Nilner K, Klinge B, Glantz PO (1996) Radiographical and histological characteristics of submerged and nonsubmerged titanium implants. An experimental study in the Labrador dog. *Clin Oral Implants Res* 7:20-26
64. Berglundh T, Lindhe J (1997) Healing around implants placed in bone defects treated with Bio-oss. An experimental study in the dog. *Clin Oral Implants Res* 8:117-124
65. Barber HD, Seckinger RJ, Silverstein K, Abughazaleh K (1996) Comparison of soft tissue healing and osseointegration of IMZ implants placed in one-stage and two-stage techniques: a pilot study. *Implant Dent* 5:11-14
66. Kohal RJ, De LaRosa M, Patrick D, Hurzeler MB, Caffesse RG (1999) Clinical and histologic evaluation of submerged and nonsubmerged hydroxyapatite-coated implants: a preliminary study in dogs. *Int J Oral Maxillofac Implants* 14:824-834
67. Levy D, Deporter DA, Pilliar RM, Watson PA, Valiquette N (1996) Initial healing in the dog of submerged versus non-submerged porous-coated endosseous dental implants. *Clin Oral Implants Res* 7:101-110
68. McDermott NE, Chuang SK, Woo VV, Dodson TB (2003) Complications of dental implants: identification, frequency, and associated risk factors. *Int J Oral Maxillofac Implants* 18:848-855
69. Ivanoff CJ, Sennerby L, Lekholm U (1996) Influence of initial implant mobility on the integration of titanium implants. An experimental study in rabbits. *Clin*

- Oral Implants Res 7:120-127
70. Cochran DL, Nummikoski PV, Higginbottom FL, Hermann JS, Makins SR, Buser D (1996) Evaluation of an endosseous titanium implant with a sandblasted and acid-etched surface in the canine mandible: radiographic results. Clin Oral Implants Res 7:240-252

Application of Commercial FEA Software

Wei Xu¹, Jason Huijun Wang², Jianping Geng³, Haw-Ming Huang⁴

¹ School of Engineering, University of Surrey, Surrey, UK

Email: drweixu@hotmail.com

² Worley Advanced Analysis (Singapore), Singapore

³ Clinical Research Institute, Second Affiliated Hospital, School of Medicine, Zhejiang University, Hangzhou, China

⁴ Graduate Institute of Medical Materials and Engineering Taipei Medical University, Taipei, Taiwan, China

5. 1 Introduction

As the Finite Element (FE) method requires a huge amount of computation, its application should be supported by advanced of computer technology. Many computer softwares have been developed and commercialised for workstation and Personal Computers (PC) in recent years. Most of the FE softwares are developed for general applications in solids, fluids, and electrical and magnetic field. There are also some FE software designed for a specific type of analysis. The FE software used for dental implant simulation is the one for general applications.

The selection of FE software is based on requirement of applications. Although the fundamental principle of FE analysis is the same, computer softwares can be developed with different features. Some commercial FE softwares have well-developed CAD function, while others provide more problem solving options. A simple dental implant FE simulation is typical solid analysis, which can be performed using most of currently available commercial FE softwares. However, when the osseointegrated interface takes into account, contact analysis is required.

In this part, two well-known FE softwares, ANSYS and ABAQUS, are used as examples to illustrate how the dental implant simulation is performed using a commercial FE software. Users who are new to the FE analysis could become familiar with the software through the step by step exercise described in the following chapters.

5.2 ANSYS

5.2.1 Introduction

ANSYS is one of the most popular commercial FE softwares. It is widely used to solve problems ranging from typical mechanical engineering to medical engineering in engineering and academic fields. It can be adapted to simulate simple linear analyses as well as the most challenging nonlinear dynamic analysis. ANSYS contains an extensive class of element types, which could virtually model any geometry and an equally extensive list of material properties. In terms of mechanical analysis, it not only can simulate the behaviour of most typical engineering materials including metals, rubber, polymers, composites, crushable/resilient foams, etc, but also biomaterials such as soft tissue and bones.

ANSYS is a user-friendly software and very simple to use. Compared to other commercial FE softwares such as ABAQUS, it not only offers users a wide range of capabilities but also powerful 3D modelling functionality. For example, users can easily create an engineering geometry within ANSYS. This is particularly useful for users without engineering background. In addition to its command line interface, ANSYS provides a Graphic User Interface (GUI). The GUI is featured in a style of step-by-step menu. Following this well structured menu, a FE model can be created by providing the geometry data, material properties, boundary conditions, and the loads applied to the model. Once the model is created, to solve the simulation is straightforward in ANSYS. Most importantly, ANSYS has very effective post process capabilities from displaying colour strain contour to plotting stress distribution on a user-defined path. Users rarely have to define parameters for controlling the numerical solution of a problem.

ANSYS is modularised a “standalone” package with three fundamental modules. They are Preprocessor, Solution and General Postprocessor modules. These modules are under the ANSYS Main Menu of the ANSYS GUI. In addition, there are some specialised modules such as Time History General Postprocessor, Topological Option and Radiation Option. FE implant simulations are covered by the first three fundamental modules. Therefore, In this chapter, we will concentrate on these fundamental modules.

Preprocessor

ANSYS Preprocessor module is the one used for creating a FE model. It consists of a number of sub-menus, which can be used for geometrical model creation, assigning element type and material properties, mesh generation, and applying constraints and loads. In the case of a complicated model geometry, ANSYS can import the model created by other softwares, including IGES, STEP, Pro Engineering, and Parasolid.

Solution

ANSYS Solution module is the one used to solve the FE model. There is some overlap between this module and Preprocessor. Either of them can apply loads and constraints to the model. The main function of the Solution module allows users to configure how they want the model to be solved, like the Analysis Type users used, how the load steps are applied to the model.

General Postprocessor

ANSYS General Postprocessor module is the one used to review the solution result of the FE model. It provides some very useful tools to view results of the solution. It includes plotting and listing stress, strain and displacement contours of the model. With plot on graphic function of the module, users can define a path on the model and plot a result (stress, strain or displacement values) on the path. Both graphic and numerical data can be easily exported and saved into a format that can be read by other softwares such as MS Excel for further process.

In order to provide a guideline for users who have no engineering background to learn how to use ANSYS for dental implant simulation, a step-by-step FE modelling example of a dental implant is described in the following sections.

5. 2. 2 Preprocess

The creation of a FE model is done by Preprocessor module. Once the geometry of the model is defined (in most cases, the geometry comes from a real application), the first thing is to convert it into a FE model. Assumptions need to be made, as the FE model is never to be the exact same as the real case. This may require some experiences and practises. The assumptions given by this step-by-step case study can be taken as a starting point for creating a FE model of dental implant.

The case used in this chapter is to simulate a biting force applied on a Bränemark “same day” dental implant. The aim of this study is to investigate the stress distribution in the bone and implant. To simplify the study, simple bone and implant structures are used, and following assumptions are made:

- (1) good osseointegration exists between bone and implant, i.e. no relative movement between bone and implant occurs under loading condition;
- (2) the implant components are treated as a continued structure;
- (3) bone is treated as homogeneous material in terms of elastic module;
- (4) the mandible is fully constrained on its ends.

5. 2. 2. 1 Selection of Element Type

The first step of FE simulations is to select element type. The selection depends on the case of study. To add element type to the model, click Add/Edit/Delete under the Element Type menu, a Element Type Window will pop up as shown in Fig.5.1.

The Add button in the window shown in the Fig.5.1 is for creating new element type to the model. Click Add button, a Library of Element Types window pops up as shown in the Fig.5.2.

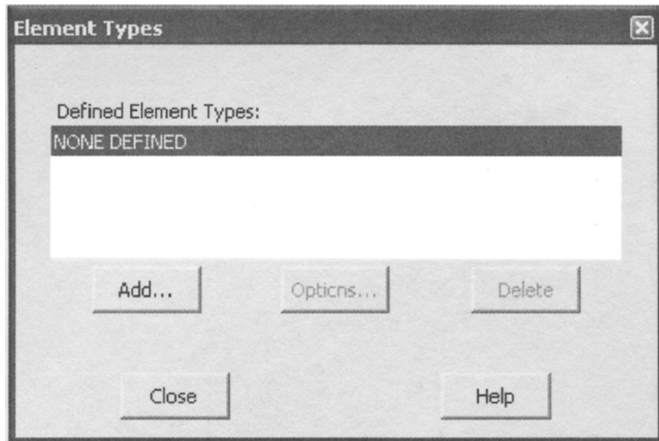


Fig. 5.1 Element Type Window

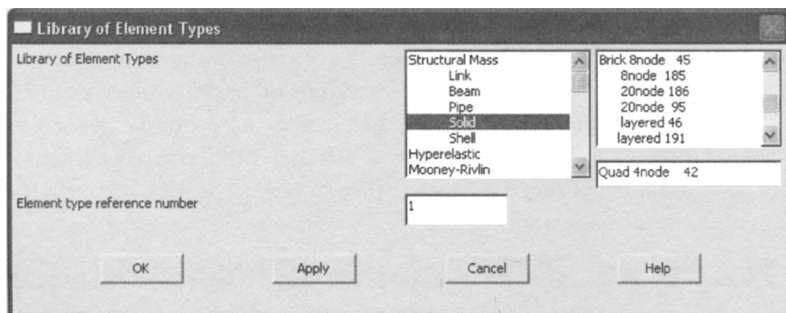


Fig. 5.2 Library of Element Types Window

For a stress analysis model, a solid structure element type should be used. As shown in the Fig.5.2, there are more than one options of the solid structure element type such as Brick 8node 45, 8node 185. Tetro Hedro element type can be used for structure analysis as well. The general guideline for selecting element type is: for regular shape such as a block, a cylinder, or a uniform section beam, Brick type element is normally used; for irregular geometry, such as 3D model of mandible, Tetro Hedro element type is used, as it can fit to the geometry well. In this example, a Tetro Hedro element type-10node Element 92 is used. To select this element type, it needs to drag the scroll bar down to the bottom of the window to see the element type. Then use the mouse to highlight the element before clicking the OK button. After the OK button is clicked, a Element Types window pops back and SOLID 92 element appears in the window as shown in the Fig.5.3.

To add more element types, clicking add button again. To quit the Element Type window, clicking the Close button.

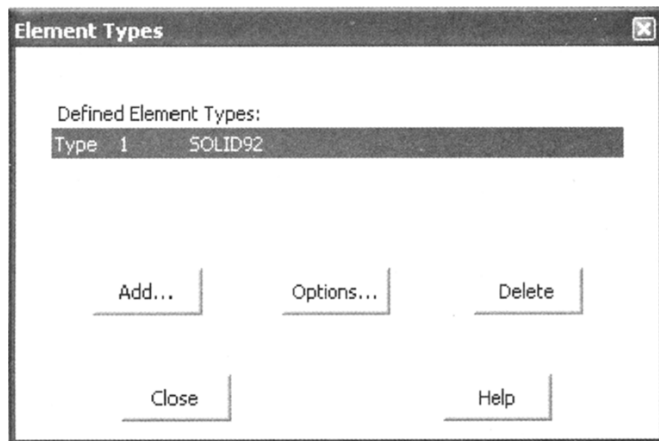


Fig. 5.3 Element Type Window with Inserted Element Type SOLID92

5.2.2.2 Assign the Material Properties

The second step of ANSYS FE simulation is to assign material properties to the model. It can be done before or after the creation of model geometry. For stress/strain analysis, there are two essential parameters need to be defined, Elastic modulus and Poisson's Ratio. To define a material property, click the Material Models under Material Properties menu, then a Define Material Model Behavior Window pops up as shown in Fig.5.4.

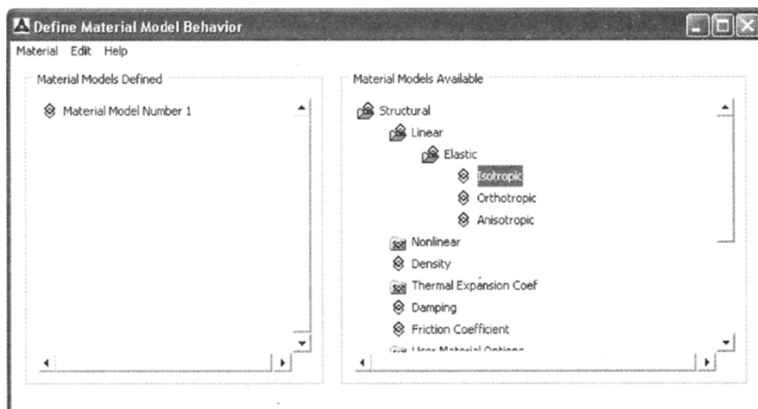


Fig. 5.4 A Define Material Model Behavior Window

In the Define Material Model Behavior Window, users can define linear, nonlinear, isotropic, orthotropic, and anisotropic properties to the model according the nature of the simulations. In this example, the bone is assumed to be isotropic and loading is in a linear range, i.e. to define linear isotropic properties to the model. Click the Isotropic, a new Linear Isotropic Properties for Materials Number

window pops up as shown in Fig.5.5. In this window, users can fill Elastic modulus and Poisson's Ratio. In this example, it is assumed that Elastic modulus and Poisson's Ratio of cortical bone are 18GPa and 0.3, respectively.

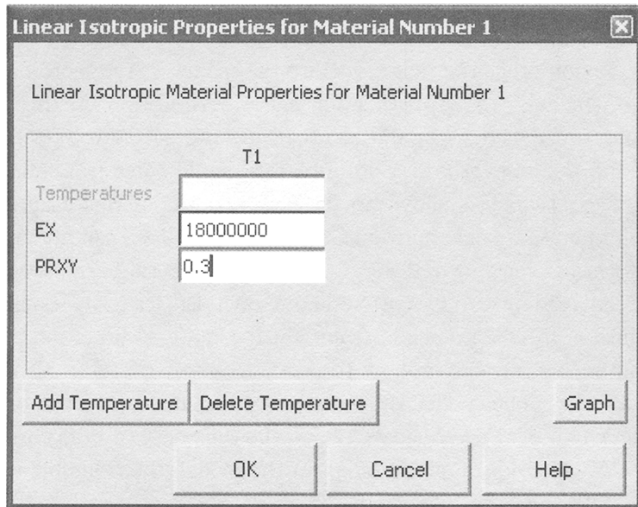


Fig. 5.5 A Linear Isotropic Properties for Materials Number Window

To add another material property, click an appropriate type of material behaviours in the Define Material Model Behavior window again. After all material properties are defined, users can close the Linear Isotropic Properties for Materials Number window by click OK and Define Material Model Behavior window by click the small red cross on right top corner.

5.2.2.3 Model Creation

The third step of the FE simulation is to create model geometry. In ANSYS, a simulation can be carried out on 2D or 3D geometry. A component with simple geometry can be simplified as a 2D case, such as a uniform cross section beam. Single dental implant simulation can also be carried out on a 2D geometry and achieve good approximation. The guideline of selection the model geometry is unless it is necessary to use 2D simulation. It will save both modelling and computation time of the simulation.

To study the same-day-teeth implant system, it deals with bridge structure of dental fixture and can not be modelled using 2D geometry. Therefore, a 3D model has to be used. As an example, an approximate 3D model is created in this section to show users how to create a 3D model in ANSYS. This model is far more close to a real same-day-teeth implant system.

To create a FE model, two critical questions need to answer, how accurate does a model need to be and where does the geometry information come from? These are not straightforward questions. To answer them, users should firstly identify what they want to get from the simulation. Is the local stress around the dental implant,

deformation of the bridge fixture, overall stress in the bone or the stress in the implant? In this example, the deformation of the bridge fixture and approximate local stress around the implant are what we are interested in. Therefore, a simplified bone structure together with an approximate geometry of the dental implant system is used.

It is very obvious that the more accurate the model is, the more difficult it will be in creating a model. For approximation and simplification, in this example, the dental implant is modelled without thread. In a more accurate model, the implant needs thread and the bone geometry information should come from human anatomy, i.e. CT scan images, which is shown in the next example of this chapter.

For model generation using human anatomy data, ANSYS can import solid model in different formats, such as IGES, STEP, Pro Engineering, Parasolid and so on. ANSYS also can read text file written in its own language, by doing this it can import coordinates from CT images, from which a more accurate model is created.

This example concentrates on how to create a simple dental implant-bone model as shown in Fig.5.6. The model shows a bridge fixture supported by three 3mm implants. The length of the implant is 12mm, the thickness of bridge plate is 3.5mm, and the depth of the bridge plate is 6mm. In the model, the mandible is modelled as a single piece with thickness of 6.5mm.

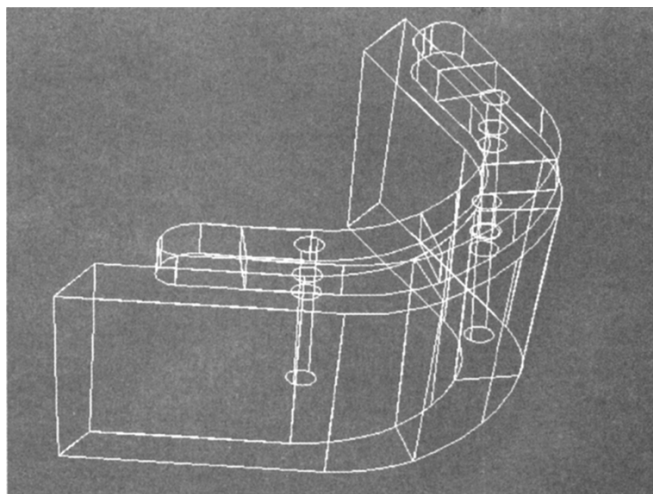


Fig. 5.6 A Simplified Dental Implant Bone Model

Creation of 3D model in ANSYS

Although there are special commands can be used to create simple geometry such as cylinder and brick, to create a 3D model in ANSYS, such as bridge plate, following steps are still recommended: create Key points from the coordinates of the plate geometries, create Line from the Key points, create Area from the Lines, and finally create volume from the Areas.

Key point is defined by coordinates in ANSYS, which is the lowest level of geometry. Unless ANSYS provides a special command to directly create a 2D or 3D geometry, model generation starts from creating Key points and follows the order described above. To create a Key point, click the Create command under the Modeling menu. A list of geometry creation command will appear including Lines, Areas, Volumes, Nodes, and Elements. The Keypoints command is the first one as shown in Fig.5.7.

Under the Keypoints command there are 7 options to create Key point in ANSYS. Among these options, the In Active CS (Coordinate System) is commonly used when the coordinates of the model are provided.

Click the In Active CS in the menu, a Create Keypoints in Active Coordinate System window appears as shown in Fig. 5. 8. This window provides space to enter the Key point number and coordinate values. The Key point number is the identification of each Key point. Each Key point has an unique Key point number.

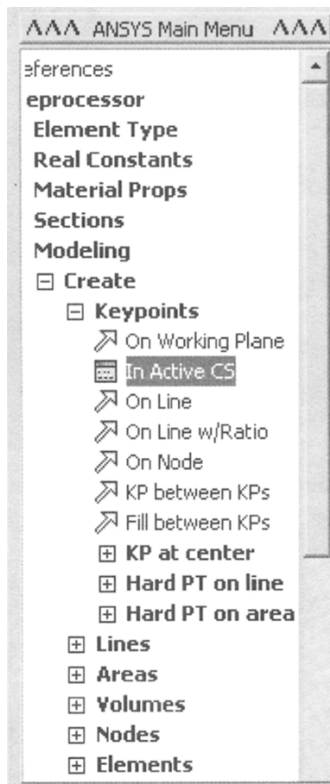


Fig. 5.7 Keypoints Creation Menu

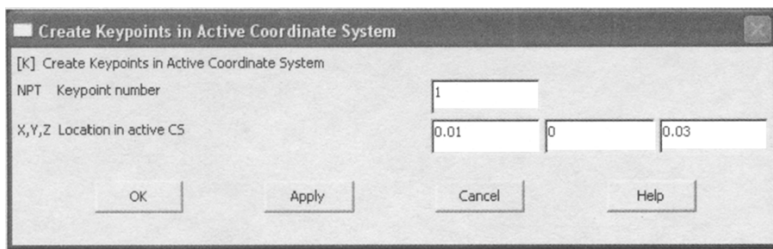


Fig. 5.8 A Create Keypoints in Active Coordinate System Window

Please note that the ANSYS uses ISO unit. The value appears in the coordinate textboxes are in meter. ANSYS has a command Scale can be used to re-scale the model. This is very useful especially when a model is imported from other CAD software or format of 3D solid model, where meter is often used as the unit. The Scale command is used to reduce the model by 1/1000.

Once necessary numbers of Key point are created, the next step is to join the Key points by Lines in the way of model goes. There are three types of lines: Straight line, Arc and Spline. A straight line is defined by two Key points, a Arc by three Key points, and a Spline by more than three Key points. Users can select them according to the requirement of the model.

To create a straight line, arc or spline through Key points, click the Lines command under the Create menu. A list of Line command will appear in the window as shown in Fig.5.9.

There are other commands in this menu which allows users to create lines. The command used to create straight line is the Straight Line command.

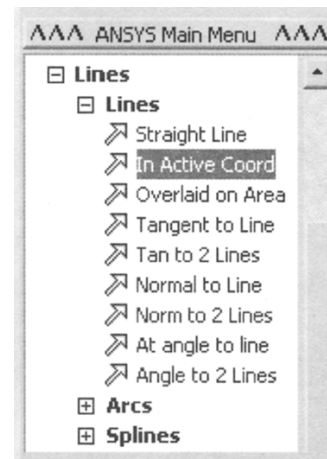


Fig. 5.9 Line Command Menu

Click the Straight Line command, a Create Straight Line window pops up as shown in Fig.5.10. Pick two Key points and join them using a straight line as shown in Fig.5.11.

In a simple model, users can create all Key points before join them by lines. But in a complicated model, it is recommended not to create all Key points at a time, otherwise it will be too confused to pick Key points to form lines. Users need to have a good plan in creating a complicated model. Experience is very important to master the skill of model creation in ANSYS.

After lines are created, the next step is to create areas from lines. To create an area, click the Areas command in ANSYS Main Menu shown in Fig. 5.7. Under the Areas, there is an Arbitrary command. In ANSYS, area can be created by both Key points and lines. It is recommended to use lines to create areas because this would generate less confusion.

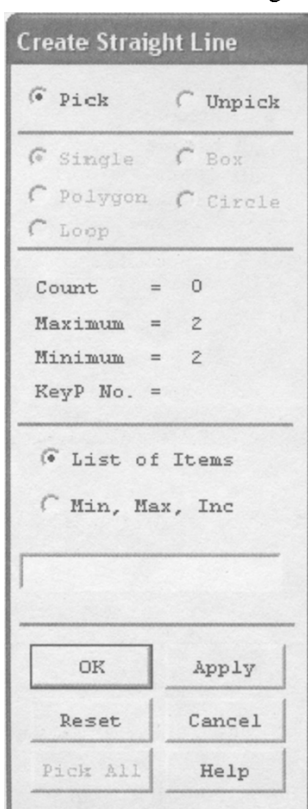


Fig. 5.10 Create Straight Line Window

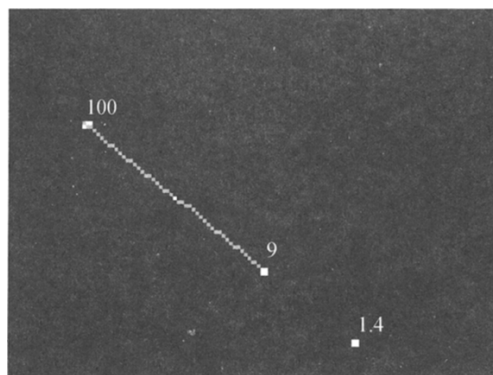


Fig. 5.11 A Straight Line Join Two Key Points

Click the By Lines command under the Arbitrary command, a Create Areas by Lines window pops up. Pick option is selected by default. Users can pick the lines in the model window to form an area as shown in Fig.5.12.

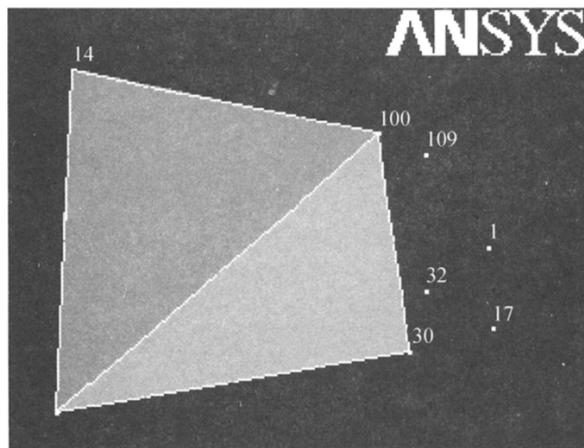


Fig. 5.12 Creating Areas by Lines

An area geometry can be used for 2D FE meshing and modelling. For 3D FE simulations, although a model can be meshed through Key points of which the model consists, meshing through volumes are much easier than using Key points of which the volume consists. And some Boolean operations such as volumetric Intersect, Add, Subtract, and Glue algorithm can only be carried out between volumes. Therefore, it is strongly recommended for beginners to follow the steps given here to create FE models.

To create a volume by areas, click the Volume command in ANSYS Main Menu shown in Fig.5.7. Under the Volume, there are six volumetric creation commands. Only the Arbitrary command allows users to create volumes from areas. A volume

can also be created by Key points. It is obvious, however, to create it by areas is much easier than directly by Key points. Fig.5.13 shows a simplified volumetric model of the same-day-teeth implant system.

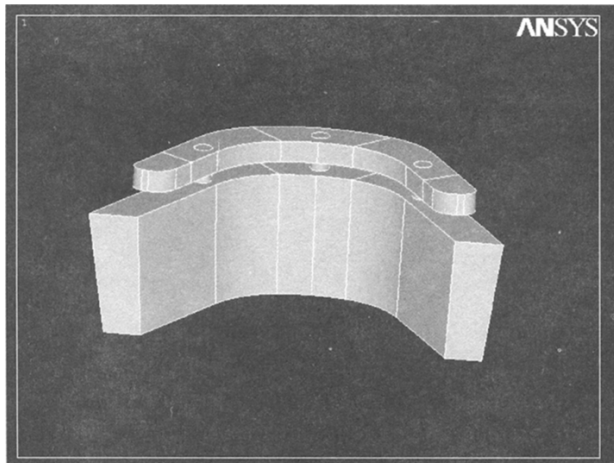


Fig. 5.13 A Simplified Volumetric Model of the Same-day-teeth Implant System

5.2.2.4 Mesh Generation

Mesh generation is the forth step of FE simulation. In this step, a 2D or 3D model is meshed with elements defined in the first step and material properties defined in the second step. The mesh process is to divide the geometrical model created in the third step into small and finite divisions. An element consists of a number of edges and nodes, which depends on the element type selected. During the mesh generation, material properties of the model are assigned. It is important to make sure each part of the model has been assigned right element type and material property.

To assign element type and material property to a model can use Default Attribs command as shown in Fig.5.14 before meshing the model.

The element type and material property can also be assigned to volume using Picked Volumes command. Click the command, a Volume Attributes window pops up. Click the volumes in the model window. After click the OK button a new one as the same pops up as shown in Fig.5.15.

In this window, users can select material number and element type number to be signed to the volume picked up.

There are two ways to generate mesh in

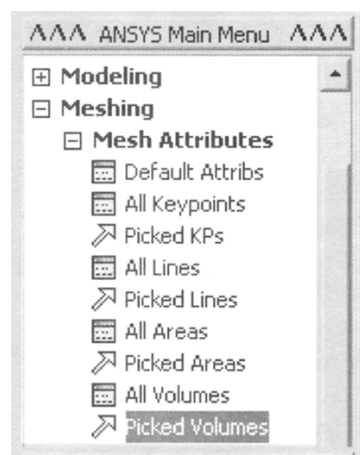


Fig. 5.14 Meshing Menu

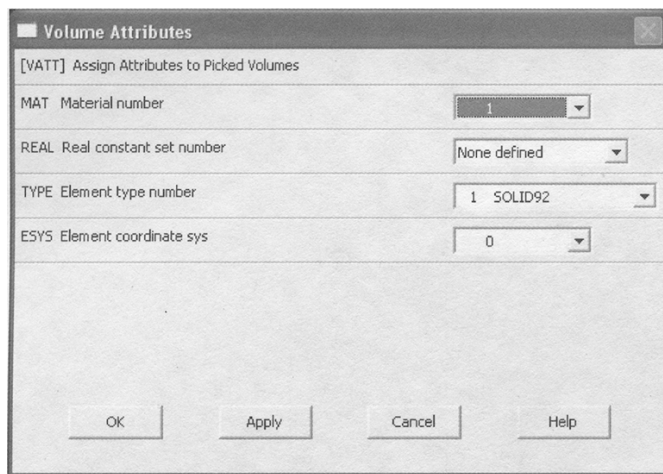


Fig. 5.15 Volume Attributes Window

ANSYS. One is Mesh Tool, the other is manual Mesh. In the Mesh Tool, users can select Smart Size to define the size of element. The analytical accuracy depends on the size of element. Extreme care and precaution has to be exercised when meshing the model. A coarse mesh on the model would cause distortion in the elements and ultimately lead to erroneous results. A very fine mesh would give quite accurate results but at the same time would cost excessive processing and computing time.

If a model involves stress concentration or a sudden change of geometry that may lead to stress distributions, an adequate mesh should be adapted with fine element at these places. But in other situations that the stress may not vary much, a coarse mesh would be sufficient enough. In ANSYS, these can be achieved using Smart Size, as it takes model geometry into account while the mesh is generating.

For manual mesh, users need to define element length on the geometry. This can be done by defining the number of elements or actual size on lines. To achieve an adequate mesh generation, experience is essential in this situation.

The beginner of ANSYS is recommended to use Mesh Tool and select Smart Size. To use Mesh Tool, click the MeshTool command in the menu as shown in Fig. 5.16, a MeshTool window pops up as shown in Fig.5.17.

In the MeshTool window, users can select mesh shape, free or mapped mesh, and option of Smart Size. As it shown in Fig.5.17, the size of element can be

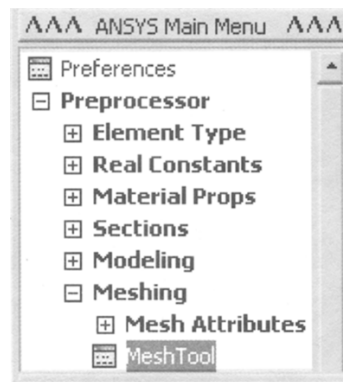


Fig. 5.16 Meshing Menu

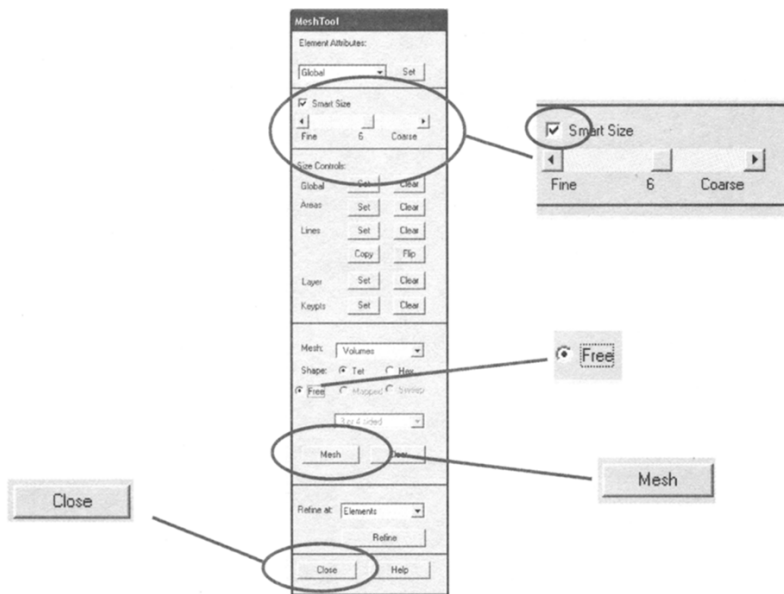


Fig. 5.17 A MeshTool Window

adjusted between 1 and 10 when the check box of the Smart Size is ticked. After all the settings are selected, click the Mesh button to start meshing, and then a Mesh Volumes window pops up. Pick the volumes to be meshed in the model window. A meshed model is shown in Fig.5.18.

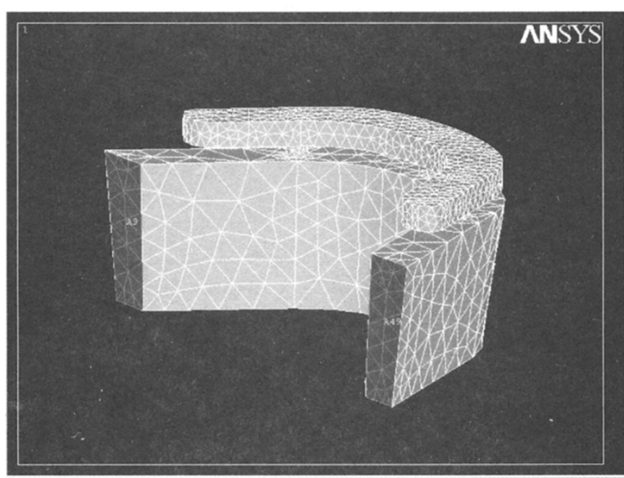


Fig. 5.18 A Meshed Implant System

5.2.2.5 Loads and Constraints

Once the model is meshed, the next step is to apply structural loads and constraints

to the model. In dental implant FEA, the structural loads are forces or pressures being put on the implant or bridge fixture and the constraints are boundary conditions of how, for example, the mandible is restrained under loading.

The structural loads can be defined in ANSYS using point force, pressure on one area, and pure moment. However, not all element types allow users to apply a pure moment to the model. The element selected for this dental implant analysis is SOLID92. Only point force and pressure can be applied to the FE model.

To define the boundary conditions of the model, we assume that the movement of the mandible is fully restrained in all directions under loading and the constraint is located at two ends of the mandible as shown in blue colour in Fig.5.19.

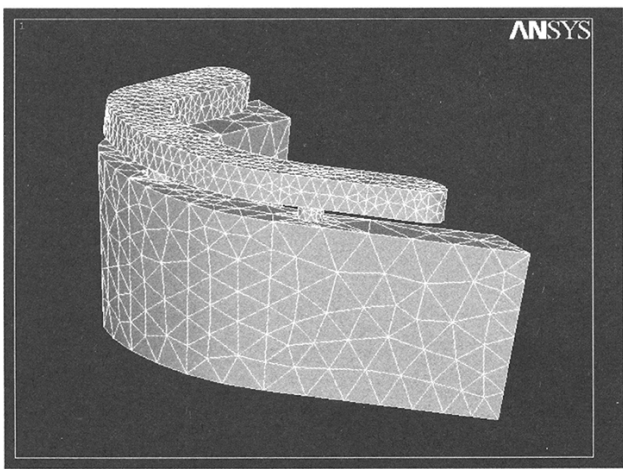


Fig. 5.19 The Restrain Locations on the Mandible

To apply loads on the model, users select force or pressure according to the requirement of simulation. The force is applied to Nodes, Keypoints or Areas. The pressure is only applied to an area. In ANSYS, loading and constraints can be done by either Preprocessor or Solution module.

To apply a force load, click Define Loads under the Load of the Preprocessor module as shown in Fig. 5.20 (a). In the ANSYS Main Menu, click Apply command to apply structural loads and constraints to the model. Once the Apply is clicked, more options appear in the ANSYS Main Menu as shown in Fig. 5.20(b). The dental implant FE simulation is a structural analysis, click the Structural command to bring more options as shown in Fig. 5.20 (c).

To apply constraints to the mandible, click the Displacement command, more options appear. These options allow users to apply displacement constraints on Nodes, Keypoints, Lines and Areas. Click the Areas command in the main menu, an Apply U,ROT on Areas window pops up as shown in Fig.5.21(a).

Click the areas on the model to highlight the areas to Apply U,ROT on Areas window be constrained. Once all areas are selected, click the OK button in the

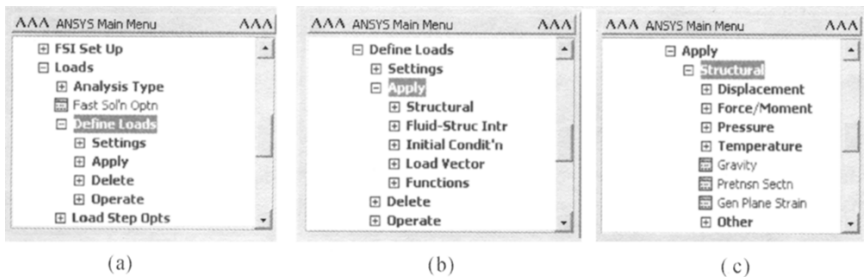


Fig. 5.20 ANSYS Main Menu for Applying Loading

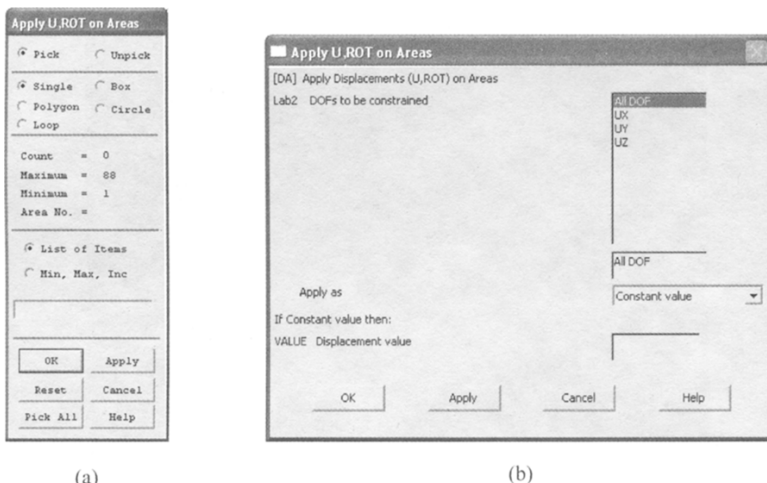


Fig. 5.21 Apply U,ROT on Areas Windows

Apply U,ROT on Areas window, a new Apply U,ROT on Areas window as shown in Fig.5.21(b). In this window, users can define the displacement in three directions, individually or together. In the dental implant model, no movement has been assumed in all three directions. To define this, select All DOF (Degree of Freedom) in the window and enter 0 in Displacement value box, and then click OK button to complete applying constraints to the model.

To apply a load (force or moment) to the model, click the Force/Moment or Pressure command. As shown in Fig. 5.22 (a), there are more options for applying load. The force/moment can be applied to Keypoints or Nodes. In ANSYS, the moment can only be applied to certain elements with rotational DOF. The pressure can be applied to Lines, Areas, Nodes or Elements.

To apply force on the dental implant, click On Nodes command in the ANSYS Main Menu, an Apply Force/Moment on Nodes window pops up as shown in Fig. 5.22 (b). Use the mouse to select one or more nodes on the implant model. Click the OK button in the Apply Force/Moment on Nodes window, a new Apply Force/Moment on Nodes window pops up. In this window, users can select which

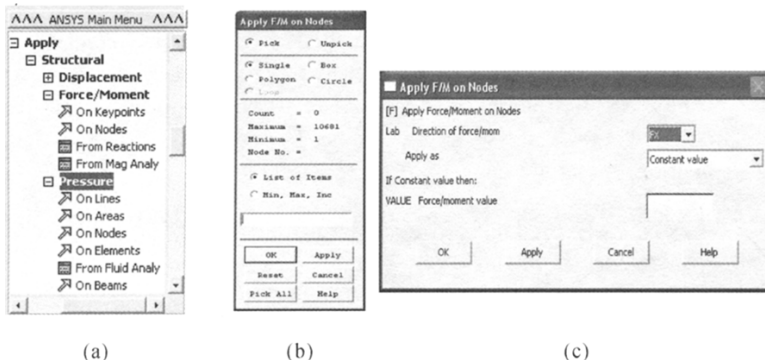


Fig. 5.22 Menu for Apply Load to ANSYS Model

direction the force will be applied. Click the arrow button, a dropdown list appears as shown in Fig.5.23. In this list, users can select one direction from x, y and z. Once the direction is selected, enter a value in the Force/moment value box. At this point, if users click OK button, the load application completed. If the Apply button is clicked, users can continue to apply force or moment to the model. To delete the applied load, click the Delete / Structure / Force/moment command.

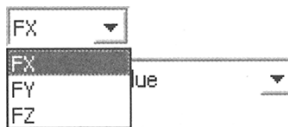


Fig. 5.23 Dropdown Window for Apply Load in Different Directions

As shown in Fig.5.24, Once the load is applied, a red arrow indicator will appear at the point where the force is applied.

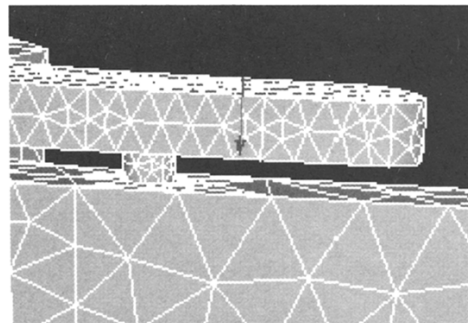


Fig. 5.24 Load Indicator on Implant Model

5.2.3 Solution

Once the mesh is completed and boundary conditions are applied, the next step is to

solve the model using solution module. This module starts Analysis type. There are three options under Analysis type, New Analysis, Re-start, and Solution control. For the first time analysis, use the New analysis. After click the New analysis command in the ANSYS Main menu, a New Analysis window pops up, as shown in Fig.5.25. In this window, users can select the Type of analysis. For the dental implant simulation, the Static analysis type is selected.

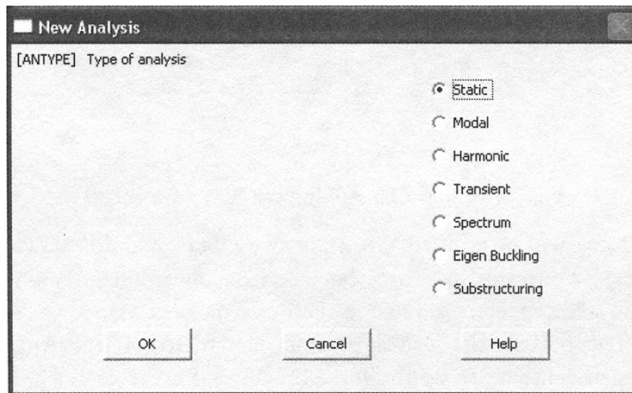


Fig. 5.25 New Analysis Window

The Solution Control option allows users to assign different parameters to the model. For static linear analysis, the default settings can be used. For other analysis such as non-linear and transient, users need to properly define these parameters. For further information about how to define these settings refers to ANSYS manual.

Before the model is solved, users also need to specify the loading steps and output format of the solution. This is done using Load Step Option command. For multi-step analysis, users need to define Printout format of the result. Click the Solution Control command in the ANSYS Main Menu, a Solution Printout Controls window appears as shown in Fig.5.26. Users can define the solution printout using the options provided in this window.

The final step of the model solution is to execute a sub-command under the Solve command. The Current LS command is one used for the first time analysis. It assigns the current load setting to the model, and then carry out the computations to solve the model.

5.2.4 Postprocess

Once the model is solved, results of the analysis can accessed using General Postprocess module in ANSYS. For structure analysis such as a dental implant system, this module provides users with three fundamental functions to review the results. They are Plot Result, List and Export Result, and Plot graphs.

5.2.4.1 Plot Result

The Plot result function allows users to generally review the results of analysis in a format of contour or vector graph. For structural analysis such as a dental implant,

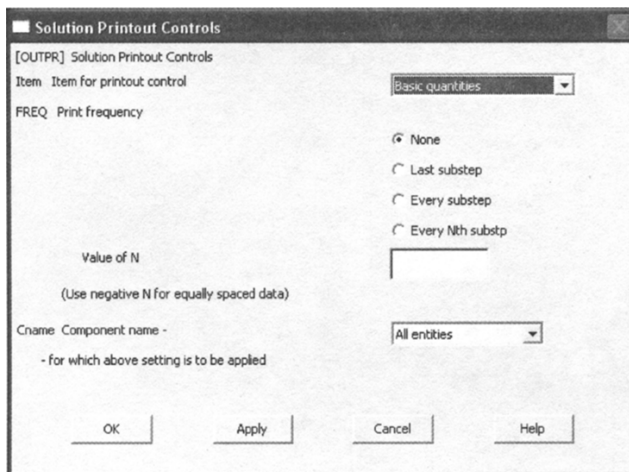


Fig. 5.26 Solution Printout Controls Window

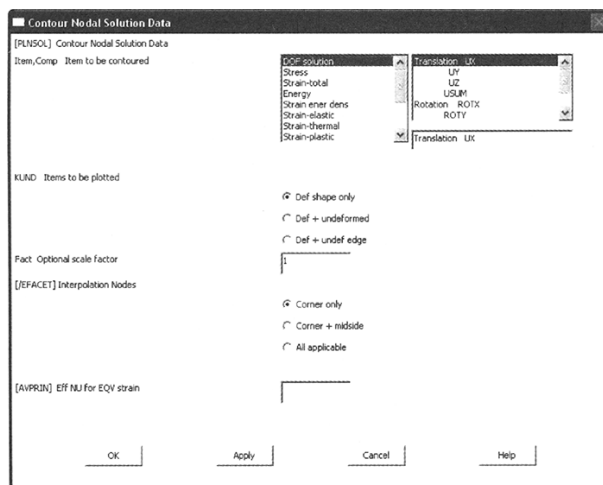


Fig. 5.27 Contour Nodal Solution Data

the stress distribution, strain level, and deformation of the structure can be shown using contour or vector plot.

To plot stress distribution contour, click the Node Solution under the Contour Plot command in the ANSYS Main Menu. A Contour Nodal Solution Data window pops up, shown in Fig. 5.27.

In the Contour Nodal Solution Data window, users can select parameters to be plotted such as stress, strain or displacement. There are many options under each of the above parameters. Fig.5.28 (a) and (b) shows that under the stress parameter, there are options of stress in x , y and z directions, shear stress in xy, yz, and xz directions, principal stresses, von Mises stress, and so on.

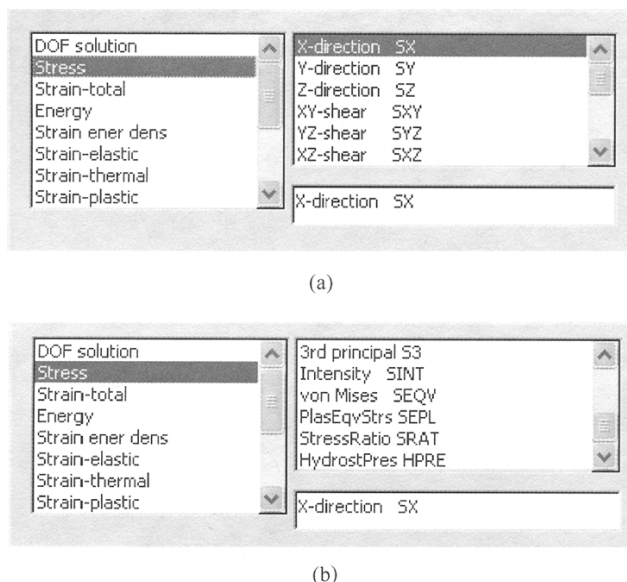


Fig. 5.28 Sub-option of Stress Contour Plot

To plot von Mises stress contour, use the mouse to highlight the von Mises ESQV option shown in Fig. 5.28 (b). Once all option in the Contour Nodal Solution Data window has been defined, click the OK button in the window, a von Mises stress contour will appear in the window as shown in Fig. 5.29. To plot strain and displacement contours is similar as to plot stress contour. The procedure of vector plot is similar as the contour plot. The only difference between the vector and contour plots is that the former uses vector indicators (small arrows) to represent the results, while the later uses colours to show the result.

The advantage of contour format is to give quick and direct graphic view of the result. Its limitation is that it only shows the result on the surface of the model and does not provide any accurate value and location.

5.2.4.2 Plot Result on Graph

Plot result on graph is a useful tool in ANSYS. It allows users to define a path across the model and plot the analysis result against the defined path to a graph. By using it, users can specify the location on the model and review the result accurately at this specific location. To plot analysis result against a path across the model, users need to define a path first. Secondly, map a specific result to the path before finally plot the result on the path. In ANSYS, the Define Path command is under Path Operations command as shown in Fig. 5.30 (a). Path can be defined by nodes, on working plane, or by location. To define path by nodes, click the By Nodes command, and then a By Nodes window pops up (Fig. 5.30 (b)). Use mouse to select a node on the model as the start of the path. Users can select two or more nodes to define a path. Once all nodes are selected, click OK in the By Nodes

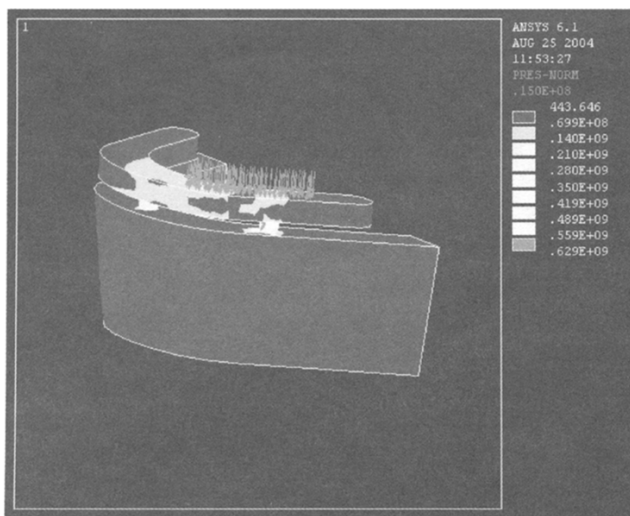


Fig. 5.29 von Mises Stress Distribution in the Dental Implant System

window, the path define is completed and a new By Nodes window pops up as shown in Fig. 5.30 (c).

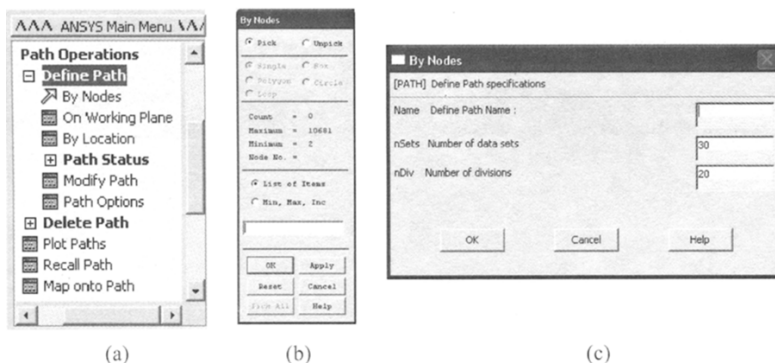


Fig. 5.30 Define Path by Nodes

Enter a path name and set number of data or number of divisions on the path. The default values are 30 and 20, respectively. Click OK to confirm the setting in this window. The next step is to map the analysis result to the path. Click the Map onto Path command, a Map Result Items onto Path window pops up as shown in Fig. 5.31.

In this window, users may enter User label for item and select the Item to be mapped as shown in Fig. 5.32. Once the settings in this window are defined, click OK to confirm the settings.

To plot the mapped result on the path, click the On Graph command under the Plot Path Item, a Plot of Path Items on Graph window pops up as shown in Fig.5.33.

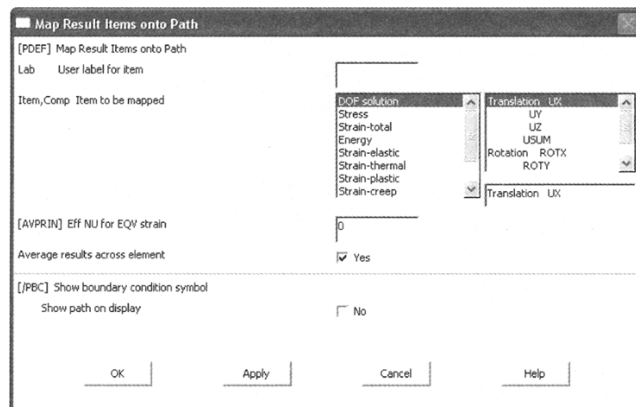


Fig. 5.31 Map Result Items on to Path Window

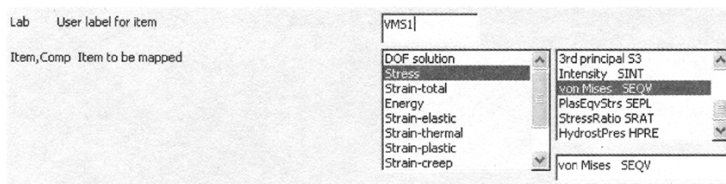


Fig. 5.32 Define Settings in the Map Result Items onto Path Window

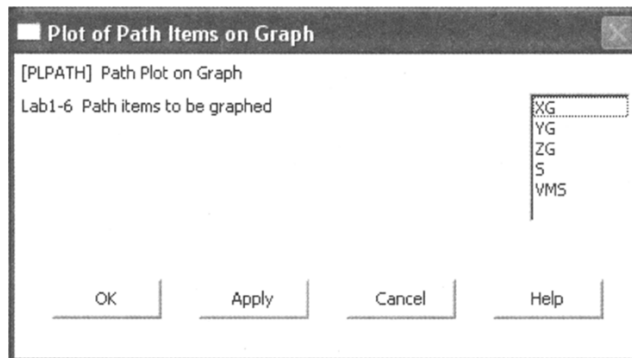


Fig. 5.33 A Plot of Path Items on Graph

Select the entered User label for item (it is VMS in this example) and click OK, a graph will appears on the window as shown in Fig. 5.34.

5.2.4.3 List and Export Result

Although ANSYS provides users with powerful graphic plotting function, its list and export result function allows users to carry out process using spreadsheet software such as Excel.

To list the result, click the Nodal Solution under the List Results command, a

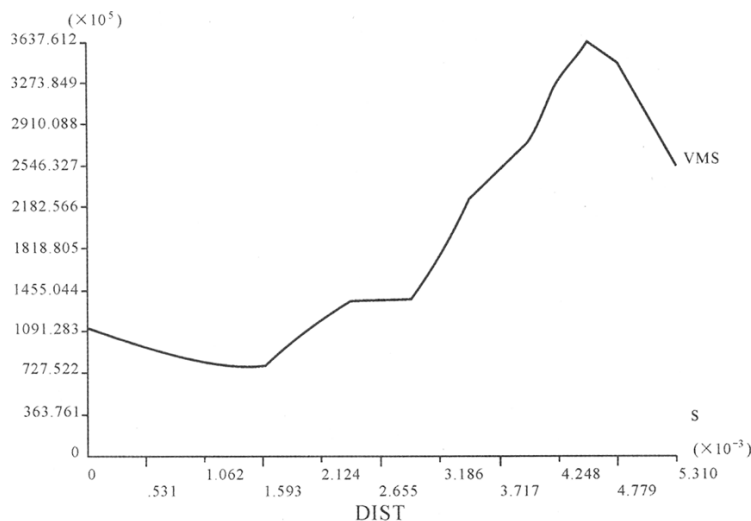


Fig. 5.34 Plot of the Result Mapped to a Path

List Nodal Solution window pops up as shown in Fig. 5.35. In this window, users selects the result to be listed. It is similar to selecting parameters to plot analysis result. Click OK after the parameter is selected; the result will appear in a popped up window (shown in Fig.5.36).

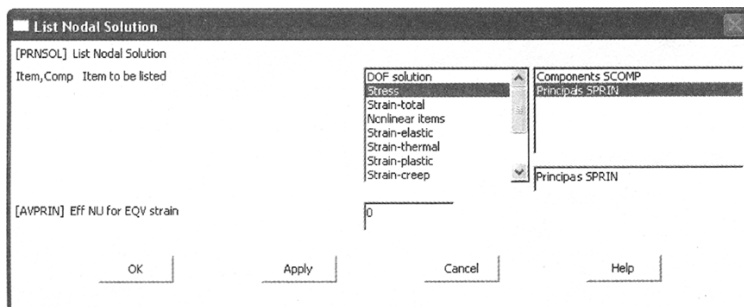


Fig. 5.35 List Nodal Solution Window

To export the listed result to a file, click File, then Save as on the PRNSOL command window. This allows users to save a text file for later use.

5.2.5 Summary

In this chapter, a step by step description of how to use commercial finite element software ANSYS to carry out FE analysis for a Brânemark same-day dental implant system is presented. It covers all the fundamental skills. In reality, the implant model may be more complicated than the one modelled in this chapter. However, the case shown in this chapter is a good starting point for those who want to use finite element analysis in their study.

PRINSOL Command					
File					
Save as ...	1	SUBSTEP=	1		
Print ...	0000	LOAD CASE=	0		
Copy to Output		ARE FOR MATERIAL	1		
Close					
	NODE	S1	S2	S3	SINT SEQ
	1	0.14968E+07-0.66373E+06-0.88193E+07	0.10316E+08	0.94337E+07	
	2	0.48716E+06-0.12048E+06-0.18176E+07	0.23047E+07	0.20748E+07	
	4	0.93042E+06	0.10818E+06-0.49458E+07	0.58762E+07	0.55113E+07
	6	0.19230E+07	0.27758E+06-0.10192E+06	0.20250E+07	0.19075E+07
	8	0.21253E+07	0.77220E+06	86261.	0.20391E+07 0.17971E+07
	10	0.33392E+07	0.13523E+07	50715.	0.32885E+07 0.28685E+07
	12	0.40543E+07	0.14420E+07	0.33819E+06	0.37162E+07 0.33055E+07
	14	0.51284E+06-0.17886E+07	0.85674E+07	0.90802E+07	0.81763E+07
	16	3138.9	-0.39077E+06-0.38326E+07	0.38357E+07	0.36547E+07
	19	0.40604E+06-0.18873E+07-0.88711E+07	0.92921E+07	0.81694E+07	

Fig. 5.36 A List Results Window

Comparing to other commercial software, ANSYS has demonstrated excellent suitability for various applications and easy to learn and use. Furthermore, the build-in preprocess and postprocess modules are very helpful for new users to learn how to use finite element software.

5.3 ABAQUS

5.3.1 Introduction

ABAQUS is a suite of powerful engineering simulation programs, based on the finite element method, that can solve problems ranging from relatively simple linear analyses to the most challenging nonlinear simulations. ABAQUS contains an extensive library of elements that can model virtually any geometry. It has an equally extensive list of material models that can simulate the behavior of most typical engineering materials including metals, rubber, polymers, composites, crushable/resilient foams, and so on.

ABAQUS is a simple-to-use software with a wide range of capabilities, even the most complicated problems can be modeled easily. For example, problems with multiple components are modeled by associating the geometry to define each component with the appropriate material models. In most simulations, even highly nonlinear ones, users only need provide the engineering data such as the geometry of the structure, its material behavior, its boundary conditions, and the loads applied to it. In a nonlinear analysis, ABAQUS automatically chooses appropriate load increments and convergence tolerances. Not only does it choose the values for these parameters, it also continually adjusts them during the analysis to ensure that an accurate solution is obtained efficiently. Users rarely has to define parameters for controlling the numerical solution of the problem.

ABAQUS consists of two main analysis modules—ABAQUS/Standard and

ABAQUS/Explicit. There are also two special-purpose add-on analysis products for ABAQUS/Standard—ABAQUS/Aqua and ABAQUS/Design. In addition, ABAQUS/Safe provides fatigue postprocessing, while ABAQUS/ADAMS, ABAQUS/CAT, ABAQUS/C-MOLD, and ABAQUS/MOLDFLOW are interfaces to ADAMS/Flex, CATIA, C-MOLD, and MOLDFLOW, respectively. ABAQUS/CAE is the complete ABAQUS environment that includes capabilities in creating ABAQUS models, interactively submitting and monitoring ABAQUS jobs, and evaluating results. ABAQUS/Viewer is a subset of ABAQUS/CAE that includes just the postprocessing function. The relationship between these modules is shown in Fig. 5.37.

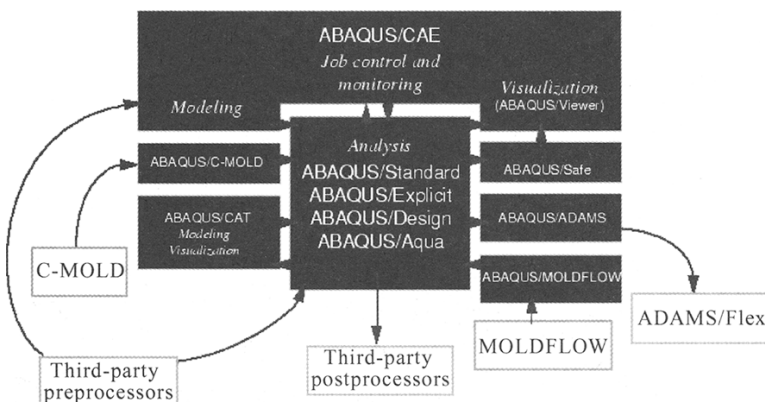


Fig. 5.37 ABAQUS Modules

ABAQUS/Standard

ABAQUS/Standard is a general-purpose analysis module that can solve a wide range of linear and nonlinear problems involving static, dynamic, thermal, and electrical response of components. This module is the main subject of this guide.

ABAQUS/Explicit

ABAQUS/Explicit is a special-purpose analysis module that uses an explicit dynamic finite element formulation. It is suitable for short-lived, transient dynamic events, such as impact and blast problems, and is also very efficient for highly nonlinear problems involving changing contact conditions such as forming simulations. ABAQUS/Explicit is not specifically covered in this guide but is described in the companion publication Getting Started with ABAQUS/Explicit. ABAQUS/CAE interface is the same for both analysis modules. In addition, the output is similar for the two modules, and ABAQUS/Viewer can be used to postprocess the results from either module.

ABAQUS/CAE

ABAQUS/CAE (Complete ABAQUS Environment) is an interactive, graphical

environment for ABAQUS. It allows models to be created quickly and easily by producing or importing the geometry of the structure to be analyzed and decomposing the geometry into meshable regions. Physical and material properties can be assigned to the geometry, together with loads and boundary conditions. ABAQUS/CAE contains very powerful options to mesh the geometry and to verify the resulting analysis model. Once the model is completed, ABAQUS/CAE can submit, monitor, and control the analysis jobs. The Visualization module can then be used to interpret the results. ABAQUS/CAE is also discussed in this guide.

5.3.2 Model an Implant in ABAQUS/CAE

This example of a GJP biomechanical optimum implant, shown in Fig. 5.38, leads readers through the ABAQUS/CAE modelling process by visiting each of the modules and showing readers the basic steps used to create and analyze a simple model.

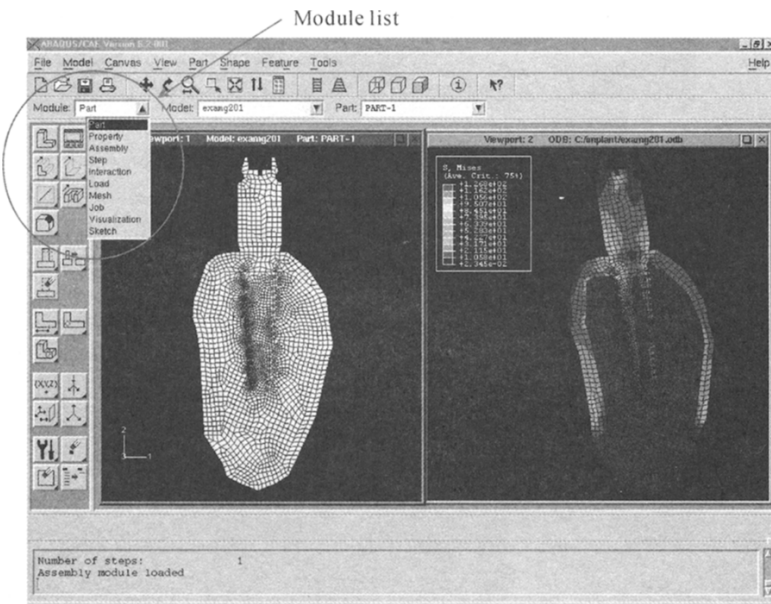


Fig. 5.38 ABAQUS/CAE Interface

Part

Sketch the two-dimensional geometry and create a part representing the implant.

Property

Define the material properties and section properties of the implant.

Assembly

Assemble the model.

Step

Configure the analysis procedure and output requests.

Load

Apply loads and boundary conditions to the implant.

Mesh

Mesh the implant.

Job

Create a job and submit it for analysis.

Visualization

View the results of the analysis.

5.3.2.1 Create a Part

We use the Part module to create each of the parts to analyze. Parts that define the geometry of individual components of the model and, therefore, are the building blocks of an ABAQUS/CAE model. We can create parts that are native to ABAQUS/CAE, or import parts created by other applications either as a geometric representation or as a finite element mesh.

We will start the implant problem by creating a two-dimensional, deformable planar part. We do this by sketching the geometry of the implant. ABAQUS/CAE automatically enters the Sketcher when creating the part. ABAQUS/CAE often displays a short message in the prompt area indicating what one should do next.

To create the implant model

- (1) If users did not already start ABAQUS/CAE, type `abaqus cae`, where `abaqus` is the command used to run ABAQUS.
- (2) Select Create Model Database from the Start Session dialog box that appears.
- (3) In the Module list located under the toolbar (see Fig. 5.38), click Part to enter the Part module.
- (4) From the main menu bar, select Part→Create to create a new part.
- (5) Name the part Frame. Choose a two-dimensional, deformable body and a planar wire base feature.
- (6) Click Continue to exit the Create Part dialog box. ABAQUS/CAE automatically enters the Sketcher. The Sketcher toolbox appears in the left side of the main window, and the Sketcher grid appears in the viewport. The Sketcher contains a set of basic tools that allow users to sketch the two-dimensional profile of the part.
- (7) After we finish the implant geometry in Sketcher, click Done to exit the Sketcher.

The implant part has been created in the screen.

5.3.2.2 Define Material Properties

There are three materials to be used in the implant model, which are called Cortical bone, Implant, and Trabecul bone, respectively. We use the Property module to create materials and to define their properties. Fig. 5.39 shows the Submenus available under the Material Manager.

To define a material

- (1) In the Module list located under the toolbar, select Property to enter the Property module.
- (2) From the main menu bar, select Material → Create to create a new material. The Create Material dialog box appears.
- (3) Name the material Trabecul, and click Continue. The material editor appears. (see Fig. 5.39)

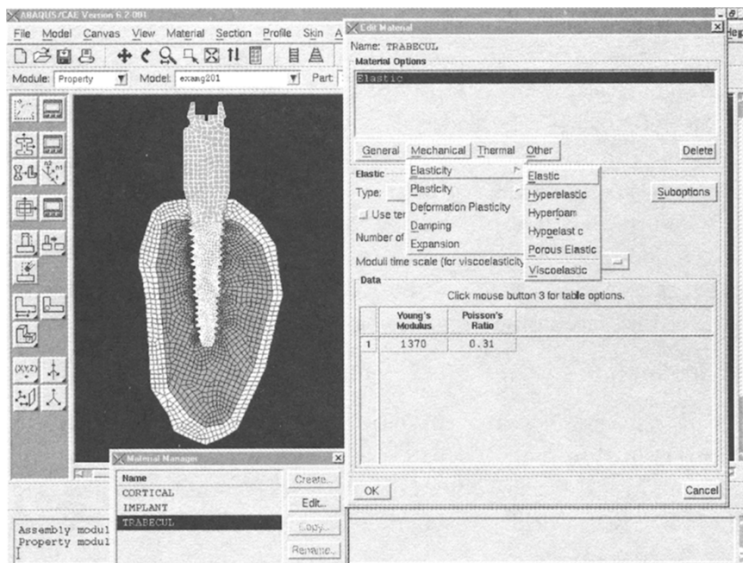


Fig. 5.39 Define Material Properties in ABAQUS/CAE

- (4) Use the menu bar under the browser area of the material editor to reveal menus containing all the available material options. When we select a material option, the appropriate data entry form appears below the menu.
- (5) Type a value of 1370 for Young's modulus and a value of 0.31 for Poisson's Ratio in the respective fields. Use [Tab] or move the cursor to a new cell and click to move between cells.
- (6) Click OK to exit the material editor.

ABAQUS uses section concept to link materials with objects. We need define the section properties of a model by creating sections in the Property module. After the section creation, we can use one of the following two methods to assign the section to the part in the current viewport:

- 1) Simply select the region from the part and assign the section to the selected region;
- 2) Use the Set toolset to create a homogeneous set containing the region and assign the section to the set.

In the implant model, we will create three sections that are behave of Cortical,

Implant, and Trabecul, respectively. The sections will be assigned to the three relative regions, see Fig. 5.39.

5.3.2.3 Define the Assembly

Each part that we create is oriented in its own coordinate system and is independent of the other parts in the model. We use the Assembly module to define the geometry of the assembly by creating instances of a part and then positioning the instances relative to each other in a global coordinate system. Although a model may contain many parts, it contains only one assembly.

We will create a single instance of the implant in this model. ABAQUS/CAE positions the instance so that the origin of the sketch that defined the implant overlays the origin of the assembly's default coordinate system.

To define the assembly

- (1) In the Module list located under the toolbar, click Assembly to enter the Assembly module.
- (2) From the main menu bar, select Instance→Create. The Create Instance dialog box appears.
- (3) In the dialog box, select Implant and click OK.

ABAQUS/CAE creates an instance of the implant. In this example the single instance of the implant defines the assembly. The implant is displayed in the 1-2 plane of the global coordinate system (a right-handed, rectangular Cartesian system). A triad in the lower-left corner of the viewport indicates the origin and orientation of the global coordinate system.

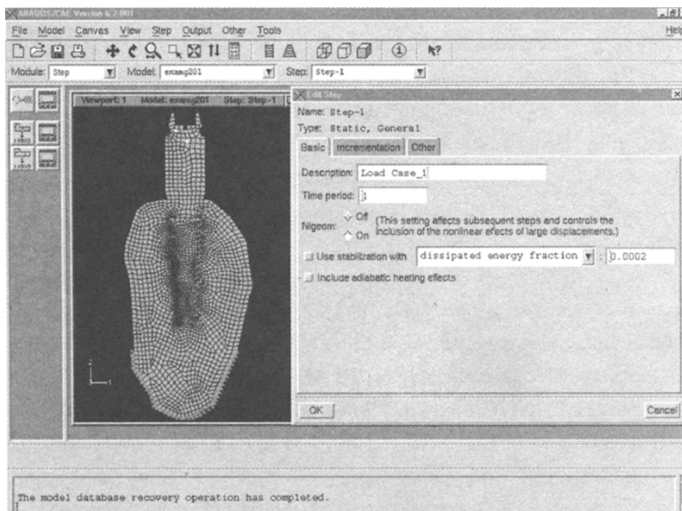


Fig. 5.40 Configuring an Analysis in ABAQUS/CAE

5.3.2.4 Define an Analysis

ABAQUS can be used to solve general static and dynamic response problems. In this example we are interested in the static response of the implant to both horizontal and vertical loads applied at the top center of the implant, with the bottom end fully constrained (see Fig. 5.40). This is a single event, so only a single analysis step is needed for the simulation. Thus the analysis will consist of two steps overall:

- 1) An initial step, in which we will apply boundary conditions that constrain the bottom end of the implant;
- 2) An analysis step, in which we will apply two concentrated loads at the top center of the implant.

ABAQUS/CAE generates the initial step automatically, but we must use the Step module to create the analysis step ourselves. The Step module also allows us to request output for any step in the analysis.

There are two kinds of analysis steps in ABAQUS: general analysis steps, which can be used to analyze linear or nonlinear response, and linear perturbation steps, which can be used only to analyze linear problems. In this simulation we will define a static, general step.

To create a static analysis step

- (1) In the Module list located under the toolbar, click Step to enter the Step module.
- (2) From the main menu bar, select Step→Create to create a step. The Create Step dialog box appears with a list of all the general procedures and a default step name of Step-1.
- (3) Change the step name to Load Case_1.
- (4) Select “Static, general” as the Procedure type, then continue. The Edit Step dialog box appears with the default settings for a static step.
- (5) Click the tabs, Basic/Incrementation/Other, to see its contents; The default values provided for the step are acceptable.
- (6) Click OK to create the step and to exit the Edit Step dialog box.

To request data output

Finite element analyses can create large amounts of output. ABAQUS allows users to control and manage this output so that only data required to interpret the results of the simulation are produced. Four types of output are available:

- 1) Results stored in a neutral binary file used by ABAQUS/Viewer for postprocessing (This file is called the ABAQUS output database file and has the extension .odb);
- 2) Printed tables of results, written to the ABAQUS data (.dat) file;
- 3) Restart data used to continue the analysis, written to the ABAQUS restart (.res) file;
- 4) Results stored in binary files for subsequent postprocessing with third-party software, written to the ABAQUS results (.fil) file.

By default, ABAQUS/CAE writes the results of the analysis to the output database (.odb) file. When a step is created, ABAQUS/CAE generates a default output request for the step. We do not need to do anything to accept these defaults. The Field Output Requests Manager can be used to request output of variables that should be written at relatively low frequencies to the output database from the entire model or from a large portion of the model. The History Output Requests Manager can be used to request output of variables that should be written to the output database at a high frequency from a small portion of the model, for example, the displacement of a single node.

Results can also be written in tabular form to the ABAQUS data (.dat) file. By default, no printout is written to the ABAQUS data file. In this implant model, we are interested in the displacements (output variable U), the reaction forces at the constrained locations (output variable RF), and the stress in the members (output variable S).

5.3.2.5 Apply Boundary Conditions and Loads to the Model

In ABAQUS analysis, prescribed conditions such as loads and boundary conditions, are step dependent, which means that users must specify the step or steps in which they become active. Now that we have defined the steps in the analysis, we can use the Load module to define prescribed conditions.

In structural analysis, boundary conditions are applied to those regions of the model where the displacements and/or rotations are known. Such regions may be constrained to remain fixed (have zero displacement and/or rotation) during the simulation or may have specified, nonzero displacements and/or rotations. The directions in which motion is possible are called Degrees of Freedom (DOF).

In this model the bottom edge portion of the implant is constrained completely, and thus, cannot move in any direction. Fig. 5.41 shows the boundary condition.

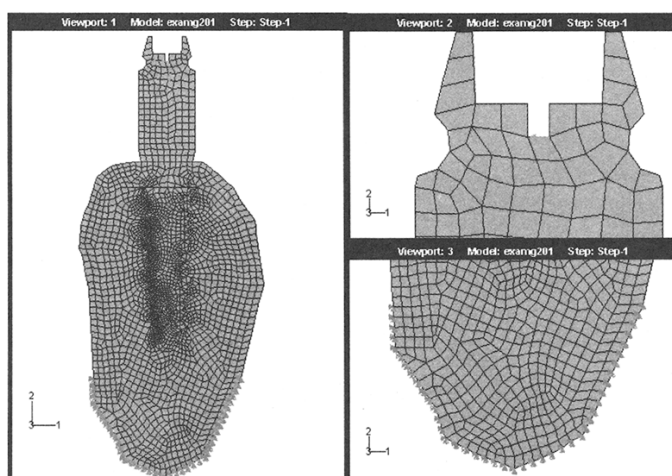


Fig. 5.41 Define Boundary Condition and Load Case in ABAQUS/CAE

To apply boundary conditions to the implant

- (1) In the Module list located under the toolbar, click Load to enter the Load module.
- (2) From the main menu bar, select BC → Create. The Create Boundary Condition dialog box appears.
- (3) In the Create Boundary Condition dialog box:
 - 1) Name the boundary condition Fixed.
 - 2) From the list of steps, select Initial as the step in which the boundary condition will be activated. All the mechanical boundary conditions specified in the Initial step must have zero magnitudes. This condition is enforced automatically by ABAQUS/CAE.
 - 3) In the Category list, accept Mechanical as the default category selection.
 - 4) In the Type for selected step list, select Displacement/Rotation, and click Continue.
- (4) In the viewport, select the vertex at the bottom edge of the implant as the region to which the boundary condition will be applied.
- (5) Click mouse button 2 in the viewport or click Done in the prompt area to indicate that we have finished selecting regions.

Then the Edit Boundary Condition dialog box appears. When we are defining a boundary condition in the initial step, all available DOFs are unconstrained by default. In the dialog box:

- 1) Toggle on U1 and U2 since all translational DOFs need to be constrained.
 - 2) Click OK to create the boundary condition and to close the dialog box.
- ABAQUS/CAE displays two arrowheads at the vertex to indicate the constrained DOFs.

To apply a load to the implant

After we have constrained the implant, we can apply two concentrated loads to the top center of the implant. In ABAQUS the term “load” (as in the Load module in ABAQUS/CAE) generally refers to anything that induces a change in the response of a structure from its initial state, including:

- 1) concentrated forces;
- 2) pressures;
- 3) nonzero boundary conditions;
- 4) body loads;
- 5) temperature (with thermal expansion of the material defined).

In this simulation two concentrated forces of 100 N are applied in the negative 1-direction and the negative 2-direction to the top center of the implant, respectively (see Fig. 5.41). These loads are applied during the static step we created in the Step module. In reality there is no such thing as a concentrated, or point, load; the load will always be applied over some finite area. However, if the area being loaded is small enough, it is an appropriate idealisation to treat the load

as a concentrated load.

To apply a concentrated force to the implant

- (1) From the main menu bar, select Load→Manager. The Load Manager appears.
- (2) At the bottom of the Load Manager, click Create. The Create Load dialog box appears.
- (3) In the Create Load dialog box:
 - 1) Name the load Force;
 - 2) From the list of steps, select Apply load as the step in which the load will be applied;
 - 3) In the Category list, accept Mechanical as the default category selection;
 - 4) In the Type for selected step list, accept the default selection of Concentrated force;
 - 5) Click Continue.
- (4) In the viewport, select the vertex at the top center of the implant as the region where the load will be applied.
- (5) Click mouse button 2 in the viewport or click Done in the prompt area to indicate that we have finished selecting regions. The Edit Load dialog box appears. In the dialog box:
 - 1) Enter a magnitude of -100.0 for CF1;
 - 2) Click OK to create the load and to close the dialog box. ABAQUS/CAE displays a downward-pointing arrow at the vertex to indicate that the load is applied in the negative 1-direction.
- (6) Repeat the above procedure to apply a concentrated load of 100.0 N in the negative 2-direction.

5.3.2.6 Mesh the Model

We use the Mesh module to generate the finite element mesh. We can choose the meshing technique that ABAQUS/CAE will use to create the mesh, the element shape, and the element type. The default meshing technique assigned to the model is indicated by the color of the model that is displayed when one enters the Mesh module; if ABAQUS/CAE displays the model in orange, it cannot be meshed without additional assistance.

In this section we will assign a particular ABAQUS element type to the model. Two-dimensional “Quadrilateral” elements will be used to model the implant. These elements are chosen because they are ideal for modelling 2D plane strain problem such as this implant.

To assign an ABAQUS element type

- (1) In the Module list located under the toolbar, click Mesh to enter the Mesh module.
- (2) From the main menu bar, select Mesh→Element Type.
- (3) In the viewport, select the entire implant as the region to be assigned an element type. In the prompt area, click Done when we finish. The Element Type dialog

box appears.

- (4) In the dialog box, select the following:
 - 1) Standard as the Element Library selection (the default).
 - 2) Linear as the Geometric Order (the default).
 - 3) Plane strain as the Family of elements.
- (5) In the Line tabbed page, accept the default element type. A description of the element type CPE4 appears at the bottom of the dialog box. ABAQUS/CAE will now associate CPE4 elements with the elements in the mesh.
- (6) Click OK to assign the element type and to close the dialog box.
- (7) In the prompt area, click Done to end the procedure.

Create the mesh

Basic meshing is a two-stage operation: first we seed the edges of the part instance, and then we mesh it. We select the number of seeds based on the desired element size or on the number of elements that we want along an edge, and ABAQUS/CAE places the nodes of the mesh at the seeds whenever possible. In this implant model, a high mesh density is required in the particular interfaces as shown in Fig. 5. 42. Along the gear edge of the implant in Fig. 5. 42, the high mesh density can be generated using “seeds along edge” technology in ABAQUS/CAE.

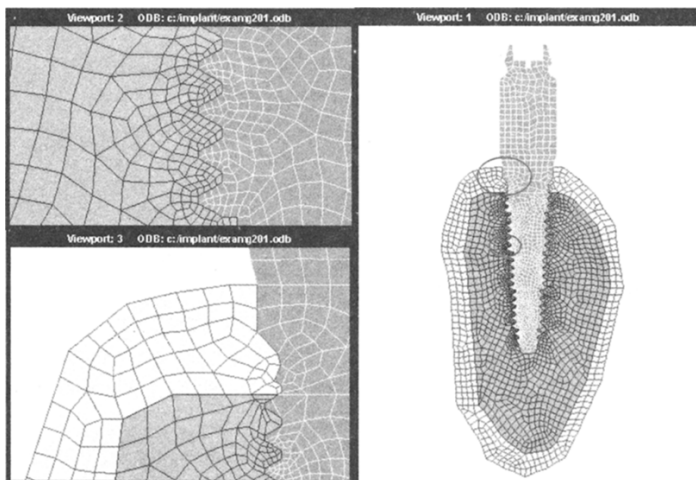


Fig. 5.42 Global Mesh and Detailed Mesh of the Implant Model

To seed and mesh the model

- (1) From the main menu bar, select Seed → Instance to seed the part instance. The prompt area displays the default element size that ABAQUS/CAE will use to seed the part instance. This default element size is based on the size of the part instance. A relatively large seed value will be used so that only coarse element density will be created in global region.

- (2) In the prompt area, specify an element size , and press Enter or click mouse button 2 in the viewport.
- (3) Click mouse button 2 in the viewport or Done in the prompt area to accept the seeding.
- (4) From the main menu bar, select Mesh→Instance to mesh the part instance.
- (5) From the buttons in the prompt area, click Yes to confirm that we want to mesh the part instance.

5.3.2.7 Create an Analysis Job and Use Keywords Editor

We have completely configured the analysis in the above sections from 2.1 to 2. 6. In this section, we will move to the Job module to create a job that is associated with our model and to add printed output requests using the Keywords Editor.

To create an analysis job

- (1) In the Module list located under the toolbar, click Job to enter the Job module.
- (2) From the main menu bar, select Job→Manager. The Job Manager appears. When we finish defining our job, the Job Manager will display a list of all jobs, the model associated with each job, the type of analysis, and the status of the job.
- (3) In the Job Manager, click Create. The Create Job dialog box appears with a list of the models in the model database, see Fig. 5.43.

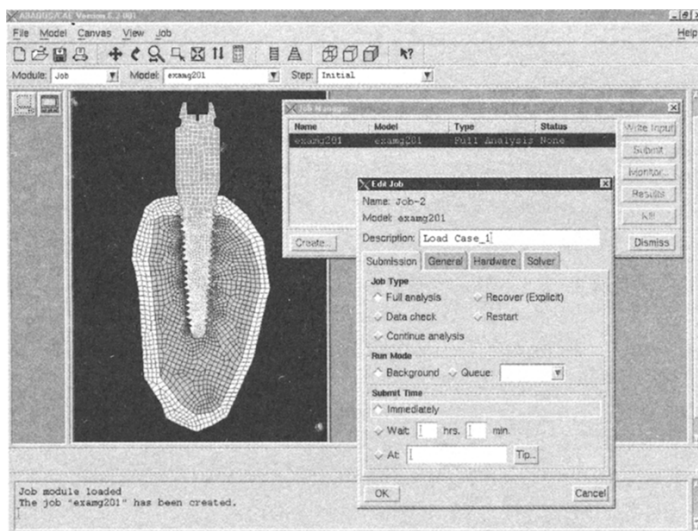


Fig. 5.43 Job Manager to Create a Job for the Implant Model

- (4) Name the job Examp201, and click Continue. The Edit Job dialog box appears.
- (5) In the Description field, type Load Case_1.
- (6) In the Submission tabbed page, select “Data check” as the Job Type to execute a check which find out any possible error in the model definition. Click the General tab, and toggle all Preprocessor Printout options. Click OK to accept all

other default job settings in the job editor and to close the dialog box.

To add printed output requests using the keywords editor

- (1) From the main menu bar, select Model → Edit Keywords and select the current model. The Edit Keywords dialog box appears containing the input file that has been generated for our model.
- (2) Only text blocks with a white background can be edited. Use the scroll bar on the right side of the dialog box to find the text blocks where the * EL PRINT and * NODE PRINT options are located (toward the bottom of the file). In each block enter data by first placing the cursor at the end of the line. For each option change the frequency at which printed output will be written to 1 and press Enter to create a new line on which we can specify the output variable names. The option blocks should resemble the following when we finish:

```
* El Print, freq = 1
S,
* Node Print, freq = 1
U,
RF,
```

- (3) When we have finished the whole editing, click OK to exit the Keywords Editor.

5.3.2.8 Run the Analysis

When the datacheck analysis completes with no error messages, run the analysis itself. To do this, edit the job definition and set the Job Type to Continue analysis; then, click Submit in the Job Manager to submit our job for analysis.

One should always perform a datacheck analysis before running a simulation to ensure that the model has been defined correctly and to check whether there is enough disk space and memory available to complete the analysis. However, it is possible to combine the datacheck and analysis phases of the simulation by setting the Job Type to “Full analysis”.

ABAQUS/CAE allows users to monitor the running procedure during the running time. By selecting “Monitor” in Job manager window, the job monitor window appears as Fig. 5.44. For multi-increments analysis we are allowed to view the half-way results before the analysis is finished. By selecting “Results” in Job manager window, the results up to the current increment will be shown in the viewport. It is convenient to check if the analysis is going to the right direction before it takes a substantial amount of time to go to a wrong direction.

If a simulation is expected to take a substantial amount of time, it may be convenient to run it in a batch queue by selecting Queue as the Run Mode.

5.3.2.9 Result Analysis in ABAQUS

ABAQUS job will generate several files that contain different information about the job analysis and the job results.

Three types of message file are available:

- 1) Log file is written to record the job procedure;

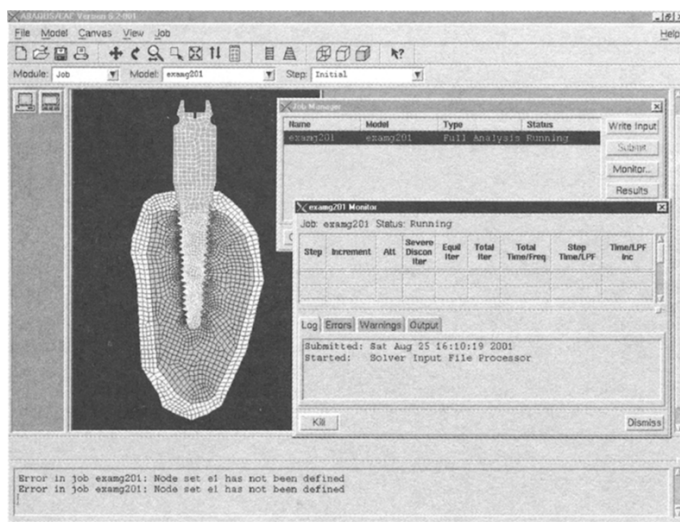


Fig. 5.44 Job Monitor to Monitor Running Analysis

- 2) Status file is used to monitor the analysis;
- 3) Message file contains detailed information about the simulation's progress.

Four types of output are available:

- 1) Neutral binary output can be written to the output database (.odb) file, using the * OUTPUT option and related suboptions;
- 2) Printed output can be written to the printed output (.dat) file. This is only available for ABAQUS/Standard;
- 3) Restart output can be written to the restart (.res) file using the * RESTART option for the purpose of conducting restart analyses;
- 4) Results (.fil) file output can be written for third-party postprocessing.

5.3.3 Job Information Files

5.3.3.1 Log File

The job log file, `examp201.log` contains the messages similar to those shown below:

```

ABAQUS JOB examp201
Begin Solver Input File Processor
06/21/01 15:43:06
Run C:\ABAQUS\6.2-1\exec\pre.exe
ABAQUS/STANDARD is running on a Category B machine
and has checked out the Enabling Token
from the license server on pc001
06/21/01 15:43:15
End Solver Input File Processor
Begin ABAQUS/Standard Analysis

```

06/21/01 15:43:15

Run C:\ABAQUS\6.2-1\exec\standard.exe

ABAQUS/STANDARD is running on a Category B machine
and has checked out the Enabling Token
from the license server on pc001

06/21/01 15:43:41

End ABAQUS/Standard Analysis

ABAQUS JOB examg201 COMPLETED

5.3.3.2 Status File

Monitor the simulation while it is running by looking at the status file, examg201.sta. When ABAQUS has finished the analysis, the status file will contain information similar to the following:

SUMMARY OF JOB INFORMATION:

STEP	INC	ATT	SEVERE	EQUIL	TOTAL	TOTAL	STEP	INC OF	DOF	IF
					DISCON	ITERS	ITERS	TIME/	TIME/LPF	TIME/LPF
								MONITOR	RIKS	
					ITERS			FREQ		
1	1	1	0	1	1	1.00	1.00		1.000	

THE ANALYSIS HAS COMPLETED SUCCESSFULLY

5.3.3.3 Message File

The message file, examg201.msg, contains detailed information about the analysis. In the first part of the message file, we can look at the information for the increment control parameters.

STEP	1	INCREMENT	1	STEP TIME	0.00
		STEP	1	STATICANALYSIS	

This load case is the default load case that always appears

AUTOMATIC TIME CONTROL WITH--

A SUGGESTED INITIAL TIME INCREMENT OF	1.00
AND A TOTAL TIME PERIOD OF	1.00
THE MINIMUM TIME INCREMENT ALLOWED IS	1.000E-05
THE MAXIMUM TIME INCREMENT ALLOWED IS	1.00

CONVERGENCE TOLERANCE PARAMETERS FOR FORCE

CRITERION FOR RESIDUAL FORCE FOR A NONLINEAR PROBLEM	5.000E-03
CRITERION FOR DISP. CORRECTION IN A NONLINEAR PROBLEM	1.000E-02
INITIAL VALUE OF TIME AVERAGE FORCE	1.000E-02

AVERAGE FORCE IS TIME AVERAGE FORCE

ALTERNATE CRIT. FOR RESIDUAL FORCE FOR A NONLINEAR PROBLEM	2.000E-02
--	-----------

CRITERION FOR ZERO FORCE RELATIVE TO TIME AVRG. FORCE	1.000E-05
---	-----------

CRITERION FOR RESIDUAL FORCE WHEN THERE IS ZERO FLUX	1.000E-05
--	-----------

CRITERION FOR DISP. CORRECTION WHEN THERE IS ZERO FLUX	1.000E-03
--	-----------

CRITERION FOR RESIDUAL FORCE FOR A LINEAR INCREMENT	1.000E-08
---	-----------

FIELD CONVERSION RATIO	1.00
------------------------	------

VOLUMETRIC STRAIN COMPATIBILITY TOLERANCE FOR HYBRID SOLIDS	1.000E-05
---	-----------

AXIAL STRAIN COMPATIBILITY TOLERANCE FOR HYBRID BEAMS	1.000E-05
---	-----------

TRANS. SHEAR STRAIN COMPATIBILITY TOLERANCE FOR HYBRID BEAMS	1.000E-05
SOFT CONTACT CONSTRAINT COMPATIBILITY TOLERANCE FOR P> P0	5.000E-03
SOFT CONTACT CONSTRAINT COMPATIBILITY TOLERANCE FOR P = 0.0	0.100
DISPLACEMENT COMPATIBILITY TOLERANCE FOR DCOUP ELEMENTS	1.000E-05
ROTATION COMPATIBILITY TOLERANCE FOR DCOUP ELEMENTS	1.000E-05

TIME INCREMENTATION CONTROL PARAMETERS

FIRST EQUILIBRIUM ITERATION FOR CONSECUTIVE DIVERGENCE CHECK	4
EQUILIBRIUM ITERATION AT WHICH LOG. CONVERGENCE RATE CHECK BEGINS	8
EQUILIBRIUM ITERATION AFTER WHICH ALTERNATE RESIDUAL IS USED	9
MAXIMUM EQUILIBRIUM ITERATIONS ALLOWED	16
EQUILIBRIUM ITERATION COUNT FOR CUT-BACK IN NEXT INCREMENT	10
MAXIMUM EQUILIB. ITERS IN TWO INCREMENTS FOR TIME INCREMENT INCREASE	4
MAXIMUM ITERATIONS FOR SEVERE DISCONTINUITIES	12
MAXIMUM CUT-BACKS ALLOWED IN AN INCREMENT	5
MAXIMUM DISCON. ITERS IN TWO INCREMENTS FOR TIME INCREMENT INCREASE	6
CUT-BACK FACTOR AFTER DIVERGENCE	0.2500
CUT-BACK FACTOR FOR TOO SLOW CONVERGENCE	0.5000
CUT-BACK FACTOR AFTER TOO MANY EQUILIBRIUM ITERATIONS	0.7500
CUT-BACK FACTOR AFTER TOO MANY SEVERE DISCONTINUITY ITERATIONS	0.2500
CUT-BACK FACTOR AFTER PROBLEMS IN ELEMENT ASSEMBLY	0.2500
INCREASE FACTOR AFTER TWO INCREMENTS THAT CONVERGE QUICKLY	1.500
MAX. TIME INCREMENT INCREASE FACTOR ALLOWED	1.500
MAX. TIME INCREMENT INCREASE FACTOR ALLOWED (DYNAMICS)	1.250
MAX. TIME INCREMENT INCREASE FACTOR ALLOWED (DIFFUSION)	2.000
MINIMUM TIME INCREMENT RATIO FOR EXTRAPOLATION TO OCCUR	0.1000
MAX. RATIO OF TIME INCREMENT TO STABILITY LIMIT	1.000
FRACTION OF STABILITY LIMIT FOR NEW TIME INCREMENT	0.9500
PRINT OF INCREMENT NUMBER, TIME, ETC., EVERY 1 INCREMENTS	
THE MAXIMUM NUMBER OF INCREMENTS IN THIS STEP IS	100
LINEAR EXTRAPOLATION WILL BE USED	
CHARACTERISTIC ELEMENT LENGTH	0.297
PRINT OF INCREMENT NUMBER, TIME, ETC., TO THE MESSAGE FILE EVERY 1 INCREMENTS	
EQUATION ARE BEING REORDERED TO MINIMIZE WAVEFRONT	

In the second part of the message file, we can look at the model's behaviour as the following

```
INCREMENT 1 STARTS. ATTEMPT NUMBER 1, TIME INCREMENT      1.00
EQUILIBRIUM ITERATION      1
AVERAGE FORCE      3.46    TIME AVG. FORCE      3.46
LARGEST RESIDUAL FORCE   8.664E-11 AT NODE      2399    DOF 1
LARGEST INCREMENT OF DISP. - 0.194   AT NODE      2240    DOF 1
LARGEST CORRECTION TO DISP. - 0.194   AT NODE      2240    DOF 1
THE FORCE EQUILIBRIUM RESPONSE WAS LINEAR IN THIS INCREMENT
```

ITERATION SUMMARY FOR THE INCREMENT:

```
1 TOTAL ITERATIONS, OF WHICH
 0 ARE SEVERE DISCONTINUITY ITERATIONS AND 1 ARE EQUILIBRIUM
ITERATIONS.
```

TIME INCREMENT COMPLETED 1.00, FRACTION OF STEP COMPLETED 1.00

STEP TIME COMPLETED 1.00, TOTAL TIME COMPLETED 1.00

THE ANALYSIS HAS BEEN COMPLETED

At the end of this file the analysis summary is given as below:

ANALYSIS SUMMARY

TOTAL OF 1 INCREMENTS

0 CUTBACKS IN AUTOMATIC INCREMENTATION

1 ITERATIONS

1 PASSES THROUGH THE EQUATION SOLVER OF WHICH

1 INVOLVE MATRIX DECOMPOSITION, INCLUDING

0 DECOMPOSITION(S) OF THE MASS MATRIX

1 REORDERING OF EQUATIONS TO MINIMIZE WAVEFRONT

0 ADDITIONAL RESIDUAL EVALUATIONS FOR LINE SEARCHES

0 ADDITIONAL OPERATOR EVALUATIONS FOR LINE SEARCHES

25 WARNING MESSAGES DURING USER INPUT PROCESSING

0 WARNING MESSAGES DURING ANALYSIS

0 ANALYSIS WARNINGS ARE NUMERICAL PROBLEM MESSAGES

0 ANALYSIS WARNINGS ARE NEGATIVE EIGENVALUE MESSAGES

0 ERROR MESSAGES

THE SPARSE SOLVER HAS BEEN USED FOR THIS ANALYSIS.

JOB TIME SUMMARY

USER TIME (SEC)= 5.8000

SYSTEM TIME (SEC)= 0.8000

TOTAL CPU TIME (SEC)= 6.6000

WALLCLOCK TIME (SEC)= 24

5.3.4 Job Result Files

5.3.4.1 Postprocess with ABAQUS/CAE

Graphical postprocessing is important because of the great volume of data created during a simulation. In any realistic model it is impractical for users to interpret results in the tabular form of the data file. ABAQUS/CAE allows users to view the results graphically using a variety of methods, including deformed shape plots, contour plots, vector plots, animations, and X-Y plots.

When the job completes successfully, we are ready to view the results of the analysis with ABAQUS/CAE. From the buttons on the right edge of the Job Manager, click Results. ABAQUS/CAE loads the Visualization module, opens the output database created by the job, and displays a fast plot of the model. The fast plot is a basic representation of the undeformed model shape and is an indication that we have opened the desired file. Alternatively, we can click Visualization in the Module list located under the toolbar, select File→Open, select examg201.odb from the list of available output database files, and click OK.

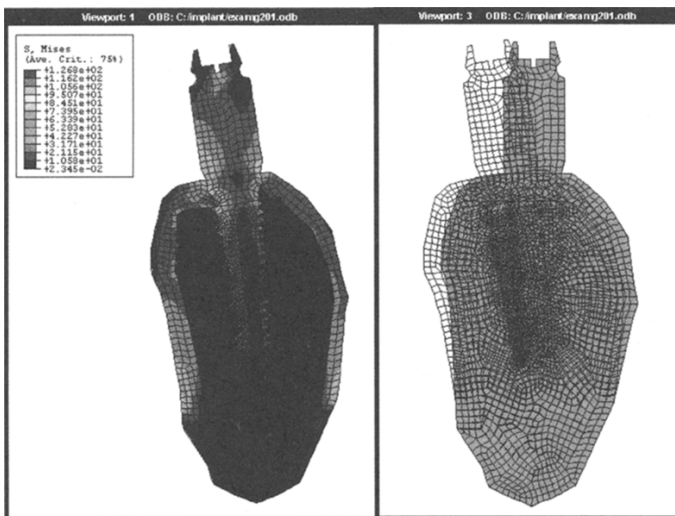


Fig. 5.45 View Analysis Results

Fig. 5.45 displays the von Mises stress contour on the deformed model shape. From the main menu bar, select Contour plot, using default setting option.

To compare the undeformed model shape with the deformed model shape

- (1) In the Basic tabbed page of the Deformed Shape Plot Options dialog box, toggle on Superimpose undeformed plot;
- (2) Click OK. By default, ABAQUS/CAE plots the undeformed model shape in green and the deformed model shape in white. The plot is shown in the right part of Fig. 5.45.

5.3.4.2 Print File Data File

After the analysis is completed, the data file, examg201.dat, will contain the tables of results requested with the * NODE PRINT and * EL PRINT options. The results from the implant simulation are shown below. The element output consists of a table of axial stress in the elements, while the node output consists of tables of nodal displacements and reaction forces.

In the first part of the print file, ABAQUS writes input deck processing information. We can look at the job scale in the print file as below:

PROBLEMSIZE

NUMBER OF ELEMENTS IS	2854
NUMBER OF NODES IS	2945
NUMBER OF NODES DEFINED BY USERS	2945
TOTAL NUMBER OF VARIABLES IN THE MODEL	5890
(DEGREES OF FREEDOM PLUS ANY LAGRANGE MULTIPLIER VARIABLES)	

If we set output requests using * El print to print the element stress at each integration point, we will have element stress output in examg201.dat as below:

ELEMENTOUTPUT

THE FOLLOWING TABLE IS PRINTED FOR ALL ELEMENTS WITH TYPE CPE4 AT THE INTEGRATION POINTS

ELEMENT	PT FOOT- NOTE	S11	S22	S33	S12
949	1	3.924	2.216	1.904	- 1.495
949	2	3.834	2.306	1.904	- 1.917
949	3	3.575	2.565	1.904	- 1.520
949	4	3.413	2.727	1.904	- 1.841
950	1	3.779	2.308	1.887	- 2.914
950	2	3.615	2.472	1.887	- 2.883
950	3	3.775	2.312	1.887	- 2.673
950	4	3.532	2.555	1.887	- 2.612
951	1	2.715	4.048	2.096	- 3.507
951	2	2.969	3.793	2.096	- 3.332
...					
1798	3	- 6.4473E - 04	1.6320E - 03	0.000	9.9250E - 04
1798	4	- 6.3243E - 04	1.6197E - 03	0.000	9.9955E - 04
1799	1	- 6.2963E - 04	1.5747E - 03	0.000	9.3184E - 04
1799	2	- 6.2656E - 04	1.5716E - 03	0.000	9.3865E - 04
1799	3	- 6.2530E - 04	1.5703E - 03	0.000	9.2794E - 04
1799	4	- 6.2228E - 04	1.5673E - 03	0.000	9.3454E - 04
MAXIMUM ELEMENT		2.8429E - 03	5.4068E - 03	0.000	1.4924E - 03
MINIMUM ELEMENT		1558	1788	1426	1789
MAXIMUM NODE		- 3.7536E - 03	- 7.0632E - 03	0.000	- 6.7281E - 03
MINIMUM NODE		1437	1558	1426	1558

We have set output requests using * Node print to print the node displacements in examg201.dat. Below is part of the node displacements output in the file.

NODEOUTPUT

THE FOLLOWING TABLE IS PRINTED FOR ALL NODES

NODE FOOT-NOTE	U1	U2
1	2.6145E - 04	- 8.1261E - 04
2	7.6767E - 05	- 1.4798E - 04
3	2.4300E - 04	- 5.9756E - 04

4	2.0798E - 04	- 4.7476E - 04
5	1.7763E - 04	- 3.8173E - 04
6	1.5107E - 04	- 3.1434E - 04
7	1.2465E - 04	- 2.5713E - 04
8	9.9932E - 05	- 2.0210E - 04
9	3.6770E - 05	- 4.0049E - 05
10	6.5746E - 05	- 1.1142E - 04
11	5.8316E - 05	- 8.4284E - 05
12	4.8597E - 05	- 6.1147E - 05
13	2.6480E - 05	- 8.8901E - 06
...		
4569	- 4.2065E - 03	- 1.3289E - 03
4570	- 1.1506E - 02	1.7034E - 03
4571	- 4.8437E - 03	- 1.7563E - 03
4572	- 1.7639E - 02	- 9.2328E - 03
MAXIMUM	5.7242E - 04	3.2395E - 02
AT NODE	4557	2120
MINIMUM	- 0.1938	- 3.5224E - 02
AT NODE	2240	1869

5.3.5 Conclusion

As an advanced finite element software for the general engineering purpose, ABAQUS package has been used widely in all engineering areas to solve problems from relatively simple linear analysis to the most challenging dynamic nonlinear simulations. To apply ABAQUS on the implant analysis and optimal design, we can look at the potential areas as the following:

- (1) Linear/nonlinear static analysis;
- (2) Linear/nonlinear dynamic analysis and impact analysis;
- (3) Nonlinear contact analysis between the implant interfaces.

ABAQUS/CAE can be used to create a complete ABAQUS analysis model. The solver (ABAQUS/Standard or ABAQUS/Explicit) reads the input file generated by ABAQUS/CAE, performs the analysis, sends information to ABAQUS/CAE to allow users to monitor the progress of the job, and generates an output database. ABAQUS/CAE is used to read the output database and view the results of the analysis.

We can perform a datacheck analysis once we have created a model. Error and warning messages are printed to the data file. After a successful datacheck analysis, estimates of the computer resources required for the simulation are printed to the data file.

Use ABAQUS/CAE to verify the model geometry and boundary conditions graphically, using the output database file generated during the datacheck phase.

It is often easiest to check for mistakes in material properties in the data (.dat) file; geometry, loads, and boundary conditions are more easily checked with a

graphical postprocessor such as ABAQUS/CAE.

Tables of results are printed in the data file. The output database file contains results for graphical postprocessing with ABAQUS/CAE.

Always check that the results satisfy basic engineering principles, such as equilibrium.

ABAQUS/CAE allows users to visualize analysis results graphically in a variety of ways.

References

1. Hibbitt, Karlsson, Sorensen (2001) ABAQUS Users' Manuals, Version 6.2, INC
2. Geng JP, Tan KBC, Liu GR (2001) Application of finite element analysis in implant dentistry: a review of literature. *J Prosthet Dent* 85:585-598
3. Geng JP, Ma QS, Xu W, Tan KBC, Liu GR (2004) Finite element analysis of four thread-form configurations in a stepped screw implant. *J Oral Rehabil* 37:236-242
4. Geng JP, Ma XX, Liu GR, Ying LA (2004) The effectiveness of element downsizing on finite element domains of infinite/finite element analysis in an implant-bone system. *Int Chin J Dent* 4: 63-66
5. Geng JP, Xu W, Tan KBC, Liu GR (2004) Finite element analysis of a biomechanical optimized stepped screw osseointegrated dental implant. *J Oral Implantol* 30:223-233
6. Gao JX, Xu W, Geng JP (2005) 3D Shape Reconstruction of Teeth by Shadow Speckle Correlation Method. *Int J Prosthodont* 18:436-437
7. Geng JP, Xu W, Yan WQ (2007) Model-based biomechanical dental implant optimization in bone-implant system. *Int Chin J Dent* 7:15-22

Index

- 30-degree load 70
2D 31, 82
3D 31, 82
3-unit prosthesis 63
- ABAQUS 92
Abutment 63
Abutment design 75
Abutment screw 69
Abutment screw failures 76
Abutment screw-abutment interface 68
Acrylic 63
Action 5
Adaptive remodelling response 82
Angled implant 71
Anisotropic material 34
ANSYS 92
Anterior mandible 87
Axial force 62
- Ball 73
Bar length 73
Bar span length 76
Bar system 76
Bar-clip 73
Beam design 73
Bending moment 69
Bioactive material 65
Bone 43
Bone 63
- Bone atrophy 82
Bone contact ratio 67
Bone density 83
Bone formation 44
Bone loss 73
Bone resorption 45
Bone resorption 82
Bone volume ratio 67
Bone/implant contact 66
Bone-implant interface 61
Bone-implant system 83
Bone-to-implant contact 49
Boundary condition 34, 35, 82
- Cancellous bone 65
Cantilever length 76
Cantilevered design 71
Chemical coating 49
Cobalt-chromium 72
Combined load 62
Combined natural tooth and implant-supported prostheses 71
Commercially pure titanium (CPTi) 65
Composite 63, 72
Compressive radial stress 66
Compressive stress 71
Computed tomography (CT) 64
Connective tissue (CT) 47
Connector design 75
Contact analysis 92

- Cortical bone 62
- Cross-sectional property 35
- Crown-abutment interface 70
- Deflection 6, 70
- Deformation 1, 15
- Degrees Of Freedom (DOF) 6
- Displacement 1
- Distortion 69
- Dynamic analysis 93
- Dynamic load 62
- Elastic modulus 63
- Element Stiffness Matrix 18
- Element type 35
- Extreme loading 70
- FEA meshes 83
- Fibro-osseous integration 43
- Fibrous tissue/implant contact 66
- Finite element method 1
- Fixed bond 65
- Fixed prosthesis 72
- Fixture-abutment interface 68
- Force 1, 6
- Force transfer 61
- Force-displacement relationship 1
- Formation of fibrosis 44
- FORTRAN 4
- Framework 72
- Geometry 35
- Gold 72
- Gold alloy 63
- Gold cylinder-abutment interface 68
- Gold retaining screw 69
- Gold retaining screw-abutment screw interface 68
- Gold retaining screw-gold cylinder interface 68
- Gold screw 69
- Gold screw failures 76
- Graphic User Interface (GUI) 93
- Healing response 45
- High rigid prostheses 71
- Horizontal force 62
- Horizontal load 71
- IGES 93
- Implant 63
- Implant fixture 48
- Implant fracture 76
- Implant geometry 63
- Implant inclination 73
- Implant position 76
- Implant prosthesis 71
- Implant supported denture 53
- Implant supported rehabilitation 53
- Implant-prosthesis connection 61
- Implant-prosthesis connection 69
- Implant-supported crown 55
- Implant-supported fixed prostheses 71
- Implant-supported overdenture 71
- Implant-supported prostheses 43
- Isotropic material 34
- Joint 5
- Junctional epithelium (JE) 47
- Load angle 70
- Load magnitude 70
- Loading 61
- Loading condition 35
- Magnet 73
- Marginal bone 66
- Material properties 35, 82
- Matrix analysis 2
- Maximum stress 63
- Maximum stress concentration 62
- Maximum tensile stress 69
- Maximum von Mises stress 65
- Moment 6
- Multiple implant prostheses 61
- Node 5
- Non-rigid connector 75
- Oblique bite force 62, 63
- Occlusal load 62
- Occlusal surface 73
- O-ring 73
- Orthotropic 84
- Osseointegration 43
- Overload 62

- Overstress 75
Parasolid 93
Passive fit 69
Peri-implant tissues 46
Poisson's Ratio 19, 34
Porcelain 63, 72
Porous coating 49
Posterior mandible 87
Postprocessor 14
Precision attachment 75
Preload 69
Preprocessor 14
Primary mineralization 45
Principal stress 66
Pro Engineering 93
Prosthetic component 48
Prosthetic failures 76
Prosthetic splinting scheme 73
Pure contact 65
Quadrilateral 15
Resilient element 75
Resin 63, 72
Rigid connector 75
Rotation 6
SAP 4
Scanning electromicroscopy 43
Screw loosening 68
Semi-precision attachment 75
Shear stress 66
Silver-palladium 72
Span length 74
Static load 62
STEP 93
Stiffener height 73
Stiffness coefficient 12
Stiffness Matrix 7, 18
Strain 3, 27
Stress 3, 15
Stress analysis 1
Stress concentration 65
Stress distribution 65, 66
Stress distribution 71
Structural analysis 1
Structure 5
Sulcus depth (SD) 47
Superstructure 70, 73
Surgical guide 49
Tensile radial stress 66
Thread design 65
Tightening torques 69
TiO₂ layer 44
Titanium 42
Titanium alloy 72
Topology 35
Trabecular bone 62
Transversely isotropic 84
Triangle 15
Triangular Element 3
Underload 62
Vertical implant 71
Vertical load 70
Vertical loading 71
Washer 70
Wolff's law 66
Young's Modulus 19